TRIBHUVAN UNIVERSITY

INSTITUTE OF ENGINEERING

PULCHOWK CAMPUS

THESIS NO:079MSPSE021

Assessment of Optimal Feeder Configuration Integrating EV Loads And Solar PV Generation for Urban Nepalese Distribution Network

By

Shekh Maquesood Alam

A THESIS

SUBMITTED TO THE DEPARTMENT OF ELECTRICAL ENGINEERING IN PARTIAL FULFILLMENT OF THE REQUIREMENTS FOR THE DEGREE OF MASTERS OF SCIENCE IN POWER SYSTEM ENGINEERING

DEPARTMENT OF ELECTRICAL ENGINEERING

LALITPUR, NEPAL

APRIL 2025

Assessment of Optimal Feeder Configuration Integrating EV Loads and Solar PV Generation for Urban Nepalese Distribution Network

by

Shekh Maquesood Alam

Thesis Supervisor

Associate Professor Mahammad Badrudoza

Assistant Professor Akhileshwar Mishra

A thesis submitted in partial fulfillment of the requirements for the degree of Master of Science in Power System Engineering

Department of Electrical Engineering,

Institute of Engineering, Pulchowk Campus,

Tribhuvan University,

Lalitpur Nepal

April 2025

त्रिभुवन विश्वविद्यालय
TRIBHUVAN UNIVERSITY
इन्जिनियरिङ्ग अध्ययन संस्थान
INSTITUTE OF ENGINEERING
पुल्चोक क्याम्पस
PULCHOWK CAMPUS
DEPARTMENT OF ELECTRICAL ENGINEERING
Pulchowk, Lalitpur

CERTIFICATE OF APPROVAL

The undersigned certify that they have read and recommended to the Institute of Engineering for acceptance, a dissertation entitled "**Assessment of Optimal Feeder Configuration Integrating EV Loads and Solar PV Generation for Urban Nepalese Distribution Network**", submitted by **Shekh Maquesood Alam** in partial fulfillment of the requirement for the award of the degree of **Master of Science in Power System Engineering**.

Asst. Prof. Akhileshwar Mishra

Department of Electrical Engineering
Pulchowk Campus, Lalitpur
(Supervisor)

Assoc. Prof. Mahammad Badrudoza

Department of Electrical Engineering
Pulchowk Campus
(Supervisor)

Dr. Sushil Aryal

Deputy Manager
Nepal Electricity Authority
(External Examiner)

Asst. Prof. Dr. Bishal Silwal

Program Coordinator
M.Sc. in Power System Engineering
Pulchowk Campus, Lalitpur

Assoc. Prof. Dr. Basanta K. Gautam

Head of Department
Department of Electrical Engineering
Pulchowk Campus, Lalitpur

April 2025

Tel: +977-1-5443081, Email: doee@pcampus.edu.np, Website: www.doee.pcampus.edu.np

COPYRIGHT

ABSTRACT

The integration of solar photovoltaic (PV) systems and electric vehicles (EVs) presents both opportunities and challenges for modern electrical distribution networks, especially in Nepal, where the shift toward decentralized renewable energy is increasing the demand on the grid. As these technologies introduce intermittent generation and variable load patterns, optimizing distribution systems, particularly radial-loop configurations, is crucial to minimize line losses, stabilize voltage, and improve overall network reliability, addressing the unique energy challenges faced by urban areas in Nepal. The main objective of this research is to identify the optimal radial-loop configuration for the Nuwakot Distribution Center, integrating EV loads and solar PV systems to minimize line losses, reduce voltage fluctuations, and enhance system stability and reliability. This includes assessing the impact of EV charging stations and solar PV generation on network performance, developing and simulating various radial-loop configurations, optimizing feeder configurations to improve efficiency and voltage stability, and minimizing losses in the distribution network. This methodology optimizes electrical distribution feeder configurations by integrating Solar PV, EV loads, and system load patterns through literature review, data collection, load flow analysis, and iterative reconfiguration, ultimately testing the optimal configuration for minimizing power loss, maintaining voltage stability, and ensuring reliability in the distribution network at Nepal Electricity Authority (NEA), Nuwakot Distribution Center (NDC). This research highlights the benefits of optimizing NEA, NDC, Nepal's urban distribution network by integrating Electric Vehicle (EV) charging loads and Solar Photovoltaic (PV) systems, with data showing a 50% reduction in daily feeder losses (from 813.79 kWh to 395.23 kWh), an improvement in minimum bus voltage from 10.44 kV to 10.80 kV, and the use of six tie switch configurations. The study demonstrates how dynamic feeder reconfiguration and the use of renewable energy sources can improve network performance while maintaining safety and reliability.

ACKNOWLEDGMENT

Throughout the writing of this thesis report, I have received a great deal of support and assistance. I would like to express my deepest gratitude to my supervisors, Associate Professor Mahammad Badrudoza and Assistant Professor Akhileshwar Mishra, Department of Electrical Engineering, Institute of Engineering, Pulchowk Campus for their exceptional guidance, support, and encouragement throughout the course of this research. Their expertise, insightful feedback, and continuous motivation have been invaluable in shaping the direction and quality of this study.

I would also like to extend my gratitude to Assistant Professor Dr. Bishal Silwal, MSc Program Coordinator for Power System Engineering (MSPSE) and Associate Professor Dr. Basanta Kumar Gautam, Head of the Department, Department of Electrical Engineering, for providing me with the opportunity to pursue this study.

In addition, I would like to acknowledge faculties from the Master's Degree in Power System Engineering program at the Institute of Engineering, Pulchowk Campus, for their guidance and suggestions.

I would also like to acknowledge my colleagues who have helped me with their valuable suggestions and have been helpful in various phases of this research.

TABLE OF CONTENTS

LIST OF FIGURES

LIST OF TABLES

LIST OF ABBREVIATIONS & ACRONYMS

A	Amperes
AMI	Advance Metering Infrastructure
AC	Alternating Current
DC	Direct Current
DERs	Distributed Energy Resources
DIgSILENT	Digital Simulation for Electrical Networks
DSO	Distribution System Operator
EV	Electric Vehicle
HPS	Hydropower Station
INPS	Integrated Nepalese Power System
IRENA	International Renewable Energy Agency
KPI	Key Performance Indicator
kVA	Kilovolt-Amperes
kWh	Kilowatt-hour
MATLAB	Matrix Laboratory
NDC	Nuwakot Distribution Center
NEA	Nepal Electricity Authority
PV	Photovoltaic
SLFE	Static Load Flow Equation

CHAPTER: 1 INTRODUCTION

1.1 Background

The integration of renewable energy sources such as solar photovoltaic (PV) systems and the increasing penetration of electric vehicles (EVs) present significant opportunities and challenges for modern electrical distribution networks. As the transition to clean energy accelerates, optimizing the design and operation of distribution systems has become essential to ensure reliability, efficiency, and sustainability. Among various network configurations, radial-loop systems offer a promising solution by balancing the trade-off between installation cost, system reliability, and operational efficiency [1].

In particular, the addition of EVs and solar PV systems into the grid poses unique challenges, primarily concerning the management of increased energy demand and intermittent renewable generation. EVs, with their growing adoption, represent a substantial load on distribution networks, potentially exacerbating issues like voltage fluctuation and line loss [2]. Meanwhile, solar PV systems, though beneficial for reducing the carbon footprint, contribute to voltage fluctuations due to their variable generation patterns [3]. Thus, it is critical to assess and optimize the radial-loop configuration of distribution networks, considering these new loads and generation sources, to minimize line losses and maintain voltage stability.

The rapid growth of renewable energy technologies and electric mobility presents both significant opportunities and challenges for power distribution networks worldwide. In Nepal, the increasing integration of solar Photovoltaic (PV) systems and the growing adoption of Electric Vehicles (EVs) are transforming the energy landscape, especially in urban areas. Nepal's energy sector, historically reliant on hydropower, is undergoing a shift towards decentralized renewable energy sources such as solar PV, which contributes to reducing dependency on conventional grid power [4]. However, the integration of these technologies into the existing distribution networks, particularly in urban areas, poses several challenges, including voltage instability and higher line losses, due to the unpredictable nature of renewable generation and the fluctuating demand from EV charging stations [5].

Conventional radial distribution systems, which are commonly used in Nepalese cities, have limitations in handling bidirectional power flow and distributed energy

resources. These systems often face issues such as line losses, voltage drops, and low system reliability when new loads like EVs and renewable generation sources like solar PV are integrated [6]. As such, there is a pressing need to optimize the configuration of these networks to ensure better integration of distributed energy, mitigate losses, and enhance voltage stability.

This research aims to assess the optimal radial-loop configuration for urban Nepalese distribution networks, focusing on the integration of EV loads and solar PV systems. By evaluating different radial-loop configurations, the study will explore strategies to minimize line losses and reduce voltage fluctuations, thus enhancing the efficiency and reliability of the network. The results of this work are expected to provide valuable insights for policymakers, utility companies, and engineers in Nepal, helping to design more robust and efficient distribution systems that can better accommodate the increasing demand for renewable energy and electric vehicles in urban areas. This research will contribute to the growing body of knowledge on optimizing power distribution networks in developing countries, with a specific focus on Nepal's unique energy challenges.

1.2 Problem Statement

The integration of renewable energy sources, particularly solar Photovoltaic (PV) systems, and the increasing adoption of Electric Vehicles (EVs) in urban areas present significant challenges for power distribution networks. In Nepal, the transition towards decentralized energy generation and electric mobility is accelerating, but the existing distribution infrastructure, especially in urban centers, is not adequately equipped to handle the complexities introduced by these technologies. As a result, issues such as increased line losses, voltage fluctuations, and grid instability have become prominent, jeopardizing the reliability and efficiency of power supply in urban Nepalese distribution networks.

Traditional radial distribution networks, which are commonly employed in Nepal, are inherently limited in their ability to manage bidirectional power flow, a characteristic feature of distributed generation systems such as solar PV. Additionally, the unpredictable charging demands of EVs, particularly during peak hours, exacerbate these challenges, leading to inefficiencies in power distribution. Current feeder configurations, which primarily focus on conventional loads and infrastructure, fail to

optimize for the dual integration of renewable energy and EVs, leaving the distribution system vulnerable to inefficiencies and performance degradation.

This research seeks to address these issues by exploring the optimal radial-loop configuration for urban Nepalese distribution networks, specifically incorporating the integration of EV loads and solar PV systems. The primary objective is to identify a configuration that minimizes line losses, reduces voltage fluctuations, and enhances overall system stability and reliability in the face of increasing demand and renewable energy generation. The study will develop models and optimization techniques tailored to the specific needs of Nepalese distribution systems, focusing on their unique operational challenges, such as high line losses, voltage instability, and the lack of advanced grid management infrastructure.

The problem is multifaceted, as it involves:

i. The need for an optimized configuration that accounts for both solar PV generation and EV load demands, which vary throughout the day.

ii. The requirement for advanced optimization algorithms that can address these challenges in a computationally efficient manner, suitable for real-time application in a developing country context.

iii. The necessity of proposing a configuration that not only minimizes technical losses but also ensures voltage stability, thereby improving the quality and reliability of electricity supply in urban areas.

Addressing this problem will contribute to the development of more sustainable, resilient, and efficient power distribution networks in Nepal, enabling the successful integration of renewable energy sources and electric mobility into the national grid. The results of this study have the potential to inform energy policy and utility strategies, ultimately helping to enhance the performance and stability of Nepal's urban power distribution systems.

1.3 Objective

1.3.1 Main Objective

The main objective of this research is to assess and identify the optimal radial-loop configuration for the urban distribution network at NEA, Nuwakot Distribution Center that integrates Electric Vehicle (EV) loads and solar Photovoltaic (PV)

systems, intending to minimize line losses, reducing voltage fluctuations, and improving overall system stability and reliability. This optimization will enhance the efficiency of the distribution network while accommodating the growing adoption of renewable energy and electric vehicles in Nuwakot, Nepal.

1.3.2 Specific Objectives

To achieve the main objective, the specific objectives are as follows:

i. To assess how the inclusion of both EV charging stations and solar PV generation affects the performance of distribution networks at the urban area of Nuwakot Distribution Center, particularly in terms of power losses, voltage stability, and load demand fluctuations.

ii. To develop models of various radial-loop configurations for distribution systems at Nuwakot DC that incorporate EV loads and solar PV systems. Simulate these models to analyze their performance under different operational conditions.

iii. To optimize the feeder configuration to determine the most efficient feeder configuration that minimizes line losses in the distribution network.

iv. To improve voltage stability and minimize voltage fluctuations caused by the integration of distributed generation and fluctuating EV charging demand.

By achieving these objectives, the study aims to contribute to a deeper understanding of how urban distribution systems in Nepal can be optimized to accommodate the future demands of renewable energy and electric mobility, while improving the efficiency and stability of the network.

1.4 Scopes of the Study

This research will focus on the assessment of optimal radial-loop configurations for urban Nepalese distribution networks, incorporating Electric Vehicle (EV) loads and solar Photovoltaic (PV) systems. While the findings may have broader applications, the primary context is based on the challenges and characteristics of Nepalese cities, where the integration of renewable energy and EVs is rapidly increasing. This research will consider the integration of solar PV systems and EV charging infrastructure into the existing power distribution network. The study will not cover other forms of renewable energy (such as wind or biomass) or advanced technologies

like energy storage systems, which are outside the scope. The optimization will address issues such as minimizing line losses, improving voltage stability, and enhancing system reliability while integrating the dynamic loads from EVs and the intermittent nature of solar energy. The study will consider different timeframes for the simulation of EV charging demand and solar generation, focusing on daily and seasonal variations. However, it will not delve into long-term grid expansion planning or explore multi-year dynamics. The research will use computer simulations to model various feeder configurations and evaluate their performance under different operating conditions, considering factors such as load variation, solar generation, and EV demand.

1.5 Limitations of the Study

Despite the comprehensive approach, several limitations exist in this study:

i. The study's findings may be limited by the availability and accuracy of data on the actual distribution network infrastructure, solar PV generation, and EV load profiles in urban Nepalese settings.

ii. During optimization process, certain assumptions will need to be made, such as uniform load distribution, standard operating conditions, and average solar generation profiles. These assumptions may not fully reflect the complexity of real-world conditions.

iii. The study will focus on radial-loop feeder configurations, which may not address all potential network optimization scenarios.

iv. The study will assume representative load profiles, but these assumptions may not fully capture the actual variability in EV charging demand, especially during peak times or in the event of unexpected EV adoption surges.

v. The focus of the research will be primarily on solar PV and EVs, without considering other distributed energy resources like wind or energy storage systems.

While this research will provide valuable insights into optimizing distribution networks with the integration of solar PV and EVs, the identified limitations highlight the need for further studies that can refine the models, gather more precise data, and explore other variables that may influence the performance of Nepalese distribution systems.

CHAPTER: 2 LITERATURE REVIEW

Different studies have been carried out to provide optimal radial and loop feeder configuration in a distribution network reducing the line loss and voltage drop. Subsection 2.1 reviews the different studies carried on distribution system feeder optimization till now. Subsection 2.2 presents the research gap between past studies and considerations of this research to address such research gap.

2.1 Previous Studies

Over the years, numerous studies have been conducted on the optimization of distribution system feeders, focusing on improving the efficiency and reliability of electrical power distribution networks. These studies have primarily concentrated on minimizing power losses, enhancing voltage stability, and ensuring the effective integration of distributed energy resources (DERs) such as solar PV systems and electric vehicles (EVs). Radial distribution networks are typically the default configuration in many power systems due to their simplicity and low installation costs. However, they are often less reliable, as any fault or failure at a single point can cause a large portion of the network to go offline [7]. In contrast, looped networks, which connect various points in a closed-loop configuration, can provide higher reliability and flexibility by offering alternative paths for electricity flow during faults or disturbances. While looped systems have higher installation costs and are more complex to operate, they can reduce system losses and improve voltage regulation [8]. The literature highlights that the optimal configuration between radial and looped systems often depends on various factors, including cost, reliability, load patterns, and integration of renewable energy sources. A hybrid approach, involving both radial and looped topologies, has been proposed as a solution to combine the cost-efficiency of radial networks with the reliability benefits of looped systems. Studies by [9] suggest that such hybrid configurations could help optimize the trade-off between system losses and reliability, especially when coupled with distributed energy resources like solar PVs and EV charging stations. The incorporation of solar PV systems into distribution networks has been widely recognized for its potential to reduce dependency on fossil-fuel-based generation and decrease greenhouse gas emissions [10]. However, solar PVs also introduce challenges, primarily due to their intermittent and variable nature. As PV output fluctuates with weather conditions, it can lead to

voltage instability and significant power quality issues such as voltage fluctuations and over-voltages during periods of high solar generation [3].

Early research in distribution system optimization focused on minimizing power losses through techniques such as load flow analysis, optimal placement of transformers, and feeder reconfiguration. For example, studies by [11] emphasized the importance of reconfiguring feeders in radial distribution networks to reduce losses and enhance voltage profiles. Various optimization algorithms, such as genetic algorithms (GA), particle swarm optimization (PSO), and simulated annealing (SA), were applied to solve these problems, yielding improved efficiency and lower operational costs in the distribution system. Recent advancements in optimization techniques have shown that Particle Swarm Optimization (PSO) is a powerful and efficient method for solving various problems related to optimal feeder configuration. In particular, the integration of Electric Vehicle (EV) charging loads and solar Photovoltaic (PV) generation into the optimization models has presented new challenges and opportunities for improving the efficiency and reliability of distribution systems.

A study on [12] used PSO for optimal feeder reconfiguration to minimize power loss in radial distribution systems. The authors demonstrated that PSO could efficiently optimize feeder switches, resulting in reduced losses and improved voltage stability. Similarly, [13] used PSO to find the optimal placement of distributed generation (DG) units in distribution systems, taking into account both active and reactive power flow, and minimizing feeder losses. This method showed significant improvements in system efficiency and reduced operational costs. Study in [14] proposed a PSO-based method for optimal feeder reconfiguration that integrates the impact of EV charging loads. The study demonstrated that PSO could adapt to fluctuating EV demands, allowing for optimal feeder reconfiguration and load balancing in real-time. The authors highlighted the advantage of PSO in handling the uncertainty and variability of EV charging patterns, which can be highly dynamic, by adjusting the configuration to optimize power distribution.

Another study by [15] focused on the combined optimization of EV charging stations and distribution network configuration. They used PSO to determine the optimal location and size of EV charging stations while minimizing power loss and ensuring voltage stability under varying EV charging loads. Study by [16] proposed a PSO-

based approach for optimal feeder configuration that incorporated both EV charging and solar PV generation. The study focused on reducing power losses and improving the voltage profile while accounting for the variability of both EV and PV. The authors demonstrated that PSO, through its ability to explore a large solution space, was able to find optimal feeder configurations that minimized losses while maintaining voltage stability in the presence of uncertain load and generation patterns. They also highlighted the advantage of PSO in handling the stochastic nature of renewable energy generation and EV charging loads. In [17] extended this work by integrating battery storage systems into the optimization model. The authors used PSO to determine the optimal configuration of feeders, placement of solar PV systems, EV charging stations, and energy storage units. The study aimed to reduce the impact of EV charging on the feeder network and to enhance the reliability of the system under varying renewable energy generation. The results showed that PSO effectively managed the dynamic fluctuations in both solar power generation and EV load while ensuring that voltage profiles were maintained and system losses minimized.

Recent studies have shifted towards integrating renewable energy sources and EVs into distribution systems. For instance, [18] presented a feeder optimization approach for systems incorporating both solar PV and EV loads, aiming to mitigate issues like voltage fluctuations and unbalanced loads. The study highlighted the challenges of bidirectional power flow and the need for dynamic adjustments to the feeder configuration to accommodate the intermittent nature of solar energy and the variable demand from EV charging stations. Similarly, [19] explored the optimal configuration of distribution feeders in the presence of EVs and distributed energy sources, proposing a hybrid optimization technique that considers both operational constraints and economic factors.

Also, [20] examined the application of Distribution Feeder Reconfiguration (DFR) in smart grids with high EV penetration. The study proposed a two-stage optimization strategy: the first stage optimized EV charging/discharging schedules using a genetic algorithm, while the second employed a modified Grey Wolf Optimization algorithm for DFR. Results showed a marked reduction in system losses and improved voltage profiles when both coordinated EV scheduling and feeder reconfiguration were employed. This research highlights the synergistic benefits of combining feeder

optimization with EV management strategies, paving the way for more resilient distribution networks. Guzman-Henao et al. [21] investigated the optimal integration of PV systems into distribution networks, analyzing technical, financial, and environmental factors. The study proposed a holistic optimization framework to determine the ideal size and location of PV systems to enhance system reliability and sustainability. Their multi-criteria decision-making approach ensured that PV integration not only improved technical performance but also met financial viability and environmental sustainability targets. This work emphasizes the importance of cross-disciplinary planning in PV deployment. Noruzi Azghandi et al. [22] presented a hybrid optimization approach combining Particle Swarm Optimization (PSO) and Artificial Bee Colony (ABC) algorithms for reconfiguring distribution feeders with integrated EVs and Distributed Generators (DGs). The objective was to minimize total energy losses and improve load balancing while considering time-of-use pricing. The proposed algorithm effectively managed dynamic EV charging demand and intermittent DG output, demonstrating superior performance compared to traditional methods. This study showcases how hybrid metaheuristic techniques can significantly enhance distribution system performance.

A study in [23] introduced an equivalent network modeling technique that accounts for harmonics generated by PV systems during feeder reconfiguration. The study stressed the importance of maintaining Total Harmonic Distortion (THD) within IEEE-519 standards to ensure power quality. By considering both harmonic content and network topology in the reconfiguration process, the study offered a practical approach to balancing renewable integration with quality standards. This contribution is particularly important in contexts where PV penetration levels are high and sensitive loads are present. Khaing et al. [24] focused on the co-optimization of Battery Energy Storage Systems (BESS) and PV in EV-integrated distribution systems. Using advanced metaheuristic algorithms such as Particle Swarm Optimization (PSO) and African Vulture Optimization Algorithm (AVOA), the authors identified optimal locations and capacities for BESS and PV units. Their objective was to minimize network costs, reduce peak demand, and improve voltage profiles. The study revealed that strategic co-placement of BESS and PV could mitigate the fluctuations associated with EV charging and PV intermittency, thereby stabilizing the network. Turan and Gökalp [25] examined the integration of EV

charging stations equipped with solar power plants, focusing on the design of protection and voltage control systems. The study identified major challenges, including bidirectional power flows and fault detection complexities due to the presence of PV sources. They proposed modified relay settings and adaptive protection schemes to accommodate the new dynamics. This work is essential in ensuring the reliability and safety of distribution systems amid increasing DER penetration. Faria et al. [26] explored aggregator-based models for managing EVs in distribution networks. Their framework allowed aggregators to coordinate EV charging and discharging based on market signals and grid constraints. The study showed that such coordination could minimize operational costs and enhance the participation of EVs in demand response programs. By integrating market-based control with technical planning, this model adds flexibility and intelligence to EV integration strategies. Knezovic and Andersen [27] assessed the potential of EVs to provide grid services through flexible charging. Their research quantified the technical and economic benefits of using EVs for frequency regulation, voltage support, and peak shaving. The study emphasized that EV flexibility, when aggregated and properly managed, could serve as a valuable grid asset rather than a disruptive load. This perspective reinforces the need to view EVs not just as consumers but as active participants in the smart grid ecosystem.

In the context of Nepal, which is experiencing an increasing adoption of solar PV and EVs, several studies have been carried out to assess the integration of these technologies into the country’s distribution networks. For example, [28] examined the impact of solar PV integration on the existing radial distribution systems in urban Nepal, identifying issues related to voltage instability and high line losses. They proposed the use of advanced optimization techniques to enhance the distribution network's performance, including feeder reconfiguration and voltage regulation.

Overall, the body of literature demonstrates the growing importance of optimizing distribution system feeders in the face of new challenges posed by renewable energy integration and electric mobility. Many studies suggest that an optimal radial-loop configuration, particularly in urban areas, can significantly improve system performance by minimizing line losses and voltage deviations. However, research on optimizing feeders for Nepal’s specific distribution systems, considering both EV loads and solar PV systems, remains limited and warrants further investigation.

2.2 Research Gap

While significant progress has been made in the optimization of distribution system feeders, particularly with the integration of renewable energy sources (such as solar PV) and Electric Vehicle (EV) loads, several gaps remain in the existing literature. These gaps highlight areas where further research is required to improve the performance and efficiency of distribution networks, especially in the context of urban areas in developing countries like Nepal. This subsection discusses the research gaps identified from past studies and outlines the considerations of this research to address these gaps.

One of the primary gaps in past studies is the limited focus on the integration of both solar PV systems and EV loads simultaneously in the optimization of distribution system feeders. While many studies have addressed feeder optimization with either solar energy or EV loads in isolation, there is a lack of research that simultaneously considers the interaction between these two emerging technologies. The combined impact of variable solar generation and fluctuating EV charging demands on the distribution network has not been fully explored, especially in the context of urban Nepalese networks, where the adoption of both technologies is growing rapidly. Most studies [19], [18] have concentrated on optimizing distribution feeders for either renewable energy or EVs, but not both in an integrated manner, leading to a limited understanding of how these factors interact within a single network.

Another significant gap is the application of optimization techniques to Nepal's specific distribution system configurations. Much of the existing research, such as that by [11] and [28], has primarily focused on developed countries with advanced infrastructure or on generalized models of distribution networks. These studies do not adequately address the unique characteristics of Nepal's distribution systems, which are often more decentralized, face high levels of power loss, and experience voltage instability due to the lack of robust grid infrastructure. The optimal radial-loop configuration for such networks has not been thoroughly studied in Nepal, and the integration of EVs and solar PV systems has not been specifically optimized for Nepalese urban environments.

Additionally, while optimization algorithms such as genetic algorithms (GA), particle swarm optimization (PSO), and simulated annealing (SA) have been widely used to solve distribution network optimization problems [11], [18] there is a need for more

context-specific and computationally efficient methods, particularly when considering the unique operational challenges in Nepalese networks. Many of the existing optimization models are computationally expensive and may not be well-suited for real-time implementation in developing countries where computational resources and access to large-scale simulation platforms are often limited. There is, therefore, a need for more accessible, low-complexity optimization approaches that can be effectively implemented in these settings.

This research aims to fill these gaps by exploring the optimal radial-loop configuration for urban Nepalese distribution networks with the integration of both EV loads and solar PV systems. Specifically, this study will simultaneously consider solar PV and EV loads. This research will assess the combined impact of both technologies on power loss, voltage deviations, and system stability, addressing the gap in understanding their interactions in urban distribution networks. It will develop a specific optimization technique to the unique features of Nepalese distribution networks, considering local conditions such as grid infrastructure, power loss, and voltage fluctuations, which have been inadequately addressed in prior studies. The research will adopt or develop low-complexity optimization algorithms to ensure that the solutions are practical for real-world implementation in Nepal, where computational resources may be limited.

By addressing these gaps, this research will contribute to the development of more efficient, reliable, and sustainable distribution networks in urban Nepal, offering valuable insights that can be applied to similar contexts in other developing countries facing similar challenges with renewable energy integration and electric mobility.

CHAPTER: 3 RESEARCH METHODOLOGY

3.1 Generalized Flowchart

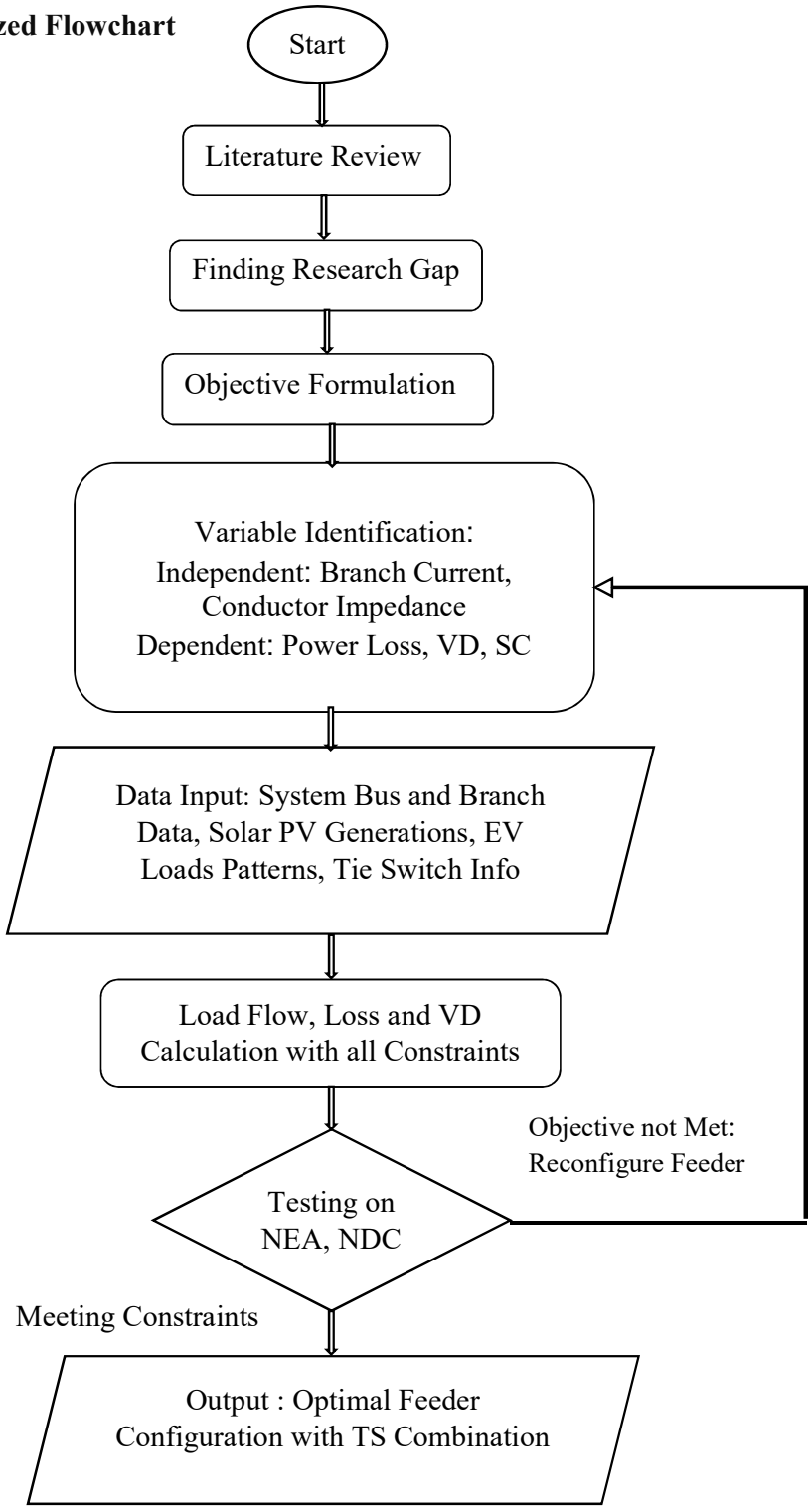

Figure 3-1: Generalized Flowchart of the Study

The flowchart in Figure 3-1 outlines a systematic methodology for optimizing electrical distribution feeder configurations, integrating Solar PV source, EV load, and system load pattern. The research methodology commences with a thorough literature review to establish an understanding of the existing knowledge related to feeder reconfiguration in power distribution systems. This initial phase helps to identify a research gap, highlighting areas where further investigation is required. Subsequently, the research progresses to objective formulation to meet the identified research gap. Following the formulation of objectives, the research involves identifying key variables. This includes identifying the independent variables, such as branch current and conductor properties like conductor type, impedance, admittance, etc. Similarly, dependent variables such as distribution power loss, bus voltage deviation (VD), and different tie switch combinations (SC) for the optimal configuration of feeders, are identified. The study then proceeds to data input, gathering comprehensive system bus and branch data, solar photovoltaic (PV) generation profiles, electric vehicle (EV) load patterns, and tie switch information. This data is collected from a real distribution system at NEA, NDC. The major parts of the analysis involve performing load flow, system loss calculation, voltage deviation calculations, and determination of the optimal tie switch combination while maintaining constraints such as bus voltage constraints, power balance constraints, conductor thermal limit constraints, and the operational constraints. This computational phase is critical for evaluating the system's performance under various configurations. If the pre-defined objectives are not met during this stage, the process necessitates reconfiguring the feeder and iterating through the calculations again until the constraints are satisfied.

Once the constraints are met, the proposed methodology is subjected to testing on real-world data from NEA, NDC to validate its applicability and effectiveness. Finally, the research culminates in the output, which is the optimal feeder configuration with tie switch (TS) combination. This solution represents the most efficient and effective arrangement that minimizes power loss, maintains voltage stability, and ensures system reliability, thereby contributing to the advancement of power distribution system optimization. Following subsections represents the specific steps of the proposed research methodology.

3.2 Analyzing Existing Studies

The first step of this study is to discuss research carried out related to distribution system optimization with the integration of EV loads and Solar PV generators. As discussed in section 2 and its subsections, there are various research carried out mainly focused on optimization of radial distribution feeders with reduced uncertainties and least computational costs. Even though number of studies has been carried out, research on optimizing feeders for Nepal's specific distribution systems, considering both EV loads and solar PV systems, remains limited and requires further investigation. With reference from different literatures, Particle Swarm Optimization (PSO) will be used for the proposed optimization. Particle Swarm Optimization (PSO) is a heuristic optimization technique inspired by the social behavior of birds flocking or fish schooling. It is widely used for solving complex optimization problems because of its simplicity and ability to find near-optimal solutions in a reasonable amount of time. In the context of distribution feeder optimization, PSO has been applied to various problems related to the efficient design and operation of electrical distribution systems. When applied to distribution feeder optimization, which involves tasks like minimizing power losses, enhancing voltage profiles, optimal placement of EVs and Distributed generations, capacitor placement, and reconfiguration, PSO has several distinct advantages over other optimization techniques. These benefits arise from PSO's inherent characteristics, making it particularly well-suited for the complex and dynamic nature of electrical distribution systems.

3.3 Data Collection

Another major stage in the study is the input data collection. The research requires various data sets to perform a comprehensive analysis. The major data required for the study is as follows:

i. Distribution Network Layout

This includes the detailed layout diagram of a distribution network having multiple radial feeder combinations so that optimal radial and loop configuration can be achieved by using controlled tie switches between them. All the generating stations, distribution transformer loads, and tie switch connecting radial feeders to have a looping operation are to be collected. The distribution line may include several

branches with different conductor types. All of this distribution network information is collected during this stage.

ii. System Bus Data and Branch Data

After collecting the detailed distribution network layout, the bus data which includes bus number, bus type, and active & reactive power injected into the bus, are collected for the load flow study. Similarly, branch data consisting of connecting buses, line resistance, line reactance, and admittance are collected to evaluate branch loss and bus voltage deviations. This branch data varies with the length of the conductor between the branches which is also collected from the network topology. All of this branch and bus data are converted into the per unit system to a common base.

iii. Solar PV Generation Data

The power generation from a solar PV cell depends on the solar radiation gain at that particular time and location. To study the effect of solar PV generations in the distribution system feeder configuration, the power generation from solar PV with respect to the time of day is to be collected.

iv. EV Load Pattern Data

Another major component of this study is the power consumption patterns of the EV charging stations. This load pattern is very intermittent in nature, and the consumption data can be collected from the smart meters installed at the charging station. After gathering all of the above-mentioned data, the next step is objective formulation, which processes the input raw data within specified constraints to give an appropriate feeder configuration as an output.

3.4 Mathematical Formulation

In this stage, a mathematical objective function is formulated with specific constraints of the system to process the given input data and result optimal feeder configuration as an output. From various literatures, it is noted that the major objective of a distribution system configuration is to minimize system line loss and bus voltage deviation, maintaining the line thermal limit, supply continuity, and reliable operations. The optimization problem can be formulated as follows [29]:

3.4.1 **Objective Function**

The objective is to minimize the total line losses and voltage deviations across the distribution network. The power loss in the distribution system is dependent on the line current flowing through it and its resistivity. The objective function to minimize distribution system loss can be expressed as [29]:

$$Min\ P = \sum_{i=1}^{n} P_{loss}(i)$$

$$\text{Or}, Min\ P = \sum_{i=1}^{n} I_i^2 . R_i \ldots\ldots\ldots\ldots\ldots\ldots\ldots (1)$$

Where, $P_{loss}(i)$: is the power loss in feeder segment i.

n: is the number of feeder segments.

Ii = Branch current in feeder segment i.

Ri = Resistance of the branch i.

The regular supply of loads with acceptable voltage limits is necessary for the distribution system operators. The voltage drop in the distribution line is dependent of current flowing through the line and its impedances. The voltage at each node is the difference between its predecessor node which is nearer to source and voltage drop in the branch connecting them. In reference to [30], another objective function to minimize the voltage drop is represented as follows:

$$Min\ V = \sum_{j=1}^{m} \Delta V(j) \ldots\ldots\ldots\ldots\ldots\ldots\ldots . (2)$$

Where, ΔV(j): is the voltage deviation at bus j

m: is the number of buses (nodes) connecting source to jth node.

The load flow studies provide the bus voltages and branch currents for a particular feeder configuration which is further used to calculate the branch loss and minimal bus voltage and thus the objective functions.

3.4.2 **Power Flow Equations**

The network's power flow is governed by equations derived from Kirchhoff's laws, which include both active and reactive power. The distribution network consists of a

set of nodes (buses) connected by lines (or branches) that are either in a radial or loop configuration. Each line has a resistance R and reactance X and each bus i has a voltage Vi, load Pi, and reactive power Qi. The power flow equations for the network are given by:

$$P_i = V_i * \sum_{k=1}^{n} V_k(G_{ik}\ Cos(\theta_i - \theta_k) + \left(B_{ik}\ Sin(\theta_i - \theta_k)\right) \dots\dots\dots\dots\dots\dots\dots (3)$$

$$Q_i = V_i * \sum_{k=1}^{n} V_k(G_{ik}\ Sin(\theta_i - \theta_k) - \left(B_{ik}\ Cos(\theta_i - \theta_k)\right) \dots\dots\dots\dots\dots\dots\dots (4)$$

Here, Pi and Qi are the active and reactive power at the bus i.

Vi and θi are the voltage magnitude and phase angle at bus i.

Gik and Bik are the real and imaginary parts of the bus-to-bus admittance matrix.

These static load flow equations (SLFE) are derived from Kirchhoff's laws considering line resistances and reactance balancing supply from source with load demand. This load flow analysis in the distribution system helps in planning, operation, and optimization. It allows utilities like NEA, NDC to ensure voltages stay within acceptable limits, minimize power losses, and integrate renewable energy sources effectively. For example, if a new solar farm is added, load flow studies can predict voltage fluctuations and help in designing control strategies. Newton-Raphson and Gauss-Seidel methods are the commonly used methods to solve load flow equations. The Newton-Raphson method, which is known for its fast convergence rate when applied to large networks, is used to calculate load flow solutions in this proposed methodology.

3.4.3 **Line Losses**

The power losses in each feeder are calculated based on the difference between the power supplied and the power consumed:

$$P_{loss}(i) = \sum_{j=1}^{n} [\left(V_i - V_j\right)^2 . G_{ij}] \dots\dots\dots\dots\dots\dots\dots\dots (5)$$

Where, G_{ij} is the conductance of the feeder between buses i and j.

The bus voltage at each bus is calculated using the load flow equation. By using the voltage difference between the node and its resistance, the power loss in each branch

can be evaluated. The total sum of individual branch loss is known as total distribution system loss. By using an optimal tie switch combination, the branch loss can be minimized by reducing the magnitude of current and distance between load and source.

3.4.4 Optimization Constraints

I. Voltage Constraints

Voltage constraints are enforced to maintain voltage within a permissible range at each bus:

$$V_{min} \leq V_i \leq V_{max} \quad for\ all\ i$$

Where, Vmin and Vmax are the minimum and maximum allowable voltages for each bus, ensuring voltage stability. As per Chapter (4), Rule (40), Sub-Rule (1) and (2) of Electricity Regulation 2050, The standard supply voltage shall be maintained as 230/400 Volts and the fluctuation shall not be allowed for more than five percent in standard volts. To maintain this voltage standard, NEA, NDC being a Nepalese utility, have to maintain the primary voltage of 11/0.4 kV distribution transformer. Similarly, as per Chapter (4), Rule (41), Sub-Rule (1) and (2) of Electricity Regulation 2050, The standard supply voltage shall be maintained as 3.3, 6.6, 11, 22, and 33 Kilo Volts and the fluctuation shall not be allowed for more than five percent in standard volts. Thus the voltage constraints for this study are defined using the above-mentioned standard and are set to a minimum of 10.45 kV (0.95 p.u.) to a maximum of 11.55 (1.05 p.u.) kV. The proposed methodology maintains the minimal system bus voltage within the specified standard of 0.95 p.u.

II. Power Balance Constraints

EV charging demand and solar generation are variable and are modeled as time-varying load profiles. These profiles must be incorporated into the power flow equations as dynamic loads. The load at each bus, particularly for EVs, will be constrained by the maximum charging capacity and the solar power generation will be bounded by the available irradiance at each time step.

$$P_{EV}(i) = f(t).P_{EV,Max}(i) \ldots\ldots\ldots\ldots\ldots\ldots (6)$$

$$P_{PV}(i) = g(t).P_{PV,Max}(i) \ldots\ldots\ldots\ldots\ldots\ldots (7)$$

Here, $P_{EV}(i)$ is the EV charging load at bus i at time t.

$P_{PV}(i)$ is the Solar PV generation at bus i at time t.

$f(t)$ & $g(t)$ are the functions representing the time-dependent variation of EV demand and solar generation.

The total power generated (including from solar PV systems) and the total load (including EVs) must balance:

$$P_{Grid}(i) + P_{PV}(i) = P_{Load}(i) + P_{EV}(i) \dots\dots\dots\dots\dots\dots (8)$$

As an electricity utility, it is compulsory to maintain the continuous power supply. Continuously maintaining the distribution system load (transformer load, EV loads, line loss) in balance with power generated by solar PV generators and other sources is known for the performance analysis indicator on a distribution center. This study maintains the supply and demand balance with the protection of islanding of load centers during the operation of various tie switch combinations maintaining supply reliability.

III. Line Flow Limits

The power flowing through each line must not exceed its thermal limit:

$$P_{Line} \leq P_{Thermal}\ for\ all\ line\ sections\ l$$

Here, $P_{Thermal}$ is the maximum thermal limit of the conductor used.

In a distribution network, there are various types of conductors used for various branches connecting source to load. Each individual conductor has its own current carrying capability which is defined by its material properties and size. This capacity is known as the conductor thermal capacity and it indicates the maximum amperes that the specific conductor can bear at particular climatic conditions. While performing various feeder configurations in this study, the line current is maintained below its specified thermal capability so as to prevent the conductor from overheating and sag & clearance standard limits.

By solving the above optimization problem within the described constraints, the optimal radial-loop configuration can be determined to minimize line losses, reduce voltage fluctuations, and enhance overall system reliability and efficiency.

3.5 System Modeling and Validation

After collecting the above-mentioned data and formulating the research methodology with specified constraints, the system is modeled and its result is validated as per technical requirements of the system. This involves developing a comprehensive model of the urban distribution network, including both conventional and distributed energy resources such as solar PV and EV charging stations. The distribution network is modeled using standard electrical network elements (such as feeders, transformers, and buses) in a software environment. The power flow equations is derived and used for simulations to assess network performance under different configurations. The next step involves modeling the load profiles, specifically focusing on the variability of EV loads and the intermittency of solar generation. EV load profiles will be based on representative charging patterns, including both residential and public EV charging demand. Solar PV generation will be modeled as a function of time of day, season, and geographical location, using typical meteorological data for urban Nepalese environments. Various simulation scenarios will be executed to evaluate the performance of different configurations. These simulations will assess key performance indicators (KPIs), including line losses, voltage profiles, system reliability, and power flow stability under varying solar generation and EV charging demand. The results will be compared for each configuration to determine the optimal configuration for the urban distribution network. The proposed optimal configuration will be validated through comparison with benchmark cases and existing studies in similar contexts. The feasibility and practical implementation of the results will be evaluated, considering the specific characteristics of Nepalese distribution networks.

CHAPTER: 4 RESULTS AND DISCUSSION

4.1 System Under Consideration

The system considered for this research will focus on the typical urban distribution network in Nepal, integrating Electric Vehicle (EV) loads and solar Photovoltaic (PV) systems into the existing power grid. The test system for the proposed methodology will be based on the radial-loop configuration of the Nuwakot Distribution Center, operated by the Nepal Electricity Authority, located in Nuwakot, Nepal. Nuwakot, situated in the Bagmati Province and to the immediate north of Kathmandu, the capital city of Nepal, is known for its diverse cultural landscape and rapidly growing economy. The demand for agricultural, industrial, and commercial electricity is increasing significantly, driven in part by its strategic location along a major highway connecting Nepal's capital with China. The Nuwakot Distribution Center includes six 33/11 kV substations and 19 radial 11 kV distribution feeders. Additionally, approximately 742 11/0.4 kV distribution transformers are installed across the district, and they serve a total of 613 kilometers of radial 11 kV feeders. The district's various consumer categories are supplied through 400/230 V low-tension distribution lines, consuming approximately 40 million units of electrical energy annually.

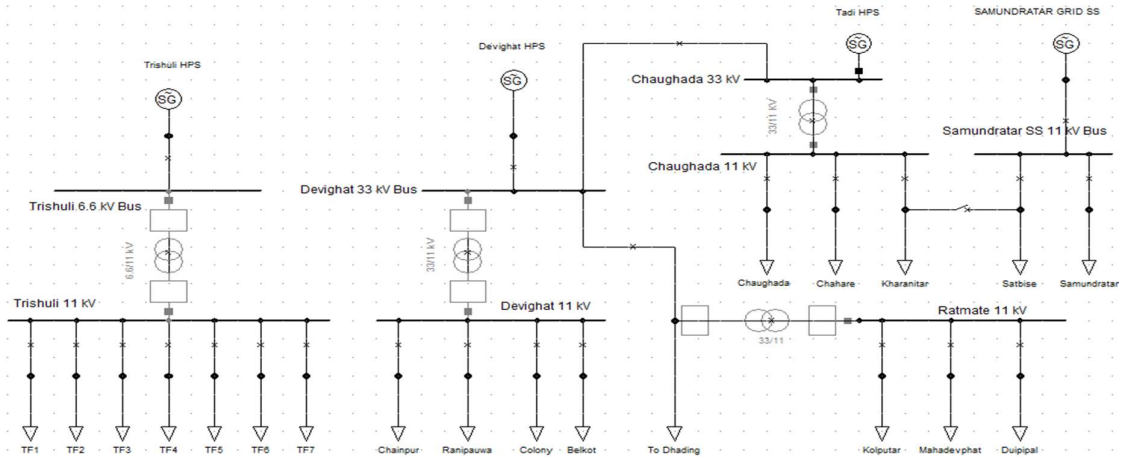

Figure 4-1: Typical Layout of Feeder and Substation Arrangements at Nuwakot DC

The figure above illustrates the typical distribution layout of the NEA, Nuwakot Distribution Center. The feeder under consideration is the radially configured Battar Feeder (TF4), which originates from the Trishuli Hydropower Station substation, along with Feeders No. 5 and 3 from the Devighat Hydropower Station. These

feeders collectively supply the major load centers in Bidur Municipality, Nuwakot District. The proposed methodology will be used to determine the optimal radial and loop configuration, as well as the best locations for Electric Vehicle (EV) charging stations and Solar Photovoltaic (PV) generation within these areas.

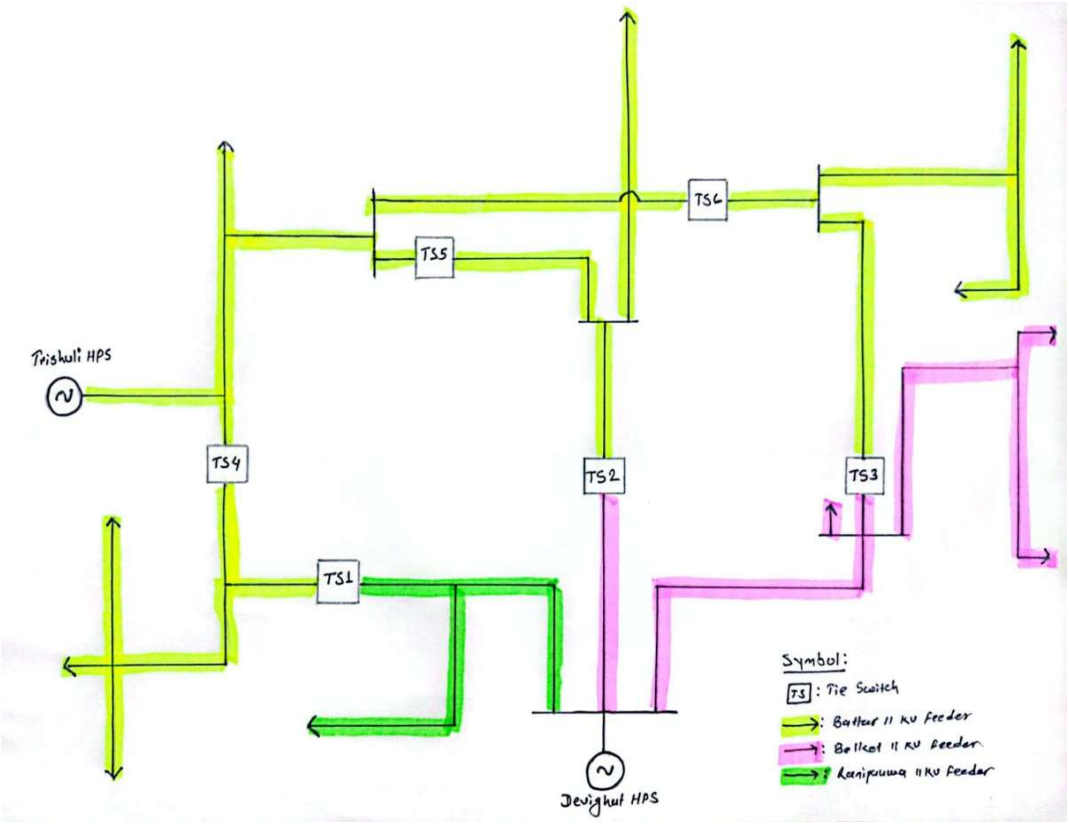

Figure 4-2*:* Typical Layout of Feeder and Tie Switch Arrangements at Nuwakot DC

Figure 4-2 represents the feeders and tie switch combination layout for the study system under consideration. The two generation sources are connected to load of Bidur Municipality via a radial and loop configuration of three feeders and six number of tie switches.

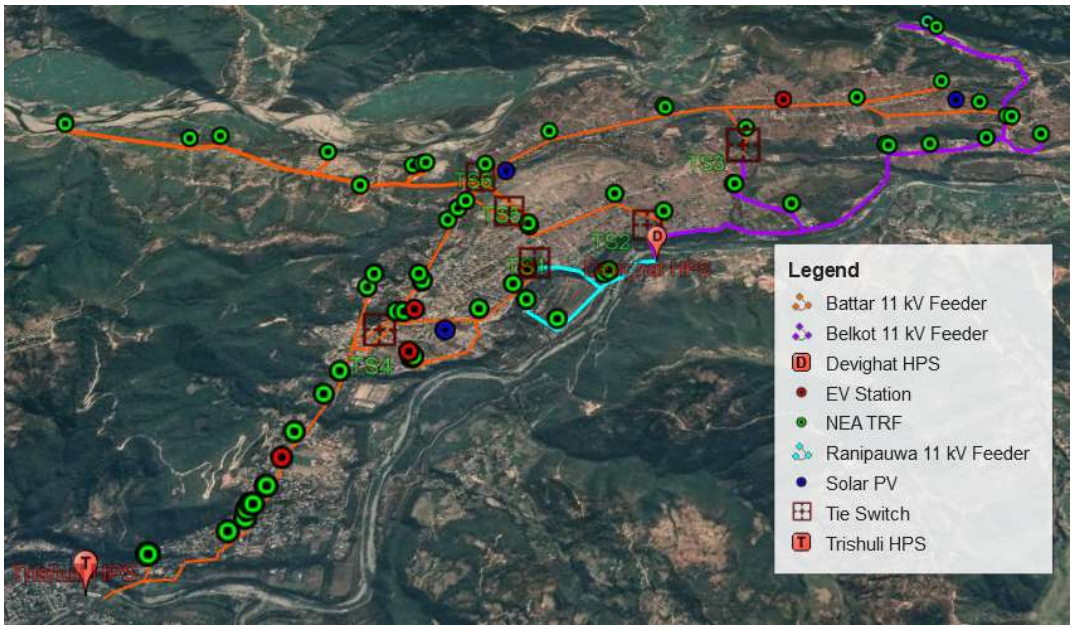

Figure 4-3*:* Layout of Existing Distribution System for the Study

The main urban area of Nuwakot District is located within Bidur Municipality, which accounts for approximately one-fourth of the total energy consumption in the district. There are currently six operational EV charging stations in this area, with an additional 20 stations under installation. Bidur Municipality also has high solar generation potential, as it falls within a region with strong solar radiation. Notably, the largest solar project in Nepal, a 25 MW peak capacity plant, is located within Bidur Municipality. This makes the area highly suitable for connecting rooftop PV installations and small solar PV farms to the low-voltage distribution system. The Nepal Electricity Authority (NEA) is in the process of developing policies for the implementation of net metering systems, which further enhances the feasibility of integrating solar generation. The key characteristics of the system to be considered are as follows:

4.1.1 **Urban Distribution Network**

The study will model a radial-loop configuration of distribution network, under urban area of Nuwakot Distribution Center, Nuwakot District, Nepal. The network consists of the typical distribution components such as buses, feeders, transformers, EV charging station, Solar PV generators and substations. Various network topologies

will be simulated, and the effects of different radial-loop configurations along with effect of EV loads and solar generators on line losses, voltage stability, and overall system performance will be assessed.

4.1.2 Electric Vehicle (EV) Loads

EV charging stations will be incorporated into the network as time-varying loads. The load profiles of different EV charging stations is collected from the data provided by Advance Metering Infrastructure installed at NEA and a load profile is analyzed accordingly. The EV charging load profiles will be modeled based on typical urban driving and charging behaviors. This includes both residential EVs (charging at home) and public EV charging stations (e.g., fast-charging stations located in key urban areas). The variability in charging demand based on factors such as time of day, seasonality, and location will be considered.

4.1.3 Solar PV System

Solar PV systems will be included as distributed generation sources within the distribution network. These systems will be modeled at various locations within the urban network, considering factors like geographical position, installation capacity, and local solar radiation. The intermittent nature of solar power generation will be taken into account, and its impact on the power flow and voltage stability will be analyzed.

4.2 System Data Collection

4.2.1 Branch and Bus Data at NDC

The system under consideration consists of three radial feeder of NEA, NDC supplying at urban area of Bidur Municipality Ward No. 1, 2, 4, 5, and 6. The overall distribution center is modeled as 51 bus system with branch connecting them. All of this system data is collected from database of NEA, NDC.

i. Bus Data

The bus data primarily consists of three types of buses. One of these is the generator bus, which represents the power generation sources in the system. Two hydropower stations, the Trishuli Hydropower Station (HPS) and the Devighat Hydropower Station, are available at the NEA NDC and are included as generator buses in the system. The generating bus connecting Trishuli HPS is named as bus-1 while the generating bus connecting Devighat HPS is named as bus-46. Here, the bus

connecting largest capacity generator is of Trishuli HPS and therefore the bus-1 is also taken as slack bus or reference bus. For the purpose of this study, a bus located near a region with the potential for solar PV generation installation is also considered as a generation bus. The solar PV generation is included hypothetically to the buses 14, 20, and 29 for the study of its behavior using proposed methodology. Remaining 46 number of buses are taken as load bus which includes six number of buses connected to EV charging station namely Bus-8, 12, 13, 14, 15, and 18. The detail of bus system and its type is as represented in the Table 4-1.

Table 4-1 Detail of Bus Data Information for System under Study

Bus ID	Bus Type	Source	Bus Number
3	Swing Bus	HEP	1
2	PV Bus	HEP	46
		Solar PV	14, 20, 29
1	Load Bus	NEA TRF	0, 2, 3, 4, 5, 6, 7, 9, 10, 11, 16, 17, 19, 21, 22, 23, 24, 25, 26, 28, 30, 31, 32, 33, 34, 35, 36, 37, 38, 39, 40, 41, 42, 43, 44, 45, 47, 48, 49, 50, 51
		EV Charging	8, 12, 13, 15, 18, 27

Here, the solar PV generation and EV Charging loads vary with respect to time and are of an intermittent nature. The bus data for those buses can be obtained from hourly PV generation patterns and EV charging load patterns. However, the hourly load supplied through individual transformers of NEA, and NDC cannot be determined exactly. The load consumed by existing consumers of NEA, NDC from various categories is treated as the NEA transformer load. Around sixty-five 11/0.4 kV distribution transformers are used to supply different consumer classes of NEA, NDC. The behavior of the NEA TRF load is analyzed using the overall system load curve of NEA, NDC. The hourly system load patterns of various substations at NEA, NDC can be determined from the historical hourly energy consumption data and the system peak demand data. By using the historical energy consumption pattern of all of the substations present at NEA, NDC, a generalized system load factor for each hour is evaluated.

By using the generalized system consumption behavior of system demand as represented in the Figure 4-4, the hourly demand injected at the load bus connecting distribution transformer of NEA, NDC are determined and used for the load flow studies. The hourly demand at each individual system load bus is evaluated to

replicate the system load curve, using measured data from different sub-stations of NEA, NDC. The details of the hourly per unit bus data calculated in 1000 kVA base power as represented in ANNEX A.

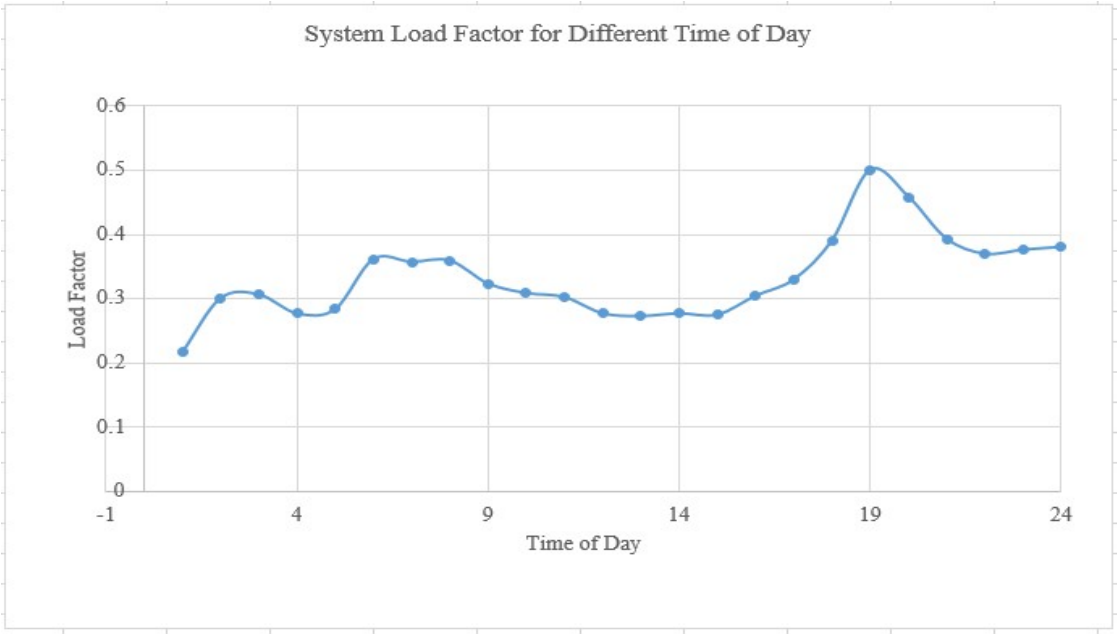

Figure 4-4: Overall System Load Factor behavior for Different Time of Day at NEA, NDC

ii. Branch Data

The system under consideration for the study at NDC consists of three different radial feeder having various conductor types, such as ACSR Weasel, ACSR Rabbit, and 100 and 50 Sq. mm XLPE Conductors, the distribution line parameters specifically resistance, reactance, and charging susceptance vary accordingly. The specific conductor type used in each branch of the distribution network has been obtained from the records of the NEA Nuwakot Distribution Center. The standard per-unit values for these conductor parameters have been sourced from various standards and are then multiplied by the length of each branch to determine the actual line parameters for each specific branch of the distribution network. There are six number of tie switches as represented in Table 4-2, which may change the feeder configuration as per the requirement of load flow of NEA, NDC.

ANNEX B: System Branch Data represents the details of the branch data for the system under consideration. The bus connecting the branch, length of branch and the type of conductor used in that particular branch is determined. With the base voltage

of 11 kV, and base power of 1000 kVA the base impedance is found to be 121 Ohms. Using the branch data and base impedance value, the per unit resistance, reactance and charging susceptance value is evaluated. Since the branch data is dependent with the tie switch combinations and it is also further dependent of feeder configurations, there are various branch data set for various tie switch combinations. The tie switch combination is arranged such that the islanded mode of operation is avoided. Even if there are six different tie switch available for larger number of feeder configuration options, only eight number of tie switch configuration are available for the load flow to avoid islanding of particular load centers. Thus there are eight set of branch data used for the load flow study. In these switch combinations; logic "0" represents the off/open condition of a tie switch, while logic "1" represents the on/closed condition. The first digit in the logic represents tie switch TS1, and it continues up to the 6th digit for tie switch TS6.The sample branch data for various tie switch combinations are represented in ANNEX B: System Branch Data.

Table 4-2 Tie Switch and Respective Bus for Testing System

S.N.	Tie Switch	Connecting Bus
1	TS1	15-47
2	TS2	44-45
3	TS3	40-41
4	TS4	10-12
5	TS5	18-42
6	TS6	42-19

4.2.2 Solar PV Generation Data

The solar PV system is also considered for the study of the effect of intermittent solar power generation on radial-loop feeder configuration. Since NEA is currently facilitating small rooftop solar generators to share the power with grid by introducing new legislative framework regarding the net metering infrastructure. Bidur Municipality under the working zone of NEA, NDC has high solar generation potential, as it falls within a region with strong solar radiation. Notably, the largest solar project in Nepal, a 25 MW peak capacity plant, is located within Bidur Municipality. This makes the area highly suitable for connecting rooftop PV installations and small solar PV farms to the low-voltage distribution system.

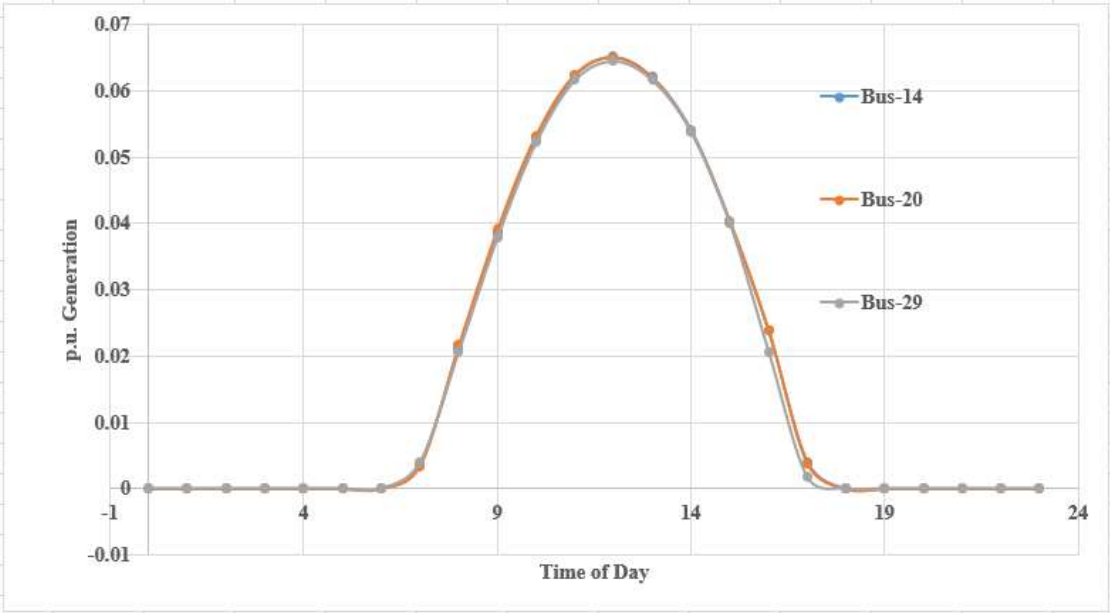

Figure 4-5: Sample PV Generation Plot for Different Time of Day at NEA, NDC

As mentioned earlier NEA is in the process of developing policies for the implementation of net metering systems, which further enhances the feasibility of integrating solar generation. Considering these facts, three number of solar PV generating station are hypothetically added as generator bus in the testing system under consideration. The location of solar PV generation is selected so as there are existing solar PV farm and has high potential of construction of small solar PV farm in near future. This study consists of three solar PV generation capable of generating 100 kWp solar energy. The hourly generation potential of the solar PV generation as represented in the Figure 4-5 is determined by using the Global Solar Atlas [31], which is an online platform that provides high-quality solar resource data and maps for countries worldwide. It is managed by the International Renewable Energy Agency (IRENA) and serves as a tool to facilitate the development of solar energy projects by providing essential data on solar power potential. Using geographical location coordinate as represented in the Table 4-3 in the [31], the hourly generation injected via solar PV generation bus can be estimated.

Variations in the solar PV generation affects the power injection to its nearer with respect to time. The details of hourly per unit power injected to solar PV connected bus calculated using [31] is as represented in ANNEX C: Solar PV Data.

Table 4-3 Solar PV Generation Capacity with Locations

S.N.	Bus No.	Generation Capacity, kWp	Latitude	Longitude
1	14	100	27.866722°	85.125952°
2	20	100	27.872964°	85.136628°
3	29	100	27.888647°	85.148597°

4.2.3 EV Load Data

The main urban area and thus the settlement of the majority of the population of Nuwakot District is within Bidur Municipality, which accounts for approximately one-fourth of the total energy consumption in the district. As it is the headquarters of Nuwakot district and lies on the only highway connecting Nepal to China i.e. Kerung-Galchhi Highway, there is an increasing trend of using electrical vehicles at an alarming rate. As Nepal imports most of the electrical vehicles from China via Kerung-Galchhi Highway, there are hundreds of electrical vehicles passing through Bidur municipality. Also, there are a large number of public vehicles in the Nuwakot district running on electricity. Therefore, the number of EV charging stations is increasing day by day. There are currently six operational EV charging stations in this area, with an additional 20 stations under installation. In the near future, the EV charging load will dominate the total system demand of this area as public diesel vehicles are completely being overtaken by electrical vehicles.

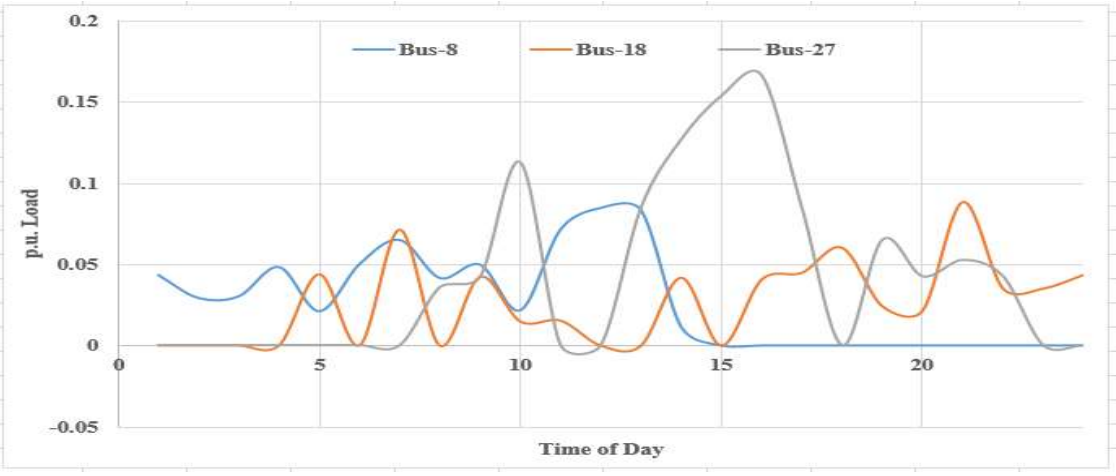

Figure 4-6: Sample EV Demand Plot for Different Time of Day at NEA, NDC

This study considers the effect of charging station loads in load flow and thus radial-loop feeder configuration as percentage share of energy consumed by EV charging stations at NEA, NDC is increasing day-by-day in total energy consumptions of Nuwakot district. The hourly power consumption pattern of the EV charging station as represented in the Figure 4-6 is collected from the smart meter installed in the existing EV charging station and Advance Metering Infrastructure (AMI) installed at NEA, NDC. Table 4-4 represents the details of the existing charging stations installed at the testing system under consideration.

Table 4-4 Existing EV Charging Station with Demand

S.N.	Bus No.	Charger Type	Approved Demand, KVA
1	8	CCS/GBT	180
2	12	CCS/GBT	200
3	13	CCS/GBT	150
4	15	GB/T	200
5	18	CCS/GBT	200
6	27	CCS	200

For the date of 17th February 2025, the hourly demand data for different buses connecting different EV charging loads are represented in the ANNEX D: EV Charging Data. This intermittent EV load consumption pattern is used to analyze the effect of charging loads in radial-loop distribution feeder configuration.

4.2.4 Tie Switch Data

A Numerical Load Break Switch (LBS) is used in the distribution systems under consideration to remotely control the flow of electricity. It is designed to operate under normal load conditions, providing the ability to remotely open or close the line sections of a distribution system as per the requirement of distribution system operator. Six number of such tie switch connections are used in the system under study as represented in the Table 4-2.

4.3 Power Flow Study Results

4.3.1 Simulation model

When various distribution data such as distribution system layout, tie switch details, system bus data, system branch data, solar PV generation data, and EV charging data is collected from NEA, NDC and various sources, load flow study and optimization of tie switch to generate optimal radial-loop feeder configuration is performed in Python

Jupyter Notebook. This simulating model takes input raw data from csv file, performs load flow study using Newton Raphson Method of load flow study, calculates and compares the system loss and minimum bus voltage for every tie switch combinations and results the best tie switch schemes for every hours of day. Also it is capable of maintaining voltage deviation constraints, conductor thermal limit constraints and prevention of loads from islanded operations. The detail of the simulation program is as represented in ANNEX G: Python Code for Simulation.

4.3.2 System Loss and Voltage Deviation

i. Without EV Load and Solar PV Generation

The load flow study of the existing distribution system at NEA NDC without considering the solar PV generation and EV charging load is performed first. The hourly bus data for different time of day is used for load flow analysis while the branch data is taken for the tie switch combination of the logic “000111” as existing system without configuration has tie switch TS1, TS2 and TS3 normally off while TS4, TS5 and TS6 are normally on condition.

Figure 4-7 represents the total distribution system loss at NEA, NDC, without integrating solar PV generation and EV charging load. The system loss varies accordingly to the system load demand. The system load demand is maximum during the morning and evening hours of the day. The system branch loss is also maximum during the time of system peak demand. The maximum hourly system loss for NEA, NDC is about 122.463 kW at 19:00 PM while the morning peak hourly loss is about 104.193 kW at 6:00 AM. The hourly system loss varies from the minimum of 22.202 kW to the maximum of 122.463 kW, resulting a total daily feeder loss of 1432.77 kWh.

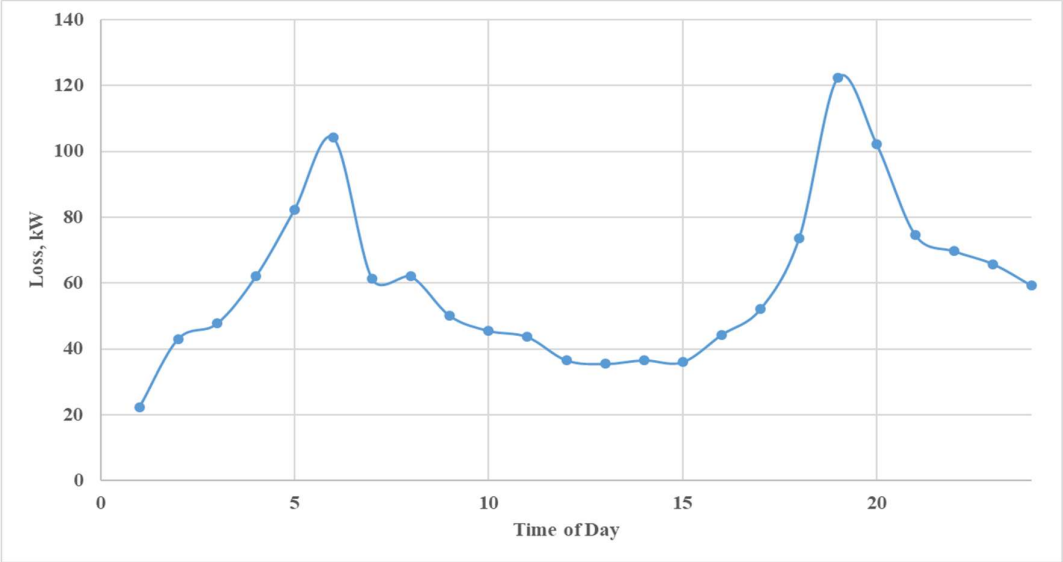

Figure 4-7: System (Feeder) Loss Without PV Generatoin and EV Load Vs. Time of Day at NEA, NDC

Similarly, Figure 4-10 represents the minimum bus voltage and time of day plot for the NEA, NDC without integration of the solar PV and EV charging load in the system. As the branch voltage drop is also dependent of the branch current flowing through the bus, the bus voltage is different for different hourly sytem load demand. For this scenario, the variation of bus voltage is from 10.7986 kV at 1:00 AM to 10.3017 kV at 19:00 PM. The minimum system bus voltage is about 0.936524 i.e. 10.3017 kV at 19:00 PM for that particular day. The detailed hourly system loss and minimum bus voltage without integrating solar PV and EV charging load is as represented in ANNEX E: Load Flow Results.

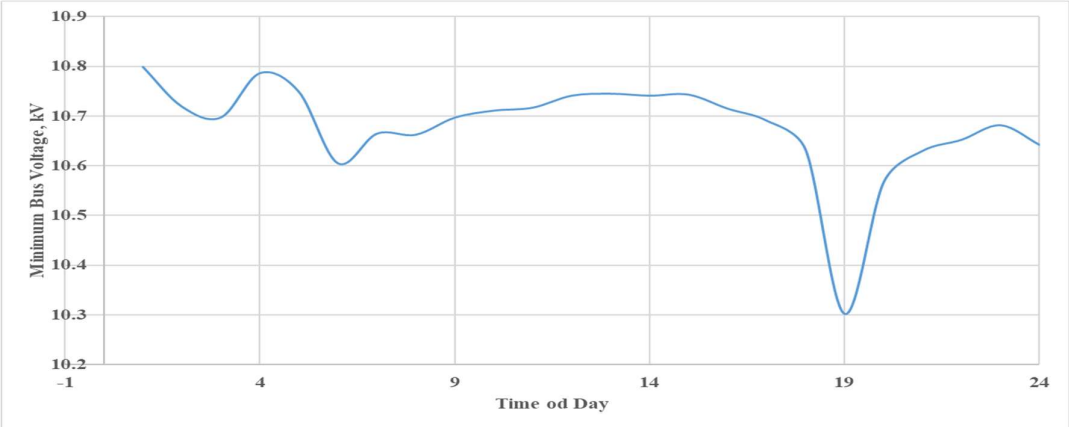

Figure 4-8: Minimum Bus Voltage Without PV Generatoin and EV Load Vs. Time of Day at NEA, NDC

ii. With EV Load and Solar PV Generation

With the above-mentioned input bus data, branch data, solar PV data and EV load data, a load flow study for the distribution system at NEA, NDC is performed using Newton Raphson Method. For Eight different combination of tie switches there are eight different set of branch data and also there is different 24 set of bus data for every hour as NEA TRF load, solar PV generation and EV station load varies with time. The major objective of this study is to minimize the system power loss and voltage drop maintaining the constraints like power balance, voltage variation limits and branch current thermal limit. Figure 4-9 represents the load flow results of test system under consideration before the feeder reconfiguration. Before reconfiguration, the feeder is operated radially using jumper connection and disconnection between two radial feeders when there is requirement of changing sources. It is noted that there are different hourly loss values for different time of day before feeder is reconfigured. The detailed hourly system loss before feeder reconfiguration is as represented in ANNEX E: Load Flow Results. Here, the cumulative system (Feeder) loss for the period of 24 hours seems to be of 19530.96 kWh.

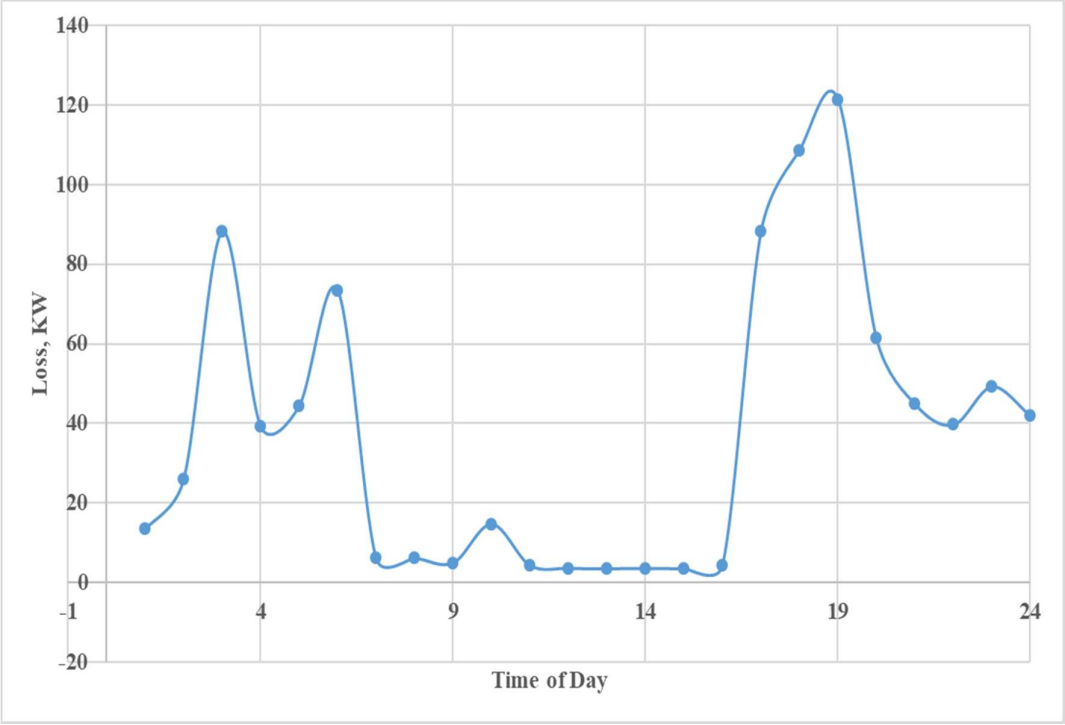

Figure 4-9: System (feeder) Loss before Reconfiguration vs. Time of Day at NEA, NDC

Similarly Figure 4-10 represents the minimum system bus voltage before the feeder reconfiguration. As substation operators at NEA, NDC maynot continuously monitor the voltage at load end, there may be voltage deviation beyond the limit set by Electricity Regulation 2050. The minimal bus voltage obtained is about 10.44 kV during evening peak hour which violates the tolerance limit of 5% for 11 kV distribution system voltage.

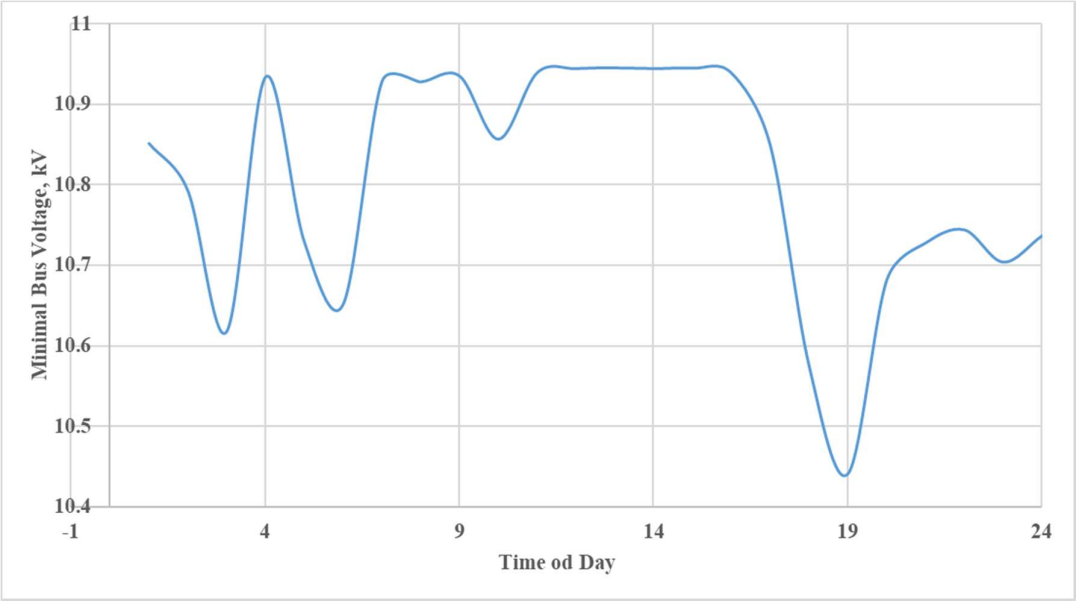

Figure 4-10: Minimum Bus Voltage before Reconfiguration Vs. Time of Day at NEA, NDC

Table 4-5 Comparison of Total System Loss and Minimum Bus Voltage Before and After Feeder Reconfiguration

S.N.	Particular	Daily Feeder Loss, kWh	Minimum Bus Voltage, KV
1	Before Feeder Configuration	19530.96	10.440925
2	After Feeder Configuration	9485.76	10.796984
Difference		10045.2	-0.356059

The total system (feeder) power loss and minimum voltage deviations for test system after reconfiguration is as represented in the Figure 4-11 and Figure 4-12 respectively. The total feeder loss for the same day after feeder reconfiguration is found to be 395.23 kWh which is about two times less than the total system loss before reconfiguration. Similarly, minimal bus voltage among all 51 buses is found to be of

10.796984 kV which is within the specified tolerance limit of 5% for 11 kV redial distribution system.

Here's a paragraph explaining the table below provided:

The Table 4-6 presents a comparison of daily total energy losses and their corresponding cost before and after implementing feeder reconfiguration in a distribution network. Initially, before reconfiguration, the total energy loss amounted to 19,531.2 kWh, which translated into a financial loss of NPR 166,015.2. After the feeder reconfiguration was carried out, the total energy loss dropped significantly to 9,484.8 kWh, resulting in a reduced energy loss cost to NPR 80,620.8. This reflects a substantial improvement, with a total reduction of 10,046.4 kWh in energy loss and a daily cost saving of NPR 85,394.4. The data clearly indicates that feeder reconfiguration is an effective strategy for minimizing energy losses and reducing operational costs in power distribution systems.

Table 4-6 Comparison of Total Daily Energy Loss and Cost of Energy before and After Feeder Reconfiguration

S.N.	**Particular**	**Daily Feeder Loss, kWh**	**Cost of Energy Loss (NPR)**
1	Before Feeder Configuration	19531.2	1,66,015.2
2	After Feeder Configuration	9484.8	80,620.8
Difference		10046.4	-85,394.4(Daily Saving)

The comparison of total system loss and minimum bus voltage before and after the configuration is as represented in Table 4-5, Figure 4-13, and Figure 4-14. The detailed hourly system loss and minimum bus voltage after feeder reconfiguration is as represented in ANNEX E: Load Flow Results.

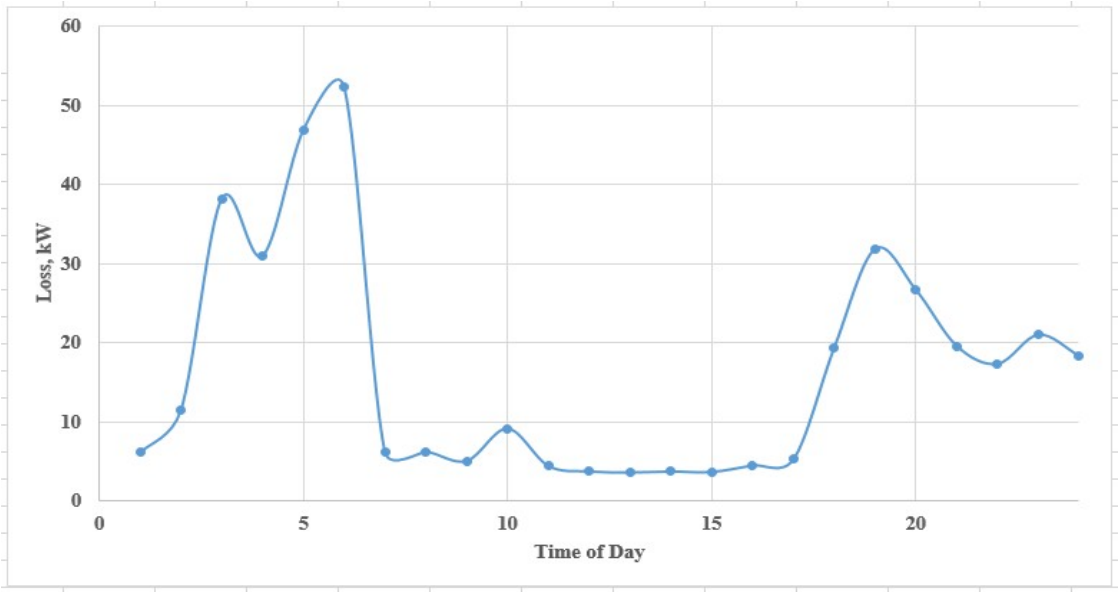

Figure 4-11: System (feeder) Loss after Reconfiguration vs. Time of Day at NEA, NDC

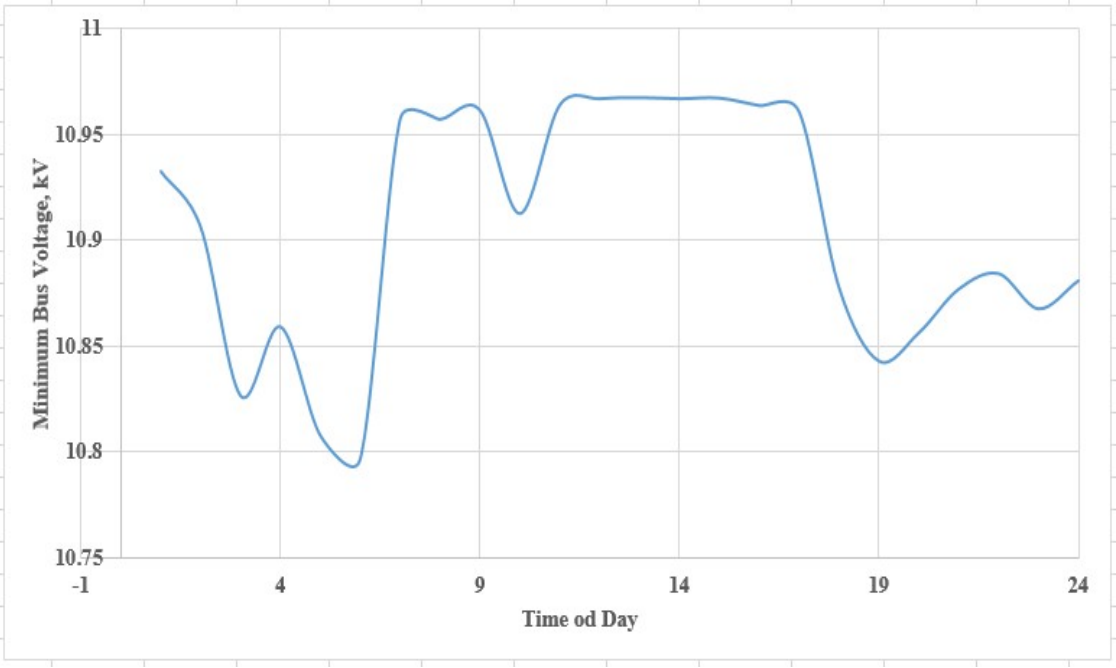

Figure 4-12: Minimum Bus Voltage after Reconfiguration vs. Time of Day at NEA, NDC

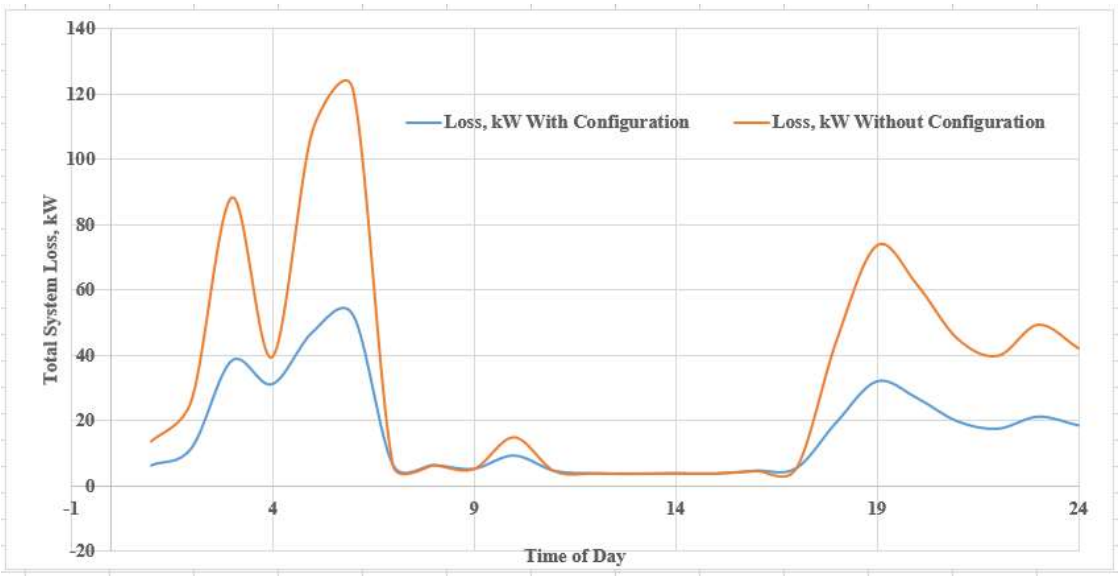

Figure 4-13: System Loss Before and After Reconfiguration vs. TOD at NEA, NDC

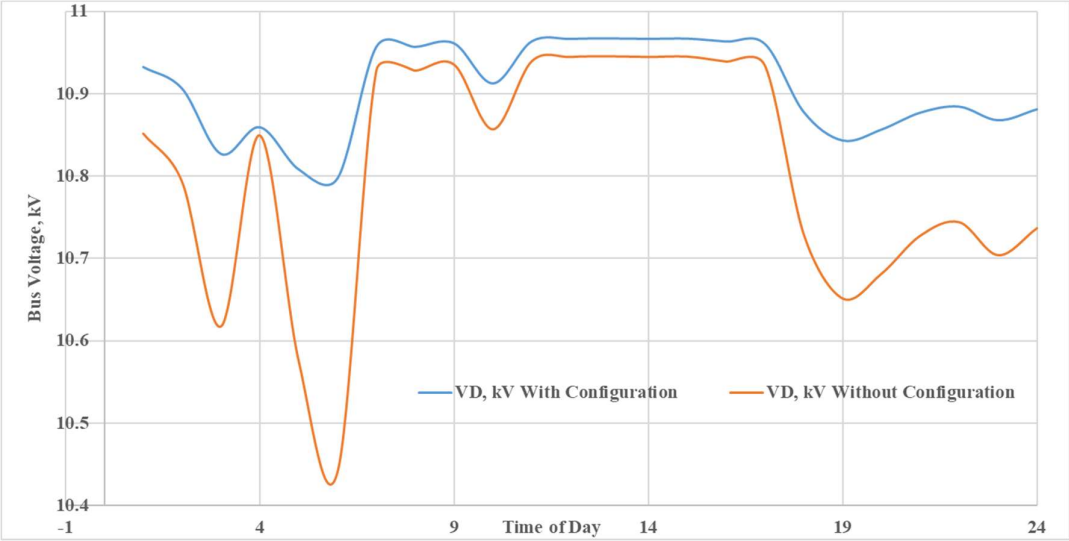

Figure 4-14: Minimal Bus Voltage Before and After Reconfiguration Vs. TOD at NEA, NDC

As discussed earlier, the line data of the distribution system varies as per the operation of tie switches and thus bus admittance matrix, which is used for load flow study in Newton Raphson algorithm, changes accordingly. Therefore, the bus admittance matrix for every possible tie switch combination and thus load flow is calculated to determine the most suitable switch combination having minimal distribution system loss. Table 4-7 represents the power loss outputs for all of the possible tie switch configuration for 1st hour. It is observed that the distribution system loss is changing

from a highest of 13.52 kW to the lowest of 6.088 kW as per the changing switch combinations. A set of distribution loss data is generated for a particular hour of a day with the various switching combinations and compared to get minimal system loss and related switch combination.

After the power flow simulations for given input data, the different tie switch combination provides different sets of total system loss and minimum bus voltage data. Comparing this data and the resulting best tie switch combination which introduces the lowest distribution system loss and maintains required bus voltage limits for different time of day for NEA, NDC ensures the objective of this study. The optimal tie switch combination for different times of day for this testing system under consideration is as represented in the Table 4-7.

Table 4-7 Combination of Tie Switches and Respective System Loss for 1st hour

S.N.	Switch Combination	Total System Loss, p.u.	System Loss, kW/hour
1	000111	0.01352123	13.52122952
2	001110	0.01264402	12.6440204
3	010101	0.00791426	7.914260037
4	011100	0.007352764	7.352764165
5	100011	0.011017852	11.01785202
6	101010	0.010139995	10.13999502
7	110001	0.00639973	6.399730096
8	111000	0.006088079	6.08807873

Table 4-8 below. Among all of the tie switch combinations for each hours of a day, these tie switch combinations give the minimum distribution system loss and bus voltage deviation for a particular day. These tie switch combinations are controlled to avoid islanding operations of load buses. For each combination of tie switches, hourly load flow analysis is performed to minimize the total branch losses and bus voltage deviations. For illustration, in these switch combinations, logic "0" represents the off/open condition of a tie switch, while logic "1" represents the on/closed condition. The first digit in the logic represents tie switch TS1, and it continues up to the 6th digit for tie switch TS6. In one case, for the 6th hour of the day, it is observed that the tie switch combination is 111000 (i.e., TS1, TS2, and TS3 are closed, while TS4, TS5, and TS6 are open). The respective values of total distribution system loss and

minimum bus voltage deviation for these tie switch combinations are represented in ANNEX E: Load Flow Results.

From the optimal Tie switch control output data as represented in Table 4-8, a generalized switching behavior for radial-loop configuration can be extracted. Here, the switching combination for the first six hours of that particular day is “111000” i.e., TS1, TS2, and TS3 are closed while the remaining tie switches are opened or isolated. During this time loads are supplied by the nearer generating sources. In the seventh hour, there is some generation from three solar PV plants as there is increased solar radiation in PV cells. Now the combination of tie switches changes as the power flow is affected by the solar PV generation. At this point, there is the least distribution loss when the tie switch combination is “001110” i.e., TS1, TS2, and TS6 are opened, and the remaining are closed. The effect of EV charging load can also be observed during the 10th hour of the day. When the EV charging load increases significantly, the load flow in the system also changes and hence the tie switch combination.

Table 4-8 Optimal Hourly Control Scheme for Tie Switches for Feeder Reconfiguration at NEA, NDC.

Time of Day	Switch Combination	Time of Day	Switch Combination
1	111000	13	001110
2	111000	14	001110
3	111000	15	001110
4	111000	16	001110
5	111000	17	001110
6	111000	18	111000
7	001110	19	111000
8	001110	20	111000
9	001110	21	111000
10	011100	22	111000
11	001110	23	111000
12	001110	24	111000

iii. With Increased Solar PV Generation (500 kWP)

The impact of solar PV generation for different plant capacity is analyzed. Previously three solar plant with 100 kW peak capacity is considered for the study. Now the impact of higher capacity solar plant is studied with consideration of 500 kW and 1000 kW peak capacity is studied.

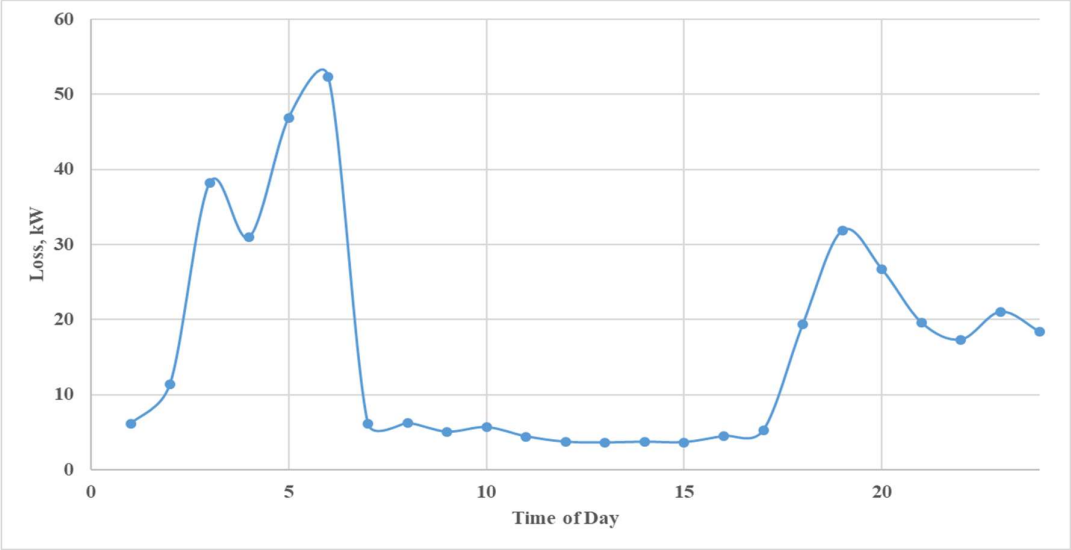

Figure 4-15: System Loss Vs. TOD for three 500 kWp Solar PV Generation

The distribution system loss for the increased capacity of solar PV generation from 100 kW peak to 500 kW peak is analysed and represented in the Figure 4-15. The daily system loss is found to be 391.748 kWh. As the capacity of solar generation is increased the additional load can be fed through nearest solar PV generation leading decrement in total system loss.

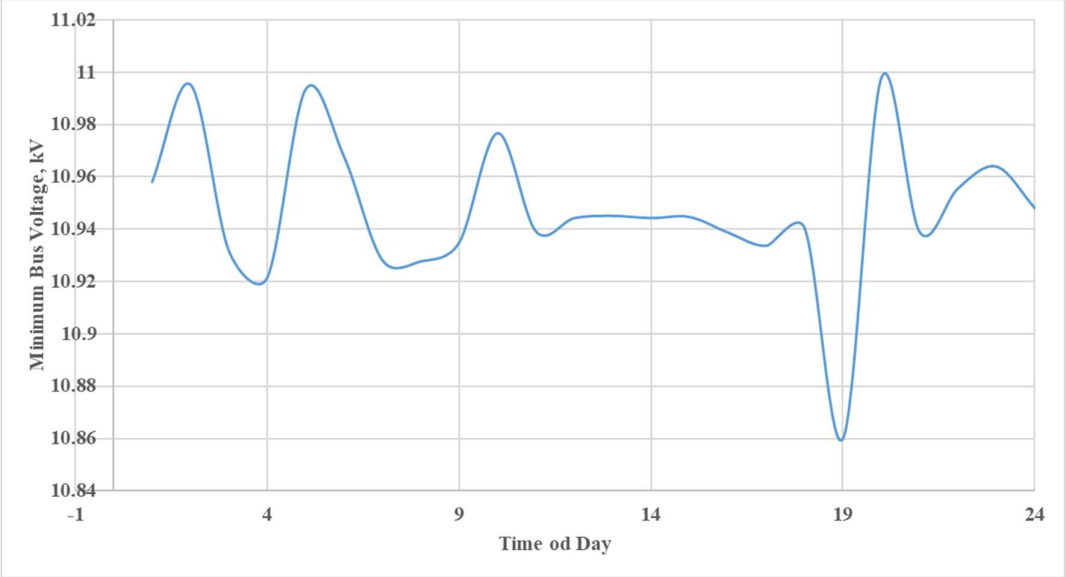

Figure 4-16: Minimum Bus Voltage Vs. TOD for three 500 kWp Solar PV Generation

Figure 4-16 represents the minimum bus voltage plot for different times of day with increased solar PV generation capacity. The minimum bus voltage for this scenario is found to be 0.9872784 p.u. i.e. 10.8600624 kV. As the source to load distance is

changed with increased solar generation, the bus voltage profile is enhanced. The detailed hourly system loss and minimum bus voltage for increased 500 kWp solar PV generation is represented in ANNEX E: Load Flow Results.

iv. With Increased Solar PV Generation (1000 kWP)

The impact of solar PV generation for different plant capacities is analyzed. Previously, three solar plants with 100 kW and 500 kW peak capacity is considered for the study. Now the impact of higher capacity solar plant is studied with consideration of 1000 kW peak capacity is studied.

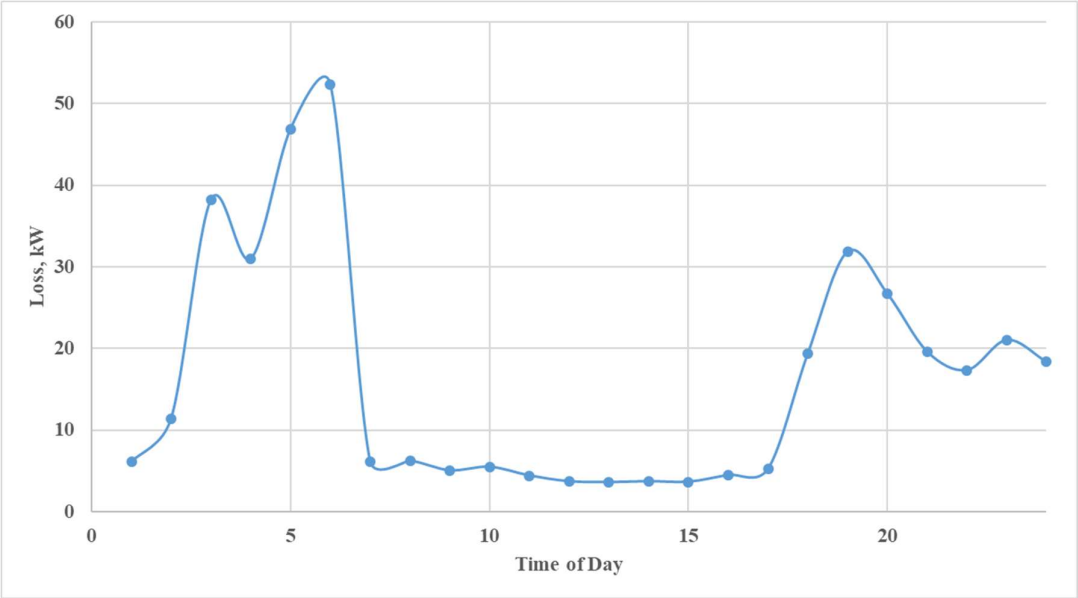

Figure 4-17: System Loss Vs. TOD for three 1000 kWp Solar PV Generation

The distribution system loss for the increased capacity of solar PV generation from 100 kW peak to 500 kW peak is analysed and represented in the Figure 4-17. The maximum daily system loss is found to be 391.575 kWh. As the capacity of solar generation is increased the additional load can be fed through nearest solar PV generation leading decrement in total system loss.

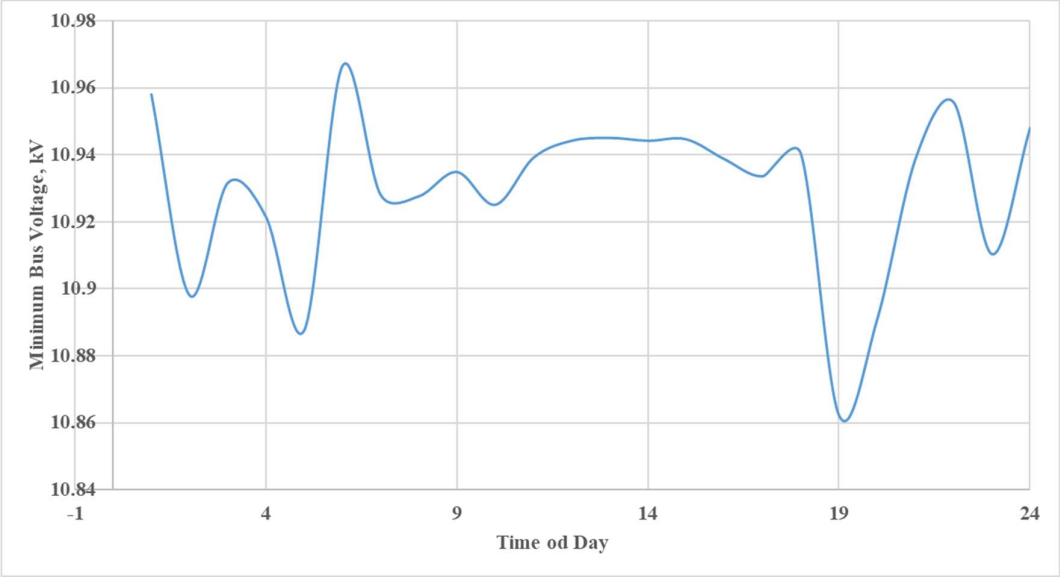

Figure 4-18: Minimum Bus Voltage Vs. TOD for three 1000 kWp Solar PV Generation

Figure 4-18 represents the minimum bus voltage plot for different times of day with increased solar PV generation capacity. The minimum bus voltage for this scenario is found to be 0.98747954 p.u. i.e. 10.86227494 kV. As the source to load distance is changed with increased solar generation, the bus voltage profile is enhanced. The detailed hourly system loss and minimum bus voltage for increased 1000 kWp solar PV generation is represented in ANNEX E: Load Flow Results.

v. With Increased Penetration of EV Charging Loads

In this section of study, the effect of increased penetration of EV charging loads is studied. As the number of EV charging stations at NEA, NDC is being increased rapidly, it is necessary to study the effect of charging loads when their contribution dominates the total system demand. For the study purpose, the upcoming EV charging stations which are under the process of construction is considered and their load demand pattern is taken from the similar charging station pattern which has alread been installed. In addition to buses 8, 12, 13, 15, 18, 27 connecting EV charging station, 14 more charging station at buses 5, 10, 16, 21, 24, 28, 30, 31, 34, 36, 42, 44, 47, 51 is considered as the laod bus with EV charging station. Figure 4-19 represents the hourly demand of the EV charging stations under consideration. The laod consumption pattern of EV charging station is so random as most of the charging station is operated by private sector. They are owened by different transportation

committee which have various number of vehicles. Also this charging stations are on very early satge of operation leading such random charging patterns. The detailed consumption pattern is as represented in the ANNEX D: EV Charging Data.

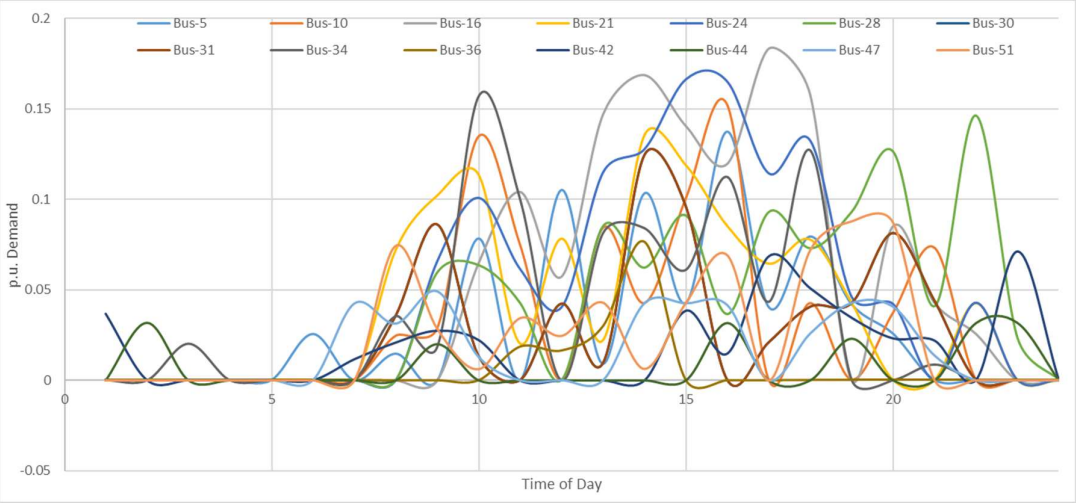

Figure 4-19: EV Demand Vs. TOD for increased EV Pentration

With this increased penetration of charging stations, power flow study is performed. As the consumption pattern is very random in nature, the tie switch combination varies frequently in the different hours of day. The total system loss for the increased number of 20 EV station is as represented in the Figure 4-20. The loss of the system varies hourly from the minimal of 3.59 kW to the maximum of 101.409 kW leading total daily power loss of 582.28 kWh.

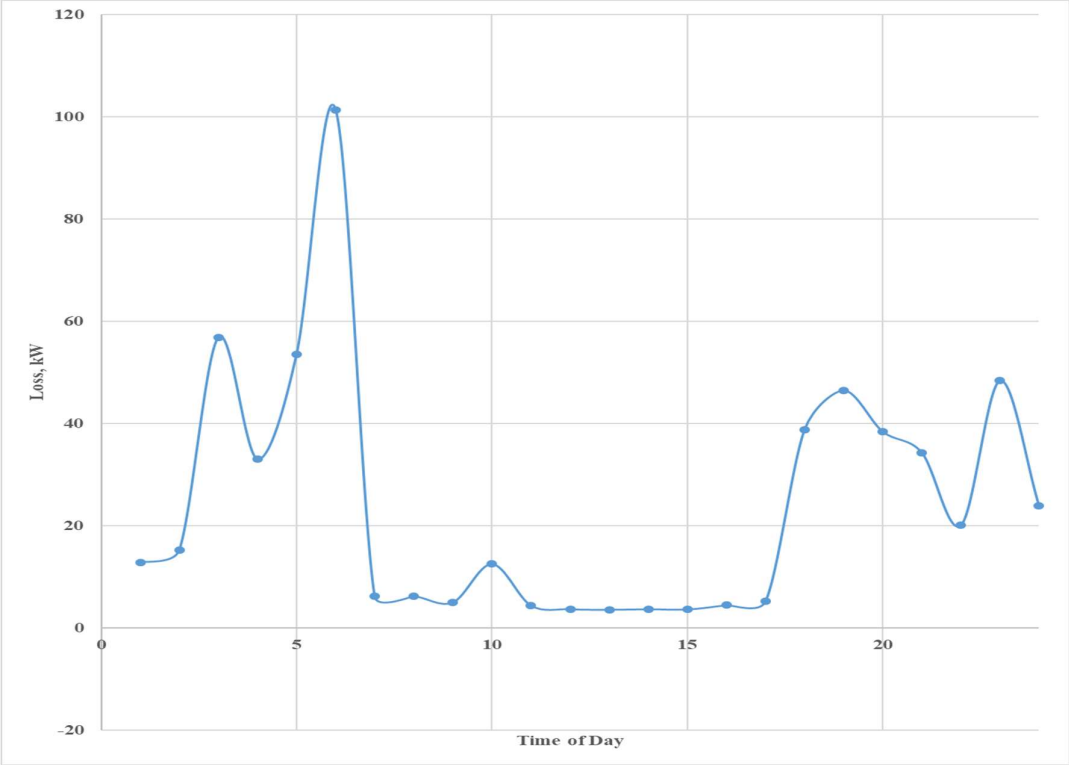

Figure 4-20: System (Feeder) Total Loss Vs. TOD for increased EV Pentration

As the increment of EV charging load effects the system power flow, the minimal bus voltages for this scenario is as represented in the Figure 4-21. The bus voltage deviates deeply as the same time when there is higher system loss. The minimal bus voltage varies hourly from the minimal of 0.961516911 p.u. i.e. 10.57668602 kV to the 0.996893586 p.u. i.e. 10.96582945.

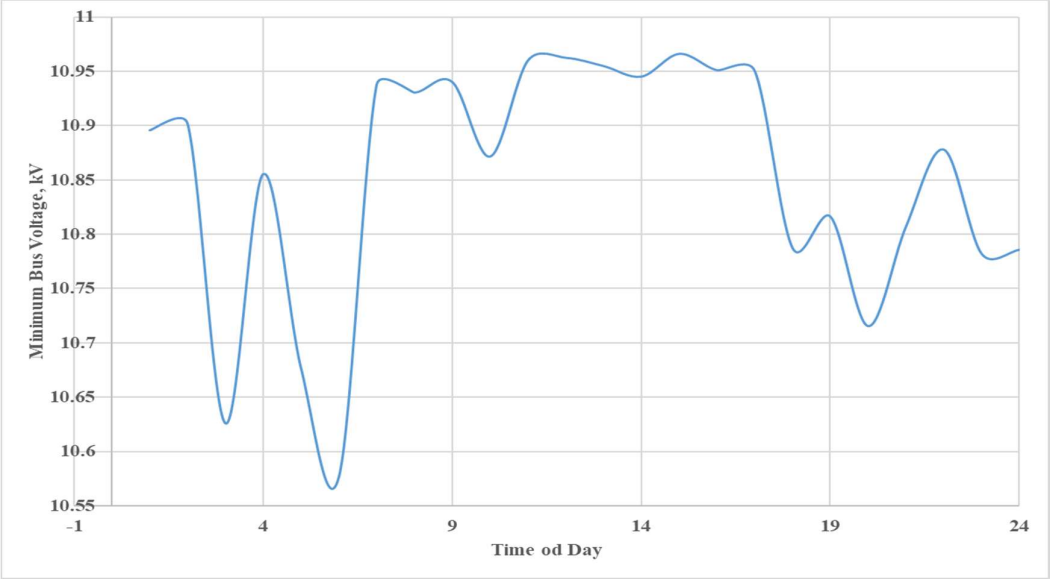

Figure 4-21: Minimal Bus Voltage Vs. TOD for increased EV penetration

The detailed hourly system loss and minimum bus voltage for an increased 20 number of EV charging load is represented in ANNEX E: Load Flow Results.

4.3.3 **Branch Current Constraints Verification**

When there is the change in feeder configuration using the various tie switch combinations, the current thermal limits of each branch conductor should be maintained. To maintain the safe distribution system operation and prevent damage of the branch conductor due to overheating, this study sets a constraint of the maximum allowable thermal limit of the branch conductor. As per IS 398 (Part 1): 2017 – Specification for ACSR Conductors and related practical analysis, the parameter along with the current carrying capacity of various conductors considered under this study is as represented in Table 4-9.

Table 4-9 Thermal Rating and Line Parameter for Conductor Used at NEA, NDC

S.N.	Conductor	Resistance, Ohm/km	Reactance, Ohm/km	Susceptance, Ohm/km	Thermal Rating at 65^{o}C, Amps
1	100 mm2 XLPE	0.194	0.11	0.00003	291
2	Rabbit ACSR	0.554	0.365	0.00000434	190
3	Weasel ACSR	0.724	0.38	0.00000375	138

For each hour of the day and the respective switching combination obtained from the above-mentioned methodology, the current flowing through the individual branch of the distribution system under consideration is calculated and compared with its allowable maximum thermal limit. The details of the branch current for the proposed feeder configuration using optimized tie switch control as mentioned in Table 4-8 are as represented in the ANNEX F: Branch Current Results.

CHAPTER: 5 CONCLUSION

In conclusion, this research provides valuable insights into optimizing the urban distribution network of Nuwakot, Nepal, through the integration of Electric Vehicle (EV) charging loads and Solar Photovoltaic (PV) systems. By focusing on a radial-loop configuration, specifically the Nuwakot Distribution Center (NDC), the study assessed the impact of these integrations on the system's performance, considering factors such as line losses, voltage stability, and overall efficiency.

The methodology involved simulating various network topologies, factoring in the time-varying nature of EV loads and the intermittent behavior of solar PV generation. It was found that incorporating EV charging stations, which are growing rapidly in Nuwakot, and leveraging the high solar potential of the region (particularly in Bidur Municipality), significantly influenced the system's performance. The load flow study, conducted using the Newton-Raphson method, revealed the following:

Reduction in System Losses: After reconfiguring the feeder network with optimal tie switch combinations, daily system (Feeder) losses were reduced by approximately 50%, from 813.79 kWh to 395.23 kWh. This reduction was achieved by dynamically adjusting the feeder configuration throughout the day, optimizing the distribution of power across the network. These findings highlight the potential for improving the efficiency of existing networks by integrating renewable energy sources and flexible charging infrastructure.

Voltage Stability: The reconfiguration also led to a notable improvement in the voltage stability of the system. Prior to reconfiguration, the minimum bus voltage during peak hours fell below the allowable limit of 5% deviation, reaching 10.44 kV, which violated the regulatory limits for an 11 kV system. After the optimal reconfiguration, the minimum bus voltage improved to 10.80 kV, staying within the acceptable range, thus ensuring a more reliable power supply for consumers.

Tie Switch Optimization: The research utilized eight distinct tie switch configurations, and through optimization, determined the best combination for each hour of the day to minimize system loss and maintain voltage within safe limits. This dynamic switching approach ensures that the system is constantly adjusted to the most efficient configuration, thereby reducing operational inefficiencies.

Thermal Rating and Safety: The study also verified that the branch currents remained within the thermal limits of the conductors, ensuring that no damage would occur to the network infrastructure. By considering the thermal ratings of the ACSR and XLPE conductors used in the system, the research ensured that the proposed feeder configurations would not lead to overheating, thus maintaining the safety and longevity of the system.

Financial Benefit: Financial analysis highlights the effectiveness of feeder reconfiguration by comparing daily total energy losses and their associated costs before and after implementation. For a particular day under consideration, prior to reconfiguration, the system (feeder) experienced an energy loss of 19,531.2 kWh per day, incurring a cost of NPR 166,015.2. Post-reconfiguration, these losses were significantly reduced to 9,484.8 kWh, with the corresponding cost dropping to NPR 80,620.8. This improvement signifies a total daily energy loss reduction of 10,046.4 kWh and a daily cost saving of NPR 85,394.4. These results confirm that feeder reconfiguration is a highly effective method for enhancing energy efficiency and lowering operational expenses in distribution networks.

Overall, this study demonstrated that optimal feeder reconfiguration and the integration of EV charging stations and solar PV systems can significantly enhance the performance of urban distribution networks. The findings are particularly relevant to regions like Nuwakot, where the demand for electricity is increasing rapidly due to urbanization, the rise in electric vehicle use, and the potential for solar energy generation. This research serves as a foundation for further development of policies and strategies for modernizing the power grid in Nepal, ensuring that it can accommodate future growth in both demand and renewable energy integration.

REFERENCES

[1] S. Chakraborty and S. Sen, "Optimal configuration of radial and looped distribution networks considering power quality indices," *Journal of Electrical Engineering & Technology,* vol. 15, no. 2, pp. 078-1086, 2020.

[2] X. Huang, X. Zhang and Y. Wu, "Electric vehicle charging optimization in smart grids: A review of methodologies and applications," *IEEE Transactions on Smart Grid,* vol. 10, no. 3, pp. 3470-3481, 2019.

[3] B. Zhao, Z. Li and X. Zhang, "Voltage fluctuation and line loss reduction in distribution systems with renewable energy integration," *Renewable and Sustainable Energy Reviews,* vol. 121, 2020.

[4] S. Shrestha, B. Koirala and T. Sharma, "Solar energy potential and its integration into Nepal's energy grid," *Energy Policy Journal,* pp. 89-102, 2020.

[5] S. Karki, S. Shrestha and B. Upreti, "Challenges and opportunities in integrating solar energy and electric vehicles into Nepal's power grid," *Nepal Journal of Science and Technology,* pp. 25-38, 2021.

[6] A. Sapkota , K. Bhattarai and R. Sharma, " Optimization of distribution network configuration for sustainable energy integration: A case study of Nepal," *Renewable Energy Review,* pp. 112-125, 2022.

[7] R. Akbar, M. F. Hossain and S. Chowdhury, "Analysis of radial and looped distribution network configurations for optimal energy delivery," *IEEE Transactions on Power Systems,* vol. 33, no. 1, pp. 394-403, 2018.

[8] S. Kumar and R. Saini, "A review of the optimal configuration of distribution systems: Radial and looped networks," *International Journal of Electrical Power & Energy Systems,* vol. 106, pp. 435-442, 2019.

[9] A. Gupta, S. R. Pandit and A. Patel, "Optimization of hybrid radial-loop distribution network in the presence of renewable energy resources," *Energy Reports,* vol. 6, pp. 681-690, 2020.

[10] M. Hossain, L. Wang and S. Khan, "Solar power integration in distribution networks: Challenges and opportunities," *International Journal of Electrical Power & Energy Systems,* vol. 119, 2020.

[11] R. Romero, J. Martinez and S. Gracia, "Feeder reconfiguration techniques in radial distribution networks to reduce line losses," *Electric Power Systems Research,* pp. 246-253, 2017.

[12] A. Singh, "Optimal feeder reconfiguration using Particle Swarm Optimization," *International Journal of Electrical Power & Energy Systems,* vol. 57, pp. 213-221, 2014.

[13] S. Ghosh, "Optimal placement of distributed generation in a distribution system using Particle Swarm Optimization," *International Journal of Electrical Power & Energy Systems,* vol. 65, pp. 338-348, 2015.

[14] H. Khatib, "PSO-based optimal feeder reconfiguration considering EV charging load," *Energy Conversion and Management,* vol. 204, 2020.

[15] M. Rohit, "Optimization of EV charging stations in distribution networks using PSO," *International Journal of Electrical Power & Energy Systems,* vol. 124, 2021.

[16] W. Zhao, "Optimal feeder reconfiguration in distribution systems with EV load and solar PV using PSO," *Renewable and Sustainable Energy Reviews,* vol. 129, 2020.

[17] Z. Li, "Optimal feeder configuration with EV load and solar PV generation using Particle Swarm Optimization," *Renewable Energy,* vol. 165, pp. 749-758, 2021.

[18] W. Zhang, Z. Liu and L. Li, "Optimization of distribution feeders with solar and EV load integration," *Renewable Energy,* pp. 925-935, 2019.

[19] A. Gupta, P. Sharma and A. Singh, "Hybrid optimization techniques for distribution system feeders with electric vehicles and distributed energy resources," *Journal of Electrical Engineering and Technology,* pp. 217-225, 2021.

[20] S. Singh, "Real power loss minimisation of smart grid with electric vehicles using distribution feeder reconfiguration," *IET Generation, Transmission & Distribution,* vol. 13, no. 22, p. 5032–5041, 2019.

[21] J. Guzman-Henao, L. F. Grisales-Noreña, B. J. Restrepo-Cuestas and O. D. Montoya, "Optimal Integration of Photovoltaic Systems in Distribution Networks from a Technical, Financial, and Environmental Perspective," *Energies,* vol. 16, no. 1, p. 562, 2023.

[22] M. N. Azghandi, A. A. Shojaei, S. Toosi and H. Lotfi, "Optimal reconfiguration of distribution network feeders considering electrical vehicles and distributed generators," *volutionary Intelligence,* vol. 16, p. 49–66, 2023.

[23] Y. Sowmya, B. Ramesh and M. Mohanty, "Equivalent Network Technique for Feeder Reconfiguration Considering Harmonics Generating From PV Solar Sources in the Distribution System," *Journal of The Institution of Engineers (India): Series B,* vol. 101, p. 229–237, 2020.

[24] S. Khaing, N. Phu and S. Srisuwan, "Optimal Placement and Capacity of BESS and PV in EV Integrated Distribution Systems: The Tenth Feeder of Phitsanulok Substation Case Study," *Engineering Proceedings,* vol. 10, no. 6, p. 212, 2023.

[25] M. . T. Turan and E. Gökalp, "Integration Analysis of Electric Vehicle Charging

Station Equipped with Solar Power Plant to Distribution Network and Protection System Design," *Journal of Electrical Engineering & Technology,* vol. 17, p. 1239–1250, 2022.

[26] P. Faria, J. Spínola and Z. Vale, "Aggregation and Remuneration of Electricity Consumers and Prosumers for the Definition of Demand Response Programs," *Energies,* vol. 12, no. 15, p. 2928, 2019.

[27] K. Knezovic and P. . B. Andersen, "Innovative business models for aggregation of EV value," in *015 IEEE Power & Energy Society General Meeting*, Denver, CO, USA, 2015.

[28] B. Koirala, S. Shrestha and R. Sharma, "Impact of solar PV integration on Nepal's urban distribution networks," *International Journal of Electrical Power & Energy Systems,* 2020.

[29] A. Kaneko, Y. Hayashi, T. Anegawa, H. Hokazono and Y. Kuwashita, "Evaluation of an Optimal Radial-Loop Configuration for a Distribution Network With PV Systems to Minimize Power Loss," *IEEE Access,* vol. 8, pp. 220408-220421, 2020.

[30] A. Augugliaro, L. Dusonchet, S. Favuzza and E. R. Sanseverino, "Voltage regulation and power losses minimization in automated distribution networks by an evolutionary multiobjective approach," *IEEE Transactions on Power Systems,* pp. 1516-1527, August 2004.

[31] "Global Solar Atlas," [Online]. Available: https://globalsolaratlas.info/map?c=27.887404,85.142134,11&s=27.887404,85.142134&m=site.

ANNEX A: SYSTEM BUS DATA

Bus Data for Hour-1 on 17th February 2025					
Bus No	Bus ID	Initial Voltage, p.u.	Initial Angle	Injected P (p.u.)	Injected Q (p.u.)
0	1	1	0	-0.0216	-0.0104796
1	3	1	0	0	0
2	1	1	0	-0.0108	-0.0052398
3	1	1	0	-0.0433	-0.0209592
4	1	1	0	-0.0325	-0.0157194
5	1	1	0	-0.0649	-0.0314388
6	1	1	0	-0.0433	-0.0209592
7	1	1	0	-0.0649	-0.0314388
8	1	1	0	-0.0433	-0.0209592
9	1	1	0	-0.0649	-0.0314388
10	1	1	0	-0.0108	-0.0052398
11	1	1	0	-0.0541	-0.026199
12	1	1	0	-0.0974	-0.0471582
13	1	1	0	-0.0433	-0.0209592
14	2	1	0	0	0
15	1	1	0	-0.0649	-0.0314388
16	1	1	0	-0.1623	-0.078597
17	1	1	0	-0.0649	-0.0314388
18	1	1	0	-0.0108	-0.0052398
19	1	1	0	-0.238	-0.1152756
20	2	1	0	0	0
21	1	1	0	-0.0108	-0.0052398
22	1	1	0	-0.0216	-0.0104796
23	1	1	0	-0.0465	-0.0225311
24	1	1	0	-0.0032	-0.0015719
25	1	1	0	-0.0216	-0.0104796
26	1	1	0	-0.0325	-0.0157194
27	1	1	0	-0.0108	-0.0052398
28	1	1	0	-0.0433	-0.0209592
29	2	1	0	0	0
30	1	1	0	-0.0216	-0.0104796
31	1	1	0	-0.0108	-0.0052398
32	1	1	0	-0.027	-0.0130995
33	1	1	0	-0.0108	-0.0052398
34	1	1	0	-0.0216	-0.0104796
35	1	1	0	-0.0433	-0.0209592
36	1	1	0	-0.0108	-0.0052398
37	1	1	0	-0.0433	-0.0209592
38	1	1	0	-0.0108	-0.0052398
39	1	1	0	-0.0433	-0.0209592
40	1	1	0	-0.0141	-0.0068117
41	1	1	0	-0.0216	-0.0104796
42	1	1	0	-0.0249	-0.0120515
43	1	1	0	-0.0433	-0.0209592
44	1	1	0	-0.0216	-0.0104796
45	1	1	0	-0.0108	-0.0052398
46	2	1	0	1.75	0.847525
48	1	1	0	-0.0433	-0.0810297
49	1	1	0	-0.0108	-0.0202574
50	1	1	0	-0.0433	-0.0810297
47	1	1	0	-0.0108	-0.0202574

Bus Data for Hour-4 on 17th February 2025					
Bus No	Bus ID	Initial Voltage, p.u.	Initial Angle	Injected P (p.u.)	Injected Q (p.u.)
0	1	1	0	-0.0482	-0.0361188
1	3	1	0	0	0
2	1	1	0	-0.0241	-0.0180594
3	1	1	0	-0.0963	-0.0722376
4	1	1	0	-0.0722	-0.0541782
5	1	1	0	-0.1445	-0.1083564
6	1	1	0	-0.0963	-0.0722376
7	1	1	0	-0.1445	-0.1083564
8	1	1	0	-0.0963	-0.0722376
9	1	1	0	-0.1445	-0.1083564
10	1	1	0	-0.0241	-0.0180594
11	1	1	0	-0.1204	-0.090297
12	1	1	0	-0.2167	-0.1625347
13	1	1	0	-0.0963	-0.0722376
14	2	1	0	0	0
15	1	1	0	-0.1445	-0.1083564
16	1	1	0	-0.3612	-0.2708911
17	1	1	0	-0.1445	-0.1083564
18	1	1	0	-0.0002	-8.378E-05
19	1	1	0	-0.5297	-0.3973069
20	2	1	0	0	0
21	1	1	0	-0.0241	-0.0180594
22	1	1	0	-0.0482	-0.0361188
23	1	1	0	-0.1035	-0.0776554
24	1	1	0	-0.0072	-0.0054178
25	1	1	0	-0.0482	-0.0361188
26	1	1	0	-0.0722	-0.0541782
27	1	1	0	-0.0241	-0.0180594
28	1	1	0	-0.0963	-0.0722376
29	2	1	0	0	0
30	1	1	0	-0.0482	-0.0361188
31	1	1	0	-0.0241	-0.0180594
32	1	1	0	-0.0602	-0.0451485
33	1	1	0	-0.0241	-0.0180594
34	1	1	0	-0.0482	-0.0361188
35	1	1	0	-0.0963	-0.0722376
36	1	1	0	-0.0241	-0.0180594
37	1	1	0	-0.0963	-0.0722376
38	1	1	0	-0.0241	-0.0180594
39	1	1	0	-0.0963	-0.0722376
40	1	1	0	-0.0313	-0.0234772
41	1	1	0	-0.0482	-0.0361188
42	1	1	0	-0.0554	-0.0415366
43	1	1	0	-0.0963	-0.0722376
44	1	1	0	1.75	0.847525
45	1	1	0	-0.0241	-0.0180594
46	2	1	0	1.44475	0
48	1	1	0	-0.0963	-0.0722376
49	1	1	0	-0.0241	-0.0180594
50	1	1	0	-0.0963	-0.0722376
47	1	1	0	-0.0241	-0.0180594

Bus Data for Hour-8 on 17th February 2025					
Bus No	Bus ID	Initial Voltage, p.u.	Initial Angle	Injected P (p.u.)	Injected Q (p.u.)
0	1	1	0	-0.0359	-0.0173982
1	3	1	0	0	0
2	1	1	0	-0.018	-0.0086991
3	1	1	0	-0.0718	-0.0347963
4	1	1	0	-0.0539	-0.0260973
5	1	1	0	-0.1078	-0.0521945
6	1	1	0	-0.0718	-0.0347963
7	1	1	0	-0.1078	-0.0521945
8	1	1	0	-0.0718	-0.0347963
9	1	1	0	-0.1078	-0.0521945
10	1	1	0	-0.018	-0.0086991
11	1	1	0	-0.0898	-0.0434954
12	1	1	0	-0.1617	-0.0782918
13	1	1	0	-0.0718	-0.0347963
14	2	1	0	0.02116	0.01024585
15	1	1	0	-0.1078	-0.0521945
16	1	1	0	-0.2694	-0.1304863
17	1	1	0	-0.1078	-0.0521945
18	1	1	0	-0.018	-0.0086991
19	1	1	0	-0.3952	-0.1913799
20	2	1	0	0.02161	0.01046379
21	1	1	0	-0.018	-0.0086991
22	1	1	0	-0.0359	-0.0173982
23	1	1	0	-0.0772	-0.0374061
24	1	1	0	-0.0054	-0.0026097
25	1	1	0	-0.0359	-0.0173982
26	1	1	0	-0.0539	-0.0260973
27	1	1	0	-0.018	-0.0086991
28	1	1	0	-0.0718	-0.0347963
29	2	1	0	0.02062	0.0099882
30	1	1	0	-0.0359	-0.0173982
31	1	1	0	-0.018	-0.0086991
32	1	1	0	-0.0449	-0.0217477
33	1	1	0	-0.018	-0.0086991
34	1	1	0	-0.0359	-0.0173982
35	1	1	0	-0.0718	-0.0347963
36	1	1	0	-0.018	-0.0086991
37	1	1	0	-0.0718	-0.0347963
38	1	1	0	-0.018	-0.0086991
39	1	1	0	-0.0718	-0.0347963
40	1	1	0	-0.0234	-0.0113088
41	1	1	0	-0.0359	-0.0173982
42	1	1	0	-0.0413	-0.0200079
43	1	1	0	-0.0718	-0.0347963
44	1	1	0	-0.0359	-0.0173982
45	1	1	0	-0.018	-0.0086991
46	2	1	0	1.75	0.847525
48	1	1	0	-0.0718	-0.0347963
49	1	1	0	-0.018	-0.0086991
50	1	1	0	-0.0718	-0.0347963
47	1	1	0	-0.018	-0.0086991

Bus Data for Hour-12 on 17th February 2025					
Bus No	Bus ID	Initial Voltage, p.u.	Initial Angle	Injected P (p.u.)	Injected Q (p.u.)
0	1	1	0	-0.0277	-0.0134302
1	3	1	0	0	0
2	1	1	0	-0.0139	-0.0067151
3	1	1	0	-0.0555	-0.0268603
4	1	1	0	-0.0416	-0.0201453
5	1	1	0	-0.0832	-0.0402905
6	1	1	0	-0.0555	-0.0268603
7	1	1	0	-0.0832	-0.0402905
8	1	1	0	-0.0555	-0.0268603
9	1	1	0	-0.0832	-0.0402905
10	1	1	0	-0.0139	-0.0067151
11	1	1	0	-0.0693	-0.0335754
12	1	1	0	-0.1248	-0.0604358
13	1	1	0	-0.0555	-0.0268603
14	2	1	0	0.06515	0.03155215
15	1	1	0	-0.0832	-0.0402905
16	1	1	0	-0.208	-0.1007263
17	1	1	0	-0.0832	-0.0402905
18	1	1	0	-0.0139	-0.0067151
19	1	1	0	-0.305	-0.1477318
20	2	1	0	0.065	0.03147998
21	1	1	0	-0.0139	-0.0067151
22	1	1	0	-0.0277	-0.0134302
23	1	1	0	-0.0596	-0.0288749
24	1	1	0	-0.0042	-0.0020145
25	1	1	0	-0.0277	-0.0134302
26	1	1	0	-0.0416	-0.0201453
27	1	1	0	-0.0139	-0.0067151
28	1	1	0	-0.0555	-0.0268603
29	2	1	0	0.06453	0.03125236
30	1	1	0	-0.0277	-0.0134302
31	1	1	0	-0.0139	-0.0067151
32	1	1	0	-0.0347	-0.0167877
33	1	1	0	-0.0139	-0.0067151
34	1	1	0	-0.0277	-0.0134302
35	1	1	0	-0.0555	-0.0268603
36	1	1	0	-0.0139	-0.0067151
37	1	1	0	-0.0555	-0.0268603
38	1	1	0	-0.0139	-0.0067151
39	1	1	0	-0.0555	-0.0268603
40	1	1	0	-0.018	-0.0087296
41	1	1	0	-0.0277	-0.0134302
42	1	1	0	-0.0319	-0.0154447
43	1	1	0	-0.0555	-0.0268603
44	1	1	0	-0.0277	-0.0134302
45	1	1	0	-0.0139	-0.0067151
46	2	1	0	1.75	0.847525
48	1	1	0	-0.0555	-0.0268603
49	1	1	0	-0.0139	-0.0067151
50	1	1	0	-0.0555	-0.0268603
47	1	1	0	-0.0139	-0.0067151

Bus Data for Hour-14 on 17th February 2025					
Bus No	Bus ID	Initial Voltage, p.u.	Initial Angle	Injected P (p.u.)	Injected Q (p.u.)
0	1	1	0	-0.0277	-0.0134302
1	3	1	0	0	0
2	1	1	0	-0.0139	-0.0067151
3	1	1	0	-0.0555	-0.0268603
4	1	1	0	-0.0416	-0.0201453
5	1	1	0	-0.0832	-0.0402905
6	1	1	0	-0.0555	-0.0268603
7	1	1	0	-0.0832	-0.0402905
8	1	1	0	-0.0555	-0.0268603
9	1	1	0	-0.0832	-0.0402905
10	1	1	0	-0.0139	-0.0067151
11	1	1	0	-0.0693	-0.0335754
12	1	1	0	-0.1248	-0.0604358
13	1	1	0	-0.0555	-0.0268603
14	2	1	0	0.05414	0.02621806
15	1	1	0	-0.0832	-0.0402905
16	1	1	0	-0.208	-0.1007263
17	1	1	0	-0.0832	-0.0402905
18	1	1	0	-0.0139	-0.0067151
19	1	1	0	-0.305	-0.1477318
20	2	1	0	0.05381	0.02606164
21	1	1	0	-0.0139	-0.0067151
22	1	1	0	-0.0277	-0.0134302
23	1	1	0	-0.0596	-0.0288749
24	1	1	0	-0.0042	-0.0020145
25	1	1	0	-0.0277	-0.0134302
26	1	1	0	-0.0416	-0.0201453
27	1	1	0	-0.0139	-0.0067151
28	1	1	0	-0.0555	-0.0268603
29	2	1	0	0.05389	0.02610038
30	1	1	0	-0.0277	-0.0134302
31	1	1	0	-0.0139	-0.0067151
32	1	1	0	-0.0347	-0.0167877
33	1	1	0	-0.0139	-0.0067151
34	1	1	0	-0.0277	-0.0134302
35	1	1	0	-0.0555	-0.0268603
36	1	1	0	-0.0139	-0.0067151
37	1	1	0	-0.0555	-0.0268603
38	1	1	0	-0.0139	-0.0067151
39	1	1	0	-0.0555	-0.0268603
40	1	1	0	-0.018	-0.0087296
41	1	1	0	-0.0277	-0.0134302
42	1	1	0	-0.0319	-0.0154447
43	1	1	0	-0.0555	-0.0268603
44	1	1	0	-0.0277	-0.0134302
45	1	1	0	-0.0139	-0.0067151
46	2	1	0	1.75	0.847525
48	1	1	0	-0.0555	-0.0268603
49	1	1	0	-0.0139	-0.0067151
50	1	1	0	-0.0555	-0.0268603
47	1	1	0	-0.0139	-0.0067151

Bus Data for Hour-16 on 17th February 2025					
Bus No	Bus ID	Initial Voltage, p.u.	Initial Angle	Injected P (p.u.)	Injected Q (p.u.)
0	1	1	0	-0.0305	-0.0147528
1	3	1	0	0	0
2	1	1	0	-0.0152	-0.0073764
3	1	1	0	-0.0609	-0.0295057
4	1	1	0	-0.0457	-0.0221293
5	1	1	0	-0.0914	-0.0442585
6	1	1	0	-0.0609	-0.0295057
7	1	1	0	-0.0914	-0.0442585
8	1	1	0	-0.0609	-0.0295057
9	1	1	0	-0.0914	-0.0442585
10	1	1	0	-0.0152	-0.0073764
11	1	1	0	-0.0762	-0.0368821
12	1	1	0	-0.1371	-0.0663878
13	1	1	0	-0.0609	-0.0295057
14	2	1	0	0.02391	0.01157768
15	1	1	0	-0.0914	-0.0442585
16	1	1	0	-0.2285	-0.1106463
17	1	1	0	-0.0914	-0.0442585
18	1	1	0	-0.0152	-0.0073764
19	1	1	0	-0.3351	-0.1622812
20	2	1	0	0.02393	0.01159075
21	1	1	0	-0.0152	-0.0073764
22	1	1	0	-0.0305	-0.0147528
23	1	1	0	-0.0655	-0.0317186
24	1	1	0	-0.0046	-0.0022129
25	1	1	0	-0.0305	-0.0147528
26	1	1	0	-0.0457	-0.0221293
27	1	1	0	-0.0152	-0.0073764
28	1	1	0	-0.0609	-0.0295057
29	2	1	0	0.0207	0.01002259
30	1	1	0	-0.0305	-0.0147528
31	1	1	0	-0.0152	-0.0073764
32	1	1	0	-0.0381	-0.018441
33	1	1	0	-0.0152	-0.0073764
34	1	1	0	-0.0305	-0.0147528
35	1	1	0	-0.0609	-0.0295057
36	1	1	0	-0.0152	-0.0073764
37	1	1	0	-0.0609	-0.0295057
38	1	1	0	-0.0152	-0.0073764
39	1	1	0	-0.0609	-0.0295057
40	1	1	0	-0.0198	-0.0095893
41	1	1	0	-0.0305	-0.0147528
42	1	1	0	-0.035	-0.0169658
43	1	1	0	-0.0609	-0.0295057
44	1	1	0	-0.0305	-0.0147528
45	1	1	0	-0.0152	-0.0073764
46	2	1	0	1.75	0.847525
48	1	1	0	-0.0609	-0.0295057
49	1	1	0	-0.0152	-0.0073764
50	1	1	0	-0.0609	-0.0295057
47	1	1	0	-0.0152	-0.0073764

Bus Data for Hour-20 on 17th February 2025					
Bus No	Bus ID	Initial Voltage, p.u.	Initial Angle	Injected P (p.u.)	Injected Q (p.u.)
0	1	1	0	-0.0458	-0.0221801
1	3	1	0	0	0
2	1	1	0	-0.0229	-0.0110901
3	1	1	0	-0.0916	-0.0443603
4	1	1	0	-0.0687	-0.0332702
5	1	1	0	-0.1374	-0.0665404
6	1	1	0	-0.0916	-0.0443603
7	1	1	0	-0.1374	-0.0665404
8	1	1	0	-0.0916	-0.0443603
9	1	1	0	-0.1374	-0.0665404
10	1	1	0	-0.0229	-0.0110901
11	1	1	0	-0.1145	-0.0554503
12	1	1	0	-0.2061	-0.0998106
13	1	1	0	-0.0916	-0.0443603
14	2	1	0	0	0
15	1	1	0	-0.1374	-0.0665404
16	1	1	0	-0.3435	-0.1663509
17	1	1	0	-0.1374	-0.0665404
18	1	1	0	-0.0229	-0.0110901
19	1	1	0	-0.5038	-0.2439814
20	2	1	0	0	0
21	1	1	0	-0.0229	-0.0110901
22	1	1	0	-0.0458	-0.0221801
23	1	1	0	-0.0985	-0.0476873
24	1	1	0	-0.0069	-0.003327
25	1	1	0	-0.0458	-0.0221801
26	1	1	0	-0.0687	-0.0332702
27	1	1	0	-0.0229	-0.0110901
28	1	1	0	-0.0916	-0.0443603
29	2	1	0	0	0
30	1	1	0	-0.0458	-0.0221801
31	1	1	0	-0.0229	-0.0110901
32	1	1	0	-0.0572	-0.0277252
33	1	1	0	-0.0229	-0.0110901
34	1	1	0	-0.0458	-0.0221801
35	1	1	0	-0.0916	-0.0443603
36	1	1	0	-0.0229	-0.0110901
37	1	1	0	-0.0916	-0.0443603
38	1	1	0	-0.0229	-0.0110901
39	1	1	0	-0.0916	-0.0443603
40	1	1	0	-0.0298	-0.0144171
41	1	1	0	-0.0458	-0.0221801
42	1	1	0	-0.0527	-0.0255071
43	1	1	0	-0.0916	-0.0443603
44	1	1	0	-0.0458	-0.0221801
45	1	1	0	-0.0229	-0.0110901
46	2	1	0	1.75	0.847525
48	1	1	0	-0.0916	-0.0443603
49	1	1	0	-0.0229	-0.0110901
50	1	1	0	-0.0916	-0.0443603
47	1	1	0	-0.0229	-0.0110901

Bus Data for Hour-24 on 17th February 2025					
Bus No	**Bus ID**	**Initial Voltage, p.u.**	**Initial Angle**	**Injected P (p.u.)**	**Injected Q (p.u.)**
0	1	1	0	-0.038	-0.0184156
1	3	1	0	0	0
2	1	1	0	-0.019	-0.0092078
3	1	1	0	-0.0761	-0.0368312
4	1	1	0	-0.057	-0.0276234
5	1	1	0	-0.1141	-0.0552468
6	1	1	0	-0.0761	-0.0368312
7	1	1	0	-0.1141	-0.0552468
8	1	1	0	-0.0761	-0.0368312
9	1	1	0	-0.1141	-0.0552468
10	1	1	0	-0.019	-0.0092078
11	1	1	0	-0.0951	-0.046039
12	1	1	0	-0.1711	-0.0828702
13	1	1	0	-0.0761	-0.0368312
14	2	1	0	0	0
15	1	1	0	-0.1141	-0.0552468
16	1	1	0	-0.2852	-0.1381171
17	1	1	0	-0.1141	-0.0552468
18	1	1	0	-0.019	-0.0092078
19	1	1	0	-0.4183	-0.2025717
20	2	1	0	0	0
21	1	1	0	-0.019	-0.0092078
22	1	1	0	-0.038	-0.0184156
23	1	1	0	-0.0818	-0.0395936
24	1	1	0	-0.0057	-0.0027623
25	1	1	0	-0.038	-0.0184156
26	1	1	0	-0.057	-0.0276234
27	1	1	0	-0.019	-0.0092078
28	1	1	0	-0.0761	-0.0368312
29	2	1	0	0	0
30	1	1	0	-0.038	-0.0184156
31	1	1	0	-0.019	-0.0092078
32	1	1	0	-0.0475	-0.0230195
33	1	1	0	-0.019	-0.0092078
34	1	1	0	-0.038	-0.0184156
35	1	1	0	-0.0761	-0.0368312
36	1	1	0	-0.019	-0.0092078
37	1	1	0	-0.0761	-0.0368312
38	1	1	0	-0.019	-0.0092078
39	1	1	0	-0.0761	-0.0368312
40	1	1	0	-0.0247	-0.0119701
41	1	1	0	-0.038	-0.0184156
42	1	1	0	-0.0437	-0.021178
43	1	1	0	-0.0761	-0.0368312
44	1	1	0	-0.038	-0.0184156
45	1	1	0	-0.019	-0.0092078
46	2	1	0	1.75	0.847525
48	1	1	0	-0.0761	-0.0368312
49	1	1	0	-0.019	-0.0092078
50	1	1	0	-0.0761	-0.0368312
47	1	1	0	-0.019	-0.0092078

ANNEX B: SYSTEM BRANCH DATA

SN	From Bus	To Bus	Length, km	Conductor Type	R (p.u.)	X (p.u.)	B/2 (p.u.)
1	0	3	0.097	Weasel ACSR	0.000580397	0.000304628	3.0062E-09
2	1	2	0.202	100 mm2 XLPE	0.000323868	0.000183636	5.00826E-08
3	2	3	0.084	Weasel ACSR	0.000502612	0.000263802	2.60331E-09
4	2	4	0.533	100 mm2 XLPE	0.000854562	0.000484545	1.32149E-07
5	4	5	0.112	Rabbit ACSR	0.000512793	0.000337851	4.01719E-09
6	5	6	0.0853	Rabbit ACSR	0.000390547	0.00025731	3.05952E-09
7	6	7	0.144	Rabbit ACSR	0.000659306	0.00043438	5.16496E-09
8	7	8	0.39	Rabbit ACSR	0.00178562	0.001176446	1.39884E-08
9	8	9	0.482	100 mm2 XLPE	0.000772793	0.000438182	1.19504E-07
10	9	10	0.271	100 mm2 XLPE	0.000434496	0.000246364	6.71901E-08
11	10	11	0.523	Weasel ACSR	0.003129355	0.001642479	1.62087E-08
12	10	12	0.358	TS4	0.001639107	0.001079917	1.28407E-08
13	12	13	0.479	Rabbit ACSR	0.002193107	0.001444917	1.71807E-08
14	13	14	0.515	Rabbit ACSR	0.002357934	0.001553512	1.84719E-08
15	13	15	0.474	Rabbit ACSR	0.002170215	0.001429835	1.70013E-08
16	15	47	0.089	TS1	0.000407488	0.000268471	3.19223E-09
17	10	16	0.623	100 mm2 XLPE	0.00099886	0.000566364	1.54463E-07
18	16	17	0.512	100 mm2 XLPE	0.000820893	0.000465455	1.26942E-07
19	17	18	0.335	Rabbit ACSR	0.001533802	0.001010537	1.20157E-08
20	18	24	0.499	Rabbit ACSR	0.002284678	0.001505248	1.7898E-08
21	19	20	0.258	Rabbit ACSR	0.001181256	0.000778264	9.25388E-09
22	20	21	0.407	Rabbit ACSR	0.001863455	0.001227727	1.45982E-08
23	21	22	0.827	Rabbit ACSR	0.00378643	0.002494669	2.96626E-08
24	22	23	0.917	Weasel ACSR	0.005486843	0.002879835	2.84194E-08
25	24	25	0.544	Rabbit ACSR	0.002490711	0.001640992	1.95121E-08
26	25	26	0.875	Rabbit ACSR	0.004006198	0.002639463	3.13843E-08
27	26	27	0.487	Rabbit ACSR	0.002229736	0.00146905	1.74676E-08
28	27	28	1.001	Weasel ACSR	0.005989455	0.003143636	3.10227E-08
29	27	41	0.843	Weasel ACSR	0.005044066	0.002647438	2.6126E-08
30	28	29	0.617	Weasel ACSR	0.003691802	0.001937686	1.91219E-08
31	28	30	1.087	Weasel ACSR	0.006504033	0.003413719	3.3688E-08
32	30	31	0.12	Weasel ACSR	0.000718017	0.00037686	3.71901E-09
33	31	32	1.44	Weasel ACSR	0.008616198	0.004522314	4.46281E-08
34	31	33	0.091	Rabbit ACSR	0.000416645	0.000274504	3.26397E-09
35	33	34	0.148	Rabbit ACSR	0.00067762	0.000446446	5.30843E-09
36	33	35	0.391	Weasel ACSR	0.002339537	0.001227934	1.21178E-08
37	34	36	0.406	Rabbit ACSR	0.001858876	0.001224711	1.45623E-08
38	36	37	0.297	Rabbit ACSR	0.001359818	0.000895909	1.06527E-08
39	37	38	1.074	Weasel ACSR	0.006426248	0.003372893	3.32851E-08
40	38	39	0.185	Rabbit ACSR	0.000847025	0.000558058	6.63554E-09
41	38	45	1.085	Rabbit ACSR	0.004967686	0.003272934	3.89165E-08
42	39	40	0.441	Rabbit ACSR	0.002019124	0.001330289	1.58177E-08
43	40	41	0.075	TS3	0.000343388	0.00022624	2.69008E-09
44	18	42	0.538	TS5	0.00246324	0.001622893	1.92969E-08
45	42	43	0.633	Rabbit ACSR	0.002898198	0.001909463	2.27043E-08
46	43	44	0.376	Rabbit ACSR	0.001721521	0.001134215	1.34863E-08
47	44	45	0.075	TS2	0.000343388	0.00022624	2.69008E-09
48	45	46	0.243	Rabbit ACSR	0.001112579	0.000733017	8.71587E-09
49	46	48	0.387	Rabbit ACSR	0.001771884	0.001167397	1.38808E-08
50	48	49	0.507	Rabbit ACSR	0.002321306	0.00152938	1.8185E-08
51	49	50	0.265	Rabbit ACSR	0.001213306	0.00079938	9.50496E-09
52	48	47	0.561	Rabbit ACSR	0.002568545	0.001692273	2.01218E-08
53	42	19	0.499	TS6	0.002284678	0.001505248	1.7898E-08

Branch Data for Switch Combination: 000111					
SN	**From Bus**	**To Bus**	**R (p.u.)**	**X (p.u.)**	**B/2 (p.u.)**
1	0	3	0.000580397	0.000304628	3.01E-09
2	1	2	0.000323868	0.000183636	5.01E-08
3	2	3	0.000502612	0.000263802	2.6E-09
4	2	4	0.000854562	0.000484545	0.000000132
5	4	5	0.000512793	0.000337851	4.02E-09
6	5	6	0.000390547	0.00025731	3.06E-09
7	6	7	0.000659306	0.00043438	5.16E-09
8	7	8	0.00178562	0.001176446	0.000000014
9	8	9	0.000772793	0.000438182	0.00000012
10	9	10	0.000434496	0.000246364	6.72E-08
11	10	11	0.003129355	0.001642479	1.62E-08
12	10	12	0.001639107	0.001079917	1.28E-08
13	12	13	0.002193107	0.001444917	1.72E-08
14	13	14	0.002357934	0.001553512	1.85E-08
15	13	15	0.002170215	0.001429835	0.000000017
16	10	16	0.00099886	0.000566364	0.000000154
17	16	17	0.000820893	0.000465455	0.000000127
18	17	18	0.001533802	0.001010537	0.000000012
19	18	24	0.002284678	0.001505248	1.79E-08
20	19	20	0.001181256	0.000778264	9.25E-09
21	20	21	0.001863455	0.001227727	1.46E-08
22	21	22	0.00378643	0.002494669	2.97E-08
23	22	23	0.005486843	0.002879835	2.84E-08
24	24	25	0.002490711	0.001640992	1.95E-08
25	25	26	0.004006198	0.002639463	3.14E-08
26	26	27	0.002229736	0.00146905	1.75E-08
27	27	28	0.005989455	0.003143636	0.000000031
28	27	41	0.005044066	0.002647438	2.61E-08
29	28	29	0.003691802	0.001937686	1.91E-08
30	28	30	0.006504033	0.003413719	3.37E-08
31	30	31	0.000718017	0.00037686	3.72E-09
32	31	32	0.008616198	0.004522314	4.46E-08
33	31	33	0.000416645	0.000274504	3.26E-09
34	33	34	0.00067762	0.000446446	5.31E-09
35	33	35	0.002339537	0.001227934	1.21E-08
36	34	36	0.001858876	0.001224711	1.46E-08
37	36	37	0.001359818	0.000895909	1.07E-08
38	37	38	0.006426248	0.003372893	3.33E-08
39	38	39	0.000847025	0.000558058	6.64E-09
40	38	45	0.004967686	0.003272934	3.89E-08
41	39	40	0.002019124	0.001330289	1.58E-08
42	18	42	0.00246324	0.001622893	1.93E-08
43	42	43	0.002898198	0.001909463	2.27E-08
44	43	44	0.001721521	0.001134215	1.35E-08
45	45	46	0.001112579	0.000733017	8.72E-09
46	46	48	0.001771884	0.001167397	1.39E-08
47	48	49	0.002321306	0.00152938	1.82E-08
48	49	50	0.001213306	0.00079938	9.5E-09
49	48	47	0.002568545	0.001692273	2.01E-08
50	42	19	0.002284678	0.001505248	1.79E-08

Branch Data for Switch Combination: 001110					
SN	From Bus	To Bus	R (p.u.)	X (p.u.)	B/2 (p.u.)
1	0	3	0.000580397	0.000304628	3.01E-09
2	1	2	0.000323868	0.000183636	5.01E-08
3	2	3	0.000502612	0.000263802	2.6E-09
4	2	4	0.000854562	0.000484545	0.000000132
5	4	5	0.000512793	0.000337851	4.02E-09
6	5	6	0.000390547	0.00025731	3.06E-09
7	6	7	0.000659306	0.00043438	5.16E-09
8	7	8	0.00178562	0.001176446	0.000000014
9	8	9	0.000772793	0.000438182	0.00000012
10	9	10	0.000434496	0.000246364	6.72E-08
11	10	11	0.003129355	0.001642479	1.62E-08
12	10	12	0.001639107	0.001079917	1.28E-08
13	12	13	0.002193107	0.001444917	1.72E-08
14	13	14	0.002357934	0.001553512	1.85E-08
15	13	15	0.002170215	0.001429835	0.000000017
16	10	16	0.00099886	0.000566364	0.000000154
17	16	17	0.000820893	0.000465455	0.000000127
18	17	18	0.001533802	0.001010537	0.000000012
19	19	20	0.001181256	0.000778264	9.25E-09
20	20	21	0.001863455	0.001227727	1.46E-08
21	21	22	0.00378643	0.002494669	2.97E-08
22	22	23	0.005486843	0.002879835	2.84E-08
23	24	25	0.002490711	0.001640992	1.95E-08
24	25	26	0.004006198	0.002639463	3.14E-08
25	26	27	0.002229736	0.00146905	1.75E-08
26	27	28	0.005989455	0.003143636	0.000000031
27	27	41	0.005044066	0.002647438	2.61E-08
28	28	29	0.003691802	0.001937686	1.91E-08
29	28	30	0.006504033	0.003413719	3.37E-08
30	30	31	0.000718017	0.00037686	3.72E-09
31	31	32	0.008616198	0.004522314	4.46E-08
32	31	33	0.000416645	0.000274504	3.26E-09
33	33	34	0.00067762	0.000446446	5.31E-09
34	33	35	0.002339537	0.001227934	1.21E-08
35	34	36	0.001858876	0.001224711	1.46E-08
36	36	37	0.001359818	0.000895909	1.07E-08
37	37	38	0.006426248	0.003372893	3.33E-08
38	38	39	0.000847025	0.000558058	6.64E-09
39	38	45	0.004967686	0.003272934	3.89E-08
40	39	40	0.002019124	0.001330289	1.58E-08
41	40	41	0.000343388	0.00022624	2.69E-09
42	18	42	0.00246324	0.001622893	1.93E-08
43	42	43	0.002898198	0.001909463	2.27E-08
44	43	44	0.001721521	0.001134215	1.35E-08
45	45	46	0.001112579	0.000733017	8.72E-09
46	46	48	0.001771884	0.001167397	1.39E-08
47	48	49	0.002321306	0.00152938	1.82E-08
48	49	50	0.001213306	0.00079938	9.5E-09
49	48	47	0.002568545	0.001692273	2.01E-08
50	42	19	0.002284678	0.001505248	1.79E-08

Branch Data for Switch Combination: 111000					
SN	From Bus	To Bus	R (p.u.)	X (p.u.)	B/2 (p.u.)
1	0	3	0.000580397	0.000304628	3.01E-09
2	1	2	0.000323868	0.000183636	5.01E-08
3	2	3	0.000502612	0.000263802	2.6E-09
4	2	4	0.000854562	0.000484545	0.000000132
5	4	5	0.000512793	0.000337851	4.02E-09
6	5	6	0.000390547	0.00025731	3.06E-09
7	6	7	0.000659306	0.00043438	5.16E-09
8	7	8	0.00178562	0.001176446	0.000000014
9	8	9	0.000772793	0.000438182	0.00000012
10	9	10	0.000434496	0.000246364	6.72E-08
11	10	11	0.003129355	0.001642479	1.62E-08
12	12	13	0.002193107	0.001444917	1.72E-08
13	13	14	0.002357934	0.001553512	1.85E-08
14	13	15	0.002170215	0.001429835	0.000000017
15	15	47	0.000407488	0.000268471	3.19E-09
16	10	16	0.00099886	0.000566364	0.000000154
17	16	17	0.000820893	0.000465455	0.000000127
18	17	18	0.001533802	0.001010537	0.000000012
19	19	20	0.001181256	0.000778264	9.25E-09
20	20	21	0.001863455	0.001227727	1.46E-08
21	21	22	0.00378643	0.002494669	2.97E-08
22	22	23	0.005486843	0.002879835	2.84E-08
23	24	25	0.002490711	0.001640992	1.95E-08
24	25	26	0.004006198	0.002639463	3.14E-08
25	26	27	0.002229736	0.00146905	1.75E-08
26	27	28	0.005989455	0.003143636	0.000000031
27	27	41	0.005044066	0.002647438	2.61E-08
28	28	29	0.003691802	0.001937686	1.91E-08
29	28	30	0.006504033	0.003413719	3.37E-08
30	30	31	0.000718017	0.00037686	3.72E-09
31	31	32	0.008616198	0.004522314	4.46E-08
32	31	33	0.000416645	0.000274504	3.26E-09
33	33	34	0.00067762	0.000446446	5.31E-09
34	33	35	0.002339537	0.001227934	1.21E-08
35	34	36	0.001858876	0.001224711	1.46E-08
36	36	37	0.001359818	0.000895909	1.07E-08
37	37	38	0.006426248	0.003372893	3.33E-08
38	38	39	0.000847025	0.000558058	6.64E-09
39	38	45	0.004967686	0.003272934	3.89E-08
40	39	40	0.002019124	0.001330289	1.58E-08
41	40	41	0.000343388	0.00022624	2.69E-09
42	42	43	0.002898198	0.001909463	2.27E-08
43	43	44	0.001721521	0.001134215	1.35E-08
44	44	45	0.000343388	0.00022624	2.69E-09
45	45	46	0.001112579	0.000733017	8.72E-09
46	46	48	0.001771884	0.001167397	1.39E-08
47	48	49	0.002321306	0.00152938	1.82E-08
48	49	50	0.001213306	0.00079938	9.5E-09
49	48	47	0.002568545	0.001692273	2.01E-08
50	42	19	0.002284678	0.001505248	1.79E-08

ANNEX C: SOLAR PV DATA

S.N.	ToD	P.U. Solar Generation (1000 kVA Base)		
		Bus-14	Bus-20	Bus-29
1	0	0	0	0
2	1	0	0	0
3	2	0	0	0
4	3	0	0	0
5	4	0	0	0
6	5	0	0	0
7	6	0	0	0
8	7	0.003868	0.00344	0.003986
9	8	0.021156	0.021606	0.020624
10	9	0.038582	0.03911	0.037869
11	10	0.052941	0.053299	0.052273
12	11	0.062343	0.062446	0.061656
13	12	0.06515	0.065001	0.064531
14	13	0.062097	0.06192	0.061648
15	14	0.054136	0.053813	0.053893
16	15	0.040378	0.040291	0.040083
17	16	0.023906	0.023933	0.020695
18	17	0.004087	0.003856	0.001709
19	18	0	0	0
20	19	0	0	0
21	20	0	0	0
22	21	0	0	0
23	22	0	0	0
24	23	0	0	0

ANNEX D: EV CHARGING DATA

S.N.	ToD	P.U. EV Charging Load (1000 kVA Base)					
		Bus-8	Bus-12	Bus-13	Bus-15	Bus-18	Bus-27
1	1	0.043439	0	0.020994	0	0.000157	0.00017
2	2	0.029286	0	0.067741	0	0.000153	0.000169
3	3	0.030387	0.029989	0.042557	0.086355	0.000153	0.00017
4	4	0.04836	0.035294	0.035632	0	0.000153	0.000169
5	5	0.02117	0	0	0	0.044056	0.000169
6	6	0.050143	0	0.000051	0	0.000159	0.000169
7	7	0.065072	0	0	0	0.071588	0.000169
8	8	0.041607	0.041598	0.092165	0	0	0.036082
9	9	0.049805	0.042765	0.077749	0	0.042532	0.042542
10	10	0.021743	0.011921	0.084878	0	0.014941	0.113238
11	11	0.07159	0.033441	0.057696	0.056259	0.015437	0.000083
12	12	0.084833	0.025971	0.042713	0.095656	0	0.000082
13	13	0.083421	0.017725	0.008178	0.059805	0	0.085226
14	14	0.011291	0.000161	0.000187	0.040318	0.041985	0.127486
15	15	0.000067	0.02327	0.00017	0.000247	0	0.154467
16	16	0.000067	0.000103	0.00017	0.000251	0.040819	0.166964
17	17	0.000068	0.000102	0.127086	0.000247	0.04499	0.085142
18	18	0.000067	0.000102	0.000173	0.000251	0.060385	0.000156
19	19	0.000067	0.000102	0.000173	0.000247	0.024311	0.065368
20	20	0.000067	0.000101	0.000173	0.000249	0.021576	0.042809
21	21	0.000067	0.000102	0.000173	0.000249	0.088635	0.052901
22	22	0.000067	0.000103	0.000172	0.000249	0.035226	0.042769
23	23	0.000066	0.040659	0.000173	0.000249	0.035204	0.000183
24	24	0.000046	0	0.000067	0	0.043634	0.000169

S.N.	ToD	P.U. EV Charging Load (1000 kVA Base)					
		Bus-5	Bus-10	Bus-16	Bus-21	Bus-24	Bus-28
1	1	0.000182	0.000182	0.000196	0.00018	0.000187	0.000181
2	2	0.000182	0.000182	0.000195	0.00018	0.000188	0.000181
3	3	0.000183	0.000182	0.000195	0.00018	0.000188	0.000181
4	4	0.000182	0.000182	0.000196	0.00018	0.000188	0.00018
5	5	0.000182	0.000182	0.000195	0.000181	0.000188	0.00018
6	6	0.025582	0.000182	0.000195	0.000181	0.000187	0.000181
7	7	0.000084	0	0.000195	0	0.000112	0.000211
8	8	0.014737	0.024583	0	0.072063	0	0
9	9	0	0.028667	0	0.102058	0.065684	0.059442
10	10	0.0783	0.134802	0.064875	0.113537	0.100716	0.063509
11	11	0.000086	0.074665	0.104096	0.020318	0.06136	0.042527
12	12	0.105082	0	0.057356	0.078267	0.04036	0.000085
13	13	0.009157	0.08424	0.146885	0.022233	0.114733	0.085027
14	14	0.103221	0.042597	0.168591	0.135419	0.127593	0.062131
15	15	0.042694	0.100658	0.140446	0.118756	0.166206	0.090936
16	16	0.137288	0.151997	0.119644	0.085217	0.16492	0.036453
17	17	0.040353	0.000087	0.183195	0.064452	0.114259	0.092872
18	18	0.079403	0.042556	0.157653	0.077794	0.132348	0.072835
19	19	0.041944	0.000346	0.000303	0.042774	0.045947	0.092973
20	20	0.0257	0.037403	0.085234	0.000325	0.042032	0.126271
21	21	0.000188	0.073092	0.042843	0.000323	0.000321	0.040802
22	22	0.000184	0.000181	0.025684	0.042631	0.042801	0.146172
23	23	0.000183	0.000183	0.000181	0.000189	0.000181	0.023278
24	24	0.000182	0.000182	0	0.00018	0.000188	0.00018

S.N.	ToD	P.U. EV Charging Load (1000 kVA Base)							
		Bus-30	Bus-31	Bus-34	Bus-36	Bus-42	Bus-44	Bus-47	Bus-51
1	1	0.00019	0.00019	0.00018	0.00025	0.03688	0	9.7E-05	4.5E-05
2	2	0.00019	0.00019	0.00018	0.00025	0.00016	0.03175	9.7E-05	4.5E-05
3	3	0.00019	0.00019	0.02039	0.00026	0.00015	0	9.8E-05	4.4E-05
4	4	0.00019	0.00019	0.00018	0.00026	0.00016	0	9.7E-05	4.4E-05
5	5	0.00019	0.00019	0.00018	0.00026	0.00015	0	9.8E-05	4.4E-05
6	6	0.00019	0.00019	0.0002	0.00026	0.00015	0	0.00011	4.4E-05
7	7	0.00019	0.00019	7.7E-05	0.00016	0.01173	0	0.04257	4.4E-05
8	8	0.03578	0.03578	0.03563	0	0.02094	0	0.03138	0.07431
9	9	0.0861	0.0861	0.01857	0	0.02748	0.01999	0.04928	0.0285
10	10	0.01317	0.01317	0.15701	0	0.02229	0	0.01289	0.00625
11	11	0	0	0.10009	0.01866	0	0	0	0.03441
12	12	0.04232	0.04232	8.8E-05	0.0165	0	0	0	0.02458
13	13	0.00947	0.00947	0.08143	0.03002	0	0	0	0.04294
14	14	0.12459	0.12459	0.08414	0.07673	0	0	0.0427	0.00639
15	15	0.09595	0.09595	0.06121	0	0.03853	0	0.04264	0.04279
16	16	0	0	0.11242	0	0.01487	0.03163	0.04161	0.06907
17	17	0.02099	0.02099	0.04348	0	0.06856	0	0	0
18	18	0.04061	0.04061	0.12711	0.00014	0.05092	0	0.02593	0.07196
19	19	0.04263	0.04263	0.00033	0.00025	0.03461	0.02298	0.04284	0.0878
20	20	0.08134	0.08134	0.00022	0.00025	0.0232	0	0.04074	0.08705
21	21	0.04378	0.04378	0.00885	0.00033	0.022	0	0.01371	6.7E-05
22	22	0.00018	0.00018	0.00017	0.00025	0.00033	0.03158	0	8.2E-05
23	23	0.00018	0.00018	0.00017	0.00025	0.07125	0.03166	0	8.2E-05
24	24	0.00019	0.00019	0.00018	0.00025	0.00016	0	9.7E-05	0.00008

ANNEX E: LOAD FLOW RESULTS

System Loss and Minimum Bus Voltage Before Reconfiguration				
Time of Day	**Total System Loss, p.u.**	**Minimum Bus Voltage, p.u.**	**Total System Loss, kW**	**Minimum Bus Voltage, kV**
1	0.01352123	0.986482	13.52122952	10.851302
2	0.026056651	0.981152	26.05665132	10.792672
3	0.088195397	0.965226	88.19539655	10.617486
4	0.039349827	0.993967	39.34982657	10.933637
5	0.044453496	0.975371	44.45349606	10.729081
6	0.07353524	0.968306	73.53523998	10.651366
7	0.006169661	0.993465	6.16966067	10.928115
8	0.006242653	0.993426	6.242652507	10.927686
9	0.005060447	0.994083	5.060447227	10.934913
10	0.014800291	0.98696	14.80029119	10.85656
11	0.00442321	0.994469	4.423209847	10.939159
12	0.003715341	0.994932	3.715340574	10.944252
13	0.003603384	0.995009	3.603383756	10.945099
14	0.003715341	0.994932	3.715340574	10.944252
15	0.003659147	0.994971	3.659147202	10.944681
16	0.004484996	0.994431	4.484995907	10.938741
17	0.088195397	0.986283	88.19539655	10.849113
18	0.108644962	0.961393	108.6449618	10.575323
19	0.121445204	0.949175	121.4452038	10.440925
20	0.061451103	0.971033	61.45110344	10.681363
21	0.04494158	0.975236	44.94158043	10.727596
22	0.03972427	0.97672	39.7242698	10.74392
23	0.049283683	0.97308	49.28368263	10.70388
24	0.042054466	0.976046	42.05446575	10.736506
Total Loss/Minimum Bus Voltage			**896.7269737**	**10.440925**

System Loss and Minimum Bus Voltage After Reconfiguration					
Time of Day	**SC for Minimal Ploss**	**Minimal System Loss**	**Minimum Bus Voltage**	**Loss, kW**	**Bus Voltage, kV**
1	111000	0.006088079	0.99387	6.08808	10.93257
2	111000	0.011404543	0.991471	11.4045	10.906181
3	111000	0.038181506	0.98424	38.1815	10.82664
4	111000	0.030963779	0.987205	30.9638	10.859255
5	111000	0.046882814	0.982531	46.8828	10.807841
6	111000	0.052308017	0.981544	52.308	10.796984
7	001110	0.006146157	0.996125	6.14616	10.957375
8	001110	0.00621887	0.996102	6.21887	10.957122
9	001110	0.005041175	0.996491	5.04117	10.961401
10	011100	0.009131308	0.992058	9.13131	10.912638
11	001110	0.004406367	0.996719	4.40637	10.963909
12	001110	0.003701197	0.996993	3.7012	10.966923
13	001110	0.003589667	0.997039	3.58967	10.967429
14	001110	0.003701197	0.996993	3.7012	10.966923
15	001110	0.003645218	0.997016	3.64522	10.967176
16	001110	0.004467918	0.996696	4.46792	10.963656
17	001110	0.005239985	0.996422	5.23998	10.960642
18	111000	0.019363608	0.988881	19.3636	10.877691
19	111000	0.031842503	0.985733	31.8425	10.843063
20	111000	0.026670831	0.986946	26.6708	10.856406
21	111000	0.019574013	0.988821	19.574	10.877031
22	111000	0.01732301	0.989484	17.323	10.884324
23	111000	0.021017898	0.987976	21.0179	10.867736
24	111000	0.018328895	0.989183	18.3289	10.881013
Total Loss/Minimum Bus Voltage				**395.239**	**10.796984**

System Loss and Minimum Bus Voltage Without Solar PV and EV Load					
Time of Day	**SC for Minimal Ploss**	**System Loss**	**Minimum Bus Voltage**	**Loss, kW**	**Bus Voltage, kV**
1	000111	0.022202382	0.981691	22.2024	10.798601
2	000111	0.043053861	0.97443	43.0539	10.71873
3	000111	0.047703121	0.972456	47.7031	10.697016
4	000111	0.062004897	0.980553	62.0049	10.786083
5	000111	0.082404653	0.977144	82.4047	10.748584
6	000111	0.104193351	0.964064	104.193	10.604704
7	000111	0.061299564	0.969478	61.2996	10.664258
8	000111	0.062040004	0.969294	62.04	10.662234
9	000111	0.050082674	0.972418	50.0827	10.696598
10	000111	0.04554576	0.973699	45.5458	10.710689
11	000111	0.043669898	0.974247	43.6699	10.716717
12	000111	0.036575095	0.976436	36.5751	10.740796
13	000111	0.035455894	0.9768	35.4559	10.7448
14	000111	0.036576095	0.976436	36.5761	10.740796
15	000111	0.036013243	0.976618	36.0132	10.742798
16	000111	0.044290628	0.974065	44.2906	10.714715
17	000111	0.052095845	0.971868	52.0958	10.690548
18	000111	0.07370772	0.966524	73.7077	10.631764
19	000111	0.122463212	0.936524	122.463	10.301764
20	000111	0.102164109	0.960571	102.164	10.566281
21	000111	0.074523157	0.966339	74.5232	10.629729
22	000111	0.069701216	0.968372	69.7012	10.652092
23	000111	0.065812145	0.971017	65.8121	10.681187
24	000111	0.059189397	0.967449	59.1894	10.641939
Total Loss/Minimum Bus Voltage				**1432.77**	**10.301764**

System Loss and Minimum Bus Voltage After Reconfiguration with Increased Solar PV (500 kWP)					
Time of Day	**SC for Minimal Ploss**	**Minimal System Loss**	**Minimum Bus Voltage**	**Loss, kW**	**Bus Voltage, kV**
1	111000	0.006088079	0.99618724	6.08808	10.9580596
2	111000	0.011404543	0.99956767	11.4045	10.9952444
3	111000	0.038181506	0.99378829	38.1815	10.9316712
4	111000	0.030963779	0.99286232	30.9638	10.9214855
5	111000	0.046882814	0.99940256	46.8828	10.9934282
6	111000	0.052308017	0.99706672	52.308	10.9677339
7	001110	0.006146157	0.993465	6.14616	10.928115
8	001110	0.00621887	0.993426	6.21887	10.927686
9	001110	0.005041175	0.994083	5.04117	10.934913
10	011100	0.005640696	0.99787899	5.6407	10.9766689
11	001110	0.004406367	0.994469	4.40637	10.939159
12	001110	0.003701197	0.994932	3.7012	10.944252
13	001110	0.003589667	0.995009	3.58967	10.945099
14	001110	0.003701197	0.994932	3.7012	10.944252
15	001110	0.003645218	0.994971	3.64522	10.944681
16	001110	0.004467918	0.994431	4.46792	10.938741
17	001110	0.005239985	0.993967	5.23998	10.933637
18	111000	0.019363608	0.99457752	19.3636	10.9403527
19	111000	0.031842503	0.9872784	31.8425	10.8600624
20	111000	0.026670831	0.99980349	26.6708	10.9978384
21	111000	0.019574013	0.9944388	19.574	10.9388268
22	111000	0.01732301	0.99597186	17.323	10.9556905
23	111000	0.021017898	0.99671923	21.0179	10.9639115
24	111000	0.018328895	0.9952752	18.3289	10.9480272
Total Loss/Minimum Bus Voltage				**391.748**	**10.8600624**

System Loss and Minimum Bus Voltage After Reconfiguration with Increased Solar PV Generation (1000 kWP)					
Time of Day	**SC for Minimal Ploss**	**Minimal System Loss**	**Minimum Bus Voltage**	**Loss, kW**	**Bus Voltage, kV**
1	111000	0.006088079	0.99618724	6.08808	10.9580596
2	111000	0.011404543	0.9907393	11.4045	10.8981323
3	111000	0.038181506	0.99378829	38.1815	10.9316712
4	111000	0.030963779	0.99286232	30.9638	10.9214855
5	111000	0.046882814	0.98979292	46.8828	10.8877221
6	111000	0.052308017	0.9969576	52.308	10.9665336
7	001110	0.006146157	0.993465	6.14616	10.928115
8	001110	0.00621887	0.993426	6.21887	10.927686
9	001110	0.005041175	0.994083	5.04117	10.934913
10	011100	0.005468095	0.993196	5.46809	10.925156
11	001110	0.004406367	0.994469	4.40637	10.939159
12	001110	0.003701197	0.994932	3.7012	10.944252
13	001110	0.003589667	0.995009	3.58967	10.945099
14	001110	0.003701197	0.994932	3.7012	10.944252
15	001110	0.003645218	0.994971	3.64522	10.944681
16	001110	0.004467918	0.994431	4.46792	10.938741
17	001110	0.005239985	0.993967	5.23998	10.933637
18	111000	0.019363608	0.99457752	19.3636	10.9403527
19	111000	0.031842503	0.98747954	31.8425	10.8622749
20	111000	0.026670831	0.99009666	26.6708	10.8910633
21	111000	0.019574013	0.9944388	19.574	10.9388268
22	111000	0.01732301	0.99597186	17.323	10.9556905
23	111000	0.021017898	0.99185718	21.0179	10.910429
24	111000	0.018328895	0.9952752	18.3289	10.9480272
Total Loss/Minimum Bus Voltage				**391.575**	**10.8622749**

System Loss and Minimum Bus Voltage For Increased EV Penetration					
Time of Day	**SC for Minimal Ploss**	**Minimal System Loss**	**Minimum Bus Voltage**	**Loss, kW**	**Bus Voltage, kV**
1	111000	0.012861143	0.99050778	12.8611	10.8955856
2	111000	0.015284426	0.99103297	15.2844	10.9013627
3	111000	0.05686276	0.96600075	56.8628	10.6260083
4	111000	0.033066555	0.98682577	33.0666	10.8550834
5	111000	0.053535373	0.97058782	53.5354	10.676466
6	111000	0.101409045	0.96151691	101.409	10.576686
7	001110	0.006168182	0.99432032	6.16818	10.9375236
8	001110	0.006239109	0.99365677	6.23911	10.9302245
9	011100	0.005044832	0.99453627	5.04483	10.939899
10	011100	0.012529094	0.98831034	12.5291	10.8714138
11	001110	0.004420764	0.99633287	4.42076	10.9596616
12	001110	0.003711381	0.99656776	3.71138	10.9622454
13	100011	0.003590385	0.9958742	3.59038	10.9546162
14	100011	0.003701775	0.99499494	3.70178	10.9449443
15	100011	0.00364611	0.99689359	3.64611	10.9658294
16	001110	0.004480171	0.99552838	4.48017	10.9508122
17	001110	0.005245172	0.99546052	5.24517	10.9500658
18	111000	0.038846918	0.98065296	38.8469	10.7871825
19	111000	0.046495847	0.9832828	46.4958	10.8161108
20	111000	0.038413534	0.97413165	38.4135	10.7154482
21	111000	0.034311678	0.98245441	34.3117	10.8069985
22	111000	0.020135851	0.98888811	20.1359	10.8777692
23	111000	0.048393026	0.98017508	48.393	10.7819259
24	111000	0.023887005	0.98050881	23.887	10.785597
Total Loss/Minimum Bus Voltage				**582.28**	**10.576686**

ANNEX F: BRANCH CURRENT RESULTS

From Bus	To Bus	Hr-1: 111000		Hr-2: 111000		Hr-3: 111000		Hr-4: 111000	
		I (p.u.)	I (Amp)	I (p.u.)	I (Amp)	I (p.u.)	I (Amp)	I (p.u.)	I (Amp)
0	3	0.024051	1.26027	0.0333957	1.7499326	0.0612407	3.2090147	0.0602489	3.1570447
1	2	0.7714411	40.4235	1.0721586	56.181113	1.9405796	101.68637	1.9089708	100.03007
2	3	0.0721522	3.78078	0.1001855	5.2497211	0.1837174	9.6267894	0.1807421	9.4708876
2	4	0.6872641	36.0126	0.9552767	50.056499	1.7262463	90.455309	1.6981086	88.980889
4	5	0.6511654	34.1211	0.9051402	47.429349	1.6342436	85.634363	1.6075981	84.238138
5	6	0.5789392	30.3364	0.8048119	42.172141	1.4500529	75.982771	1.4263979	74.743249
6	7	0.5307754	27.8126	0.7379013	38.666026	1.3271756	69.544003	1.305517	68.409091
7	8	0.4584997	24.0254	0.6374772	33.403806	1.142666	59.875698	1.1240082	58.898029
8	9	0.410269	21.4981	0.570437	29.890901	1.0193573	53.414324	1.0027099	52.541999
9	10	0.3378965	17.7058	0.4698257	24.618866	0.8342268	43.713484	0.8206004	42.999459
10	11	0.0603336	3.16148	0.0838876	4.3957083	0.1544238	8.091808	0.1519015	7.9596385
10	12	0.1084803	5.68437	0.1507063	7.8970122	0.2770387	14.516828	0.2725286	14.280501
12	13	1.846E-08	9.7E-07	1.845E-08	9.666E-07	1.84E-08	9.642E-07	1.84E-08	9.643E-07
13	14	0.15668	8.21003	0.2176605	11.405413	0.4000771	20.964039	0.3935654	20.622829
13	15	0.2289505	11.997	0.3180354	16.665057	0.5844423	30.624777	0.5749346	30.126571
10	16	0.2654989	13.9121	0.3691657	19.344283	0.6489351	34.004201	0.6383349	33.448751
16	17	0.0844817	4.42684	0.1174711	6.1554842	0.1855701	9.723875	0.1825399	9.5650929
17	18	0.012069	0.63242	0.016782	0.8793783	0.0001952	0.0102304	0.0001941	0.01017
18	24	0.0882264	4.62306	0.1227464	6.4319104	0.2264521	11.866088	0.2219423	11.629778
19	20	0.0882264	4.62306	0.1227464	6.4319109	0.2264521	11.866089	0.2219423	11.629778
20	21	0.0761465	3.99008	0.1059433	5.5514265	0.1954704	10.242647	0.1915767	10.03862
21	22	0.0519784	2.72367	0.0723208	3.7896124	0.1334514	6.9928511	0.1307923	6.853515
22	23	0.0036267	0.19004	0.0050463	0.2644263	0.0093127	0.4879863	0.0091348	0.4786622
24	25	0.0278047	1.45697	0.0386879	2.0272437	0.0713958	3.741139	0.0700316	3.6696583
25	26	0.0640669	3.3571	0.0891408	4.6709802	0.1644881	8.6191768	0.161346	8.4545301
26	27	0.0641762	3.36283	0.0893087	4.6797757	0.1648787	8.6396453	0.1617252	8.4743995
27	28	0.1403282	7.3532	0.1952629	10.231777	0.3603834	18.88409	0.3534956	18.523172
27	41	1.899E-08	1E-06	1.895E-08	9.929E-07	1.882E-08	9.861E-07	1.887E-08	9.89E-07
28	29	0.0158149	0.8287	0.0220146	1.153563	0.0406747	2.1313522	0.0398951	2.0905038
28	30	0.0083732	0.43875	0.0116443	0.6101588	0.0214565	1.1243221	0.0210481	1.1029228
30	31	0.0302388	1.58451	0.0420836	2.2051789	0.0777098	4.0719935	0.0762227	3.9940712
31	32	0.0507017	2.65677	0.0705513	3.6968861	0.1302216	6.8236106	0.1277323	6.693175
31	33	0.1111658	5.82509	0.1546925	8.1058855	0.2855535	14.963005	0.2800937	14.676911
33	34	0.0483728	2.53473	0.0673156	3.5273398	0.1242742	6.5119678	0.1218974	6.3874237
33	35	0.1353469	7.09218	0.18834	9.8690154	0.3476555	18.217148	0.3410087	17.868857
34	36	0.1474338	7.72553	0.2051567	10.750211	0.3786822	19.842945	0.3714429	19.463608
36	37	0.1957698	10.2583	0.2724012	14.273822	0.5027114	26.342079	0.4931053	25.83872
37	38	0.228455	11.971	0.3178163	16.653575	0.5861748	30.715557	0.5749904	30.129496
38	39	0.4362914	22.8617	0.6069949	31.806534	1.11978	58.676473	1.0984024	57.556288
38	45	0.1801767	9.44126	0.2506838	13.135833	0.4625225	24.236179	0.4536896	23.773337
39	40	0.1644795	8.61872	0.2288526	11.991876	0.4222902	22.128004	0.4142234	21.705305
18	42	0.3816478	19.9983	0.5308289	27.815434	0.9785024	51.273528	0.9590563	50.254553
42	43	0.429842	22.5237	0.5977984	31.324636	1.1015952	57.723587	1.0797205	56.577352
43	44	0.4539178	23.7853	0.6312422	33.07709	1.1630015	60.941279	0.8623537	45.187336
45	46	0.9022449	47.2776	1.2549546	65.759623	2.3134699	121.22582	0.2661583	13.946696
46	48	0.4364178	22.8683	0.4852028	25.424629	0.8912955	46.703885	0.8768079	45.944732
48	49	0.1149659	6.02421	0.0835542	4.3782417	0.1533263	8.0342986	0.1508396	7.9039948
49	50	0.0229937	1.20487	0.0167112	0.8756652	0.0306664	1.606917	0.030169	1.5808544
48	47	0.3081577	16.1475	0.3849417	20.170946	0.7073173	37.063428	0.6958133	36.460616
42	19	0.3538996	18.5443	0.4922507	25.793939	0.907482	47.552055	0.8894427	46.606797
Maximum Current		**0.9022449**	**47.2776**	**1.2549546**	**65.759623**	**2.3134699**	**121.22582**	**1.9089708**	**100.03007**

From Bus	To Bus	Hr-5: 111000		Hr-6: 111000		Hr-7: 001110		Hr-8: 001110	
		I (p.u.)	I (Amp)	I (p.u.)	I (Amp)	I (p.u.)	I (Amp)	I (p.u.)	I (Amp)
0	3	0.0677873	3.5520533	0.071557	3.74959	0.0396985	2.0801997	0.0399321	2.0924412
1	2	2.1493663	112.62679	2.269715	118.933	0.8520237	44.646039	0.8570457	44.909194
2	3	0.2033559	10.655848	0.2146645	11.2484	0.1190933	6.2404908	0.1197942	6.2772141
2	4	1.9121223	100.19521	2.0192781	105.81	0.7130905	37.365942	0.717295	37.586257
4	5	1.8102676	94.858021	1.9117488	100.176	0.653511	34.243978	0.6573647	34.445909
5	6	1.6063311	84.171751	1.6964369	88.8933	0.5343075	27.997713	0.5374589	28.162849
6	7	1.4702711	77.042204	1.5527814	81.3657	0.4548222	23.832682	0.4575053	23.973276
7	8	1.2659432	66.335422	1.3370329	70.0605	0.3355617	17.583431	0.3375418	17.68719
8	9	1.1293535	59.178121	1.1927865	62.502	0.2560121	13.415035	0.257523	13.494207
9	10	0.9242631	48.431384	0.9761872	51.1522	0.1367297	7.1646356	0.1375368	7.2069305
10	11	0.1710909	8.9651651	0.1807028	9.46883	0.0995408	5.2159389	0.1001283	5.2467255
10	12	0.3068279	16.077783	0.3239973	16.9775	0.202696	10.62127	0.203892	10.683941
12	13	1.839E-08	9.636E-07	1.838E-08	9.6E-07	0.3817138	20.001805	0.3839657	20.119802
13	14	0.4430855	23.217681	0.4678729	24.5165	0.5804763	30.416958	0.5838995	30.596332
13	15	0.6472359	33.91516	0.6834232	35.8114	0.1192772	6.2501274	0.1199802	6.2869647
10	16	0.7189747	37.674274	0.759367	39.7908	0.2197247	11.513574	0.2210214	11.581519
16	17	0.2055869	10.772753	0.2171302	11.3776	0.079003	4.1397577	0.0794694	4.1641948
17	18	0.0001954	0.0102413	0.0001944	0.01019	0.1983711	10.394644	0.1995419	10.455993
18	24	0.2510155	13.15321	0.2651923	13.8961	0.8203403	42.985833	0.8251756	43.239199
19	20	0.2510155	13.153211	0.2651923	13.8961	0.1450021	7.5981096	0.145856	7.6428548
20	21	0.2166779	11.353923	0.2289183	11.9953	0.1251546	6.5581035	0.1258918	6.596729
21	22	0.1479344	7.7517646	0.1562941	8.18981	0.0854374	4.4769193	0.0859407	4.5032916
22	23	0.0103237	0.5409612	0.0109072	0.57154	0.0059707	0.3128653	0.0060059	0.3147114
24	25	0.0791462	4.1472588	0.0836199	4.38168	0.0457748	2.3985988	0.0460449	2.412752
25	26	0.1823401	9.5546234	0.1926444	10.0946	0.1054679	5.5265166	0.1060901	5.5591222
26	27	0.1827956	9.5784916	0.1931394	10.1205	0.1252946	6.5654349	0.1260337	6.6041661
27	28	0.3995163	20.934657	0.4221059	22.1183	0.0072118	0.3778965	0.0072543	0.3801257
27	41	1.879E-08	9.845E-07	1.877E-08	9.8E-07	0.413665	21.676045	0.4161055	21.803929
28	29	0.0451037	2.3634314	0.0476614	2.49746	0.2089571	10.949353	0.2101906	11.013985
28	30	0.0237768	1.2459042	0.0251153	1.31604	0.1691584	8.8639012	0.170157	8.9162253
30	31	0.0861586	4.514709	0.0910366	4.77032	0.0497957	2.6092945	0.0500898	2.6247036
31	32	0.1443642	7.5646836	0.1525282	7.99248	0.0995021	5.2139099	0.1000894	5.2446822
31	33	0.3165735	16.58845	0.3344809	17.5268	0.0048153	0.2523223	0.0048437	0.2538114
33	34	0.137778	7.2195668	0.1455739	7.62807	0.0796551	4.1739294	0.0801254	4.1985727
33	35	0.3854192	20.195968	0.4072196	21.3383	0.0402866	2.1110166	0.0405246	2.1234873
34	36	0.4198122	21.998158	0.4435554	23.2423	0.0600989	3.1491813	0.0604538	3.1677796
36	37	0.5572887	29.201928	0.5887925	30.8527	0.1396122	7.3156767	0.1404363	7.3588645
37	38	0.6497195	34.045304	0.6863912	35.9669	0.1456488	7.6319967	0.1465077	7.6770043
38	39	1.2412378	65.040863	1.3113373	68.7141	0.3051219	15.98839	0.3069222	16.082721
38	45	0.5127068	26.865837	0.5416722	28.3836	0.066309	3.4745919	0.0667001	3.4950852
39	40	0.4681219	24.529587	0.4945762	25.9158	0.0407001	2.132684	0.0409401	2.1452634
18	42	1.0844273	56.82399	1.1455427	60.0264	0.2182649	11.437079	0.219553	11.504578
42	43	1.2207522	63.967417	1.2894939	67.5695	0.1193605	6.2544899	0.1200645	6.2913789
43	44	1.2887428	67.530122	1.3612777	71.331	0.039789	2.0849434	0.0400237	2.097241
45	46	2.5639578	134.35139	2.7084867	141.925	0.324957	17.027746	0.3268739	17.128194
46	48	0.9869687	51.717158	1.0420963	54.6058	0.1985408	10.403538	0.1997095	10.464776
48	49	0.1697434	8.8945517	0.1791993	9.39004	0.0992747	5.2019923	0.099859	5.2326137
49	50	0.03395	1.7789805	0.0358414	1.87809	0.0198554	1.0404222	0.0199723	1.0465468
48	47	0.783293	41.044555	0.8270753	43.3387	0.0794168	4.1614394	0.0798843	4.1859347
42	19	1.0057429	52.70093	1.0624387	55.6718	0.3833445	20.087252	0.3856062	20.205763
Maximum Current		**2.5639578**	**134.35139**	**2.7084867**	**141.925**	**0.8520237**	**44.646039**	**0.8570457**	**44.909194**

From Bus	To Bus	Hr-9: 001110		Hr-10: 001110		Hr-11: 001110		Hr-12: 001110	
		I (p.u.)	I (Amp)	I (p.u.)	I (Amp)	I (p.u.)	I (Amp)	I (p.u.)	I (Amp)
0	3	0.0359608	1.8843433	0.03596075	1.88434334	0.03362482	1.76194082	0.03082186	1.61506562
1	2	0.7716871	40.436405	0.77168713	40.4364054	0.72149227	37.8061952	0.66127415	34.6507653
2	3	0.1078806	5.6529412	0.10788056	5.65294121	0.10087299	5.28574483	0.09246434	4.84513162
2	4	0.6458346	33.841733	0.64583461	33.8417333	0.60381466	31.6398883	0.55340594	28.9984712
4	5	0.5918678	31.013872	0.59186779	31.0138724	0.55335522	28.9958136	0.50715478	26.5749106
5	6	0.4838978	25.356247	0.48389784	25.356247	0.45240473	23.7060078	0.41462609	21.7264074
6	7	0.4119048	21.583811	0.41190479	21.5838111	0.38509315	20.1788813	0.35293108	18.4935884
7	8	0.3038894	15.923804	0.3038894	15.9238043	0.28410377	14.8870377	0.2603707	13.6434248
8	9	0.2318455	12.148702	0.23184546	12.148702	0.21674886	11.3576404	0.19864063	10.4087688
9	10	0.1238198	6.4881577	0.1238198	6.48815766	0.1157555	6.06558796	0.10608276	5.55873653
10	11	0.0901435	4.7235204	0.09014352	4.72352044	0.08427326	4.41591871	0.07723204	4.04695866
10	12	0.1835659	9.6188519	0.18356588	9.61885195	0.17161515	8.99263411	0.15727997	8.24147044
12	13	0.3456948	18.114406	0.34569478	18.1144063	0.32319273	16.9352988	0.29620027	15.5208941
13	14	0.5257194	27.547696	0.52571938	27.5476957	0.49150944	25.7550944	0.45047081	23.6046705
13	15	0.1080314	5.6608455	0.1080314	5.66084549	0.10100484	5.29265387	0.0925751	4.85093508
10	16	0.1989846	10.426791	0.19898455	10.4267906	0.18602835	9.74788546	0.17048737	8.93353834
16	17	0.0715439	3.7489002	0.0715439	3.74890023	0.06688445	3.50474511	0.06129564	3.21189155
17	18	0.1796446	9.4133777	0.17964461	9.41337767	0.16794654	8.80039893	0.15391491	8.06514126
18	24	0.7429923	38.932798	0.74299233	38.9327981	0.69466461	36.4004254	0.63668633	33.3623636
19	20	0.131341	6.8822671	0.13134098	6.88226715	0.12280424	6.43494236	0.11256165	5.89823052
20	21	0.1133621	5.9401725	0.11336207	5.94017252	0.10599312	5.55403942	0.0971518	5.09075455
21	22	0.0773859	4.0550217	0.07738591	4.05502165	0.07235482	3.79139278	0.06631863	3.47509614
22	23	0.0054072	0.2833365	0.00540719	0.28333649	0.00505515	0.26488976	0.00463287	0.24276256
24	25	0.0414545	2.172218	0.04145454	2.17221798	0.03875566	2.03079681	0.0355183	1.86115918
25	26	0.0955149	5.0049808	0.0955149	5.00498076	0.08929711	4.67916857	0.08183862	4.28834373
26	27	0.1134716	5.945914	0.11347164	5.94591401	0.10608555	5.55888281	0.09722552	5.09461714
27	28	0.0065313	0.3422401	0.0065313	0.34224014	0.00610619	0.31996439	0.00559624	0.29324312
27	41	0.374628	19.630509	0.37462804	19.6305092	0.35024095	18.3526259	0.32098761	16.8197506
28	29	0.189229	9.9156006	0.18922902	9.91560059	0.17690548	9.26984732	0.16212386	8.49529038
28	30	0.1531872	8.0270084	0.15318718	8.02700844	0.14321051	7.50423094	0.13124394	6.8771823
30	31	0.0450925	2.362846	0.04509248	2.36284603	0.04215473	2.20890784	0.03863121	2.02427541
31	32	0.0901091	4.7217165	0.09010909	4.72171647	0.08424145	4.41425182	0.07720329	4.04545262
31	33	0.0043608	0.2285053	0.00436079	0.22850535	0.00407685	0.21362709	0.00373627	0.19578064
33	34	0.0721332	3.7797818	0.07213324	3.77978183	0.0674347	3.53357835	0.06179914	3.23827483
33	35	0.0364804	1.9115712	0.03648037	1.91157115	0.03410303	1.78699859	0.03125178	1.63759348
34	36	0.0544223	2.851727	0.05442227	2.851727	0.05087654	2.66593064	0.04662384	2.44308917
36	37	0.1264298	6.624919	0.12642975	6.624919	0.11819526	6.19343137	0.10831842	5.67588542
37	38	0.1319095	6.9120562	0.13190947	6.91205619	0.1233257	6.46226667	0.11302853	5.92269498
38	39	0.2763271	14.479542	0.27632714	14.4795423	0.25833861	13.536943	0.23676069	12.4062602
38	45	0.0600532	3.1467859	0.06005317	3.14678593	0.05614486	2.94199047	0.0514565	2.69632034
39	40	0.0368601	1.9314678	0.03686007	1.93146782	0.03446107	1.80575996	0.03158327	1.65496351
18	42	0.1976612	10.357449	0.19766123	10.3574485	0.18479043	9.68301877	0.16935204	8.87404705
42	43	0.1080997	5.6644229	0.10809967	5.6644229	0.10106451	5.29578033	0.0926252	4.85356071
43	44	0.036035	1.888234	0.036035	1.88823396	0.03368972	1.76534139	0.03087637	1.61792184
45	46	0.2942946	15.421039	0.29429463	15.4210388	0.27513895	14.4172812	0.25216054	13.2132125
46	48	0.1798435	9.4238007	0.17984352	9.42380067	0.16815889	8.81152595	0.15413852	8.07685858
48	49	0.0899253	4.7120834	0.08992526	4.71208343	0.0840825	4.4059231	0.07707183	4.03856389
49	50	0.0179854	0.9424362	0.01798542	0.94243618	0.01681683	0.88120166	0.01541464	0.80772709
48	47	0.0719378	3.7695401	0.07193779	3.76954009	0.06726389	3.52462778	0.06165569	3.23075814
42	19	0.3471685	18.191629	0.34716849	18.1916287	0.32456871	17.0074006	0.29745936	15.5868706
Maximum Current		**0.7716871**	**40.436405**	**0.77168713**	**40.4364054**	**0.72149227**	**37.8061952**	**0.66127415**	**34.6507653**

From Bus	To Bus	Hr-13: 001110		Hr-14: 001110		Hr-15: 001110		Hr-16: 001110	
		I (p.u.)	I (Amp)	I (p.u.)	I (Amp)	I (p.u.)	I (Amp)	I (p.u.)	I (Amp)
0	3	0.03035472	1.59058725	0.03082186	1.61506562	0.03058829	1.6028264	0.03385841	1.77418081
1	2	0.65123946	34.1249475	0.66127415	34.6507653	0.65625674	34.3878533	0.72651122	38.0691882
2	3	0.09106295	4.77169847	0.09246434	4.84513162	0.09176364	4.80841496	0.10157373	5.3224637
2	4	0.5450061	28.5583194	0.55340594	28.9984712	0.54920596	28.7783923	0.60801614	31.8600456
4	5	0.49945626	26.1715082	0.50715478	26.5749106	0.50330547	26.3732065	0.55720598	29.1975933
5	6	0.40833104	21.3965467	0.41462609	21.7264074	0.41147852	21.5614744	0.45555359	23.8710083
6	7	0.34757199	18.2127722	0.35293108	18.4935884	0.35025149	18.3531779	0.38777391	20.319353
7	8	0.25641622	13.4362097	0.2603707	13.6434248	0.25839342	13.5398153	0.28608201	14.9906971
8	9	0.1956234	10.2506662	0.19864063	10.4087688	0.19713198	10.329716	0.21825826	11.4367328
9	10	0.1044711	5.4742859	0.10608276	5.55873653	0.10527691	5.51651033	0.11656177	6.10783701
10	11	0.07605883	3.98548249	0.07723204	4.04695866	0.07664542	4.01621996	0.08486018	4.44667336
10	12	0.15489137	8.11630805	0.15727997	8.24147044	0.15608565	8.17888812	0.17281003	9.05524574
12	13	0.29170259	15.2852155	0.29620027	15.5208941	0.29395139	15.4030528	0.32544259	17.0531917
13	14	0.44363245	23.2463405	0.45047081	23.6046705	0.44705158	23.4255029	0.49492998	25.9343308
13	15	0.09117036	4.77732706	0.0925751	4.85093508	0.09187272	4.81413065	0.10170743	5.32946924
10	16	0.1678979	8.79784974	0.17048737	8.93353834	0.16919261	8.86569276	0.18732375	9.81576441
16	17	0.06036444	3.16309668	0.06129564	3.21189155	0.06083003	3.18749362	0.06735031	3.5291561
17	18	0.15157694	7.94263189	0.15391491	8.06514126	0.1527459	8.00388537	0.16911614	8.861686
18	24	0.62702487	32.8561032	0.63668633	33.3623636	0.63185554	33.1092305	0.69949687	36.6536359
19	20	0.11085471	5.80878681	0.11256165	5.89823052	0.11170818	5.85350837	0.12365787	6.47967218
20	21	0.0956784	5.01354834	0.0971518	5.09075455	0.0964151	5.05215116	0.10672997	5.59265018
21	22	0.06531271	3.42238618	0.06631863	3.47509614	0.06581567	3.44874094	0.07285789	3.81775369
22	23	0.00456251	0.23907563	0.00463287	0.24276256	0.00459769	0.24091906	0.00509035	0.26673413
24	25	0.03497888	1.83289342	0.0355183	1.86115918	0.03524859	1.84702604	0.03902551	2.04493661
25	26	0.08059584	4.22322213	0.08183862	4.28834373	0.08121722	4.25578237	0.08991879	4.71174468
26	27	0.09574919	5.01725773	0.09722552	5.09461714	0.09648734	5.05593678	0.10682405	5.59758008
27	28	0.00551127	0.28879059	0.00559624	0.29324312	0.00555376	0.29101682	0.0061487	0.32219164
27	41	0.31611323	16.5643334	0.32098761	16.8197506	0.31855038	16.6920398	0.35267928	18.4803943
28	29	0.15966096	8.36623432	0.16212386	8.49529038	0.16089239	8.43076103	0.17813761	9.33441081
28	30	0.12925008	6.77270433	0.13124394	6.8771823	0.13024699	6.82494224	0.144208	7.55649899
30	31	0.03804415	1.99351323	0.03863121	2.02427541	0.03833767	2.00889396	0.04244844	2.22429848
31	32	0.07603059	3.98400287	0.07720329	4.04545262	0.07661693	4.01472715	0.08482811	4.44499288
31	33	0.00367952	0.19280702	0.00373627	0.19578064	0.0037079	0.19429381	0.00410524	0.21511467
33	34	0.06086016	3.18907247	0.06179914	3.23827483	0.06132964	3.21367312	0.06790446	3.5581939
33	35	0.03077674	1.61270132	0.03125178	1.63759348	0.03101426	1.62514709	0.03434071	1.79945305
34	36	0.04591529	2.40596102	0.04662384	2.44308917	0.04626955	2.42452466	0.05123104	2.68450638
36	37	0.10667277	5.5896531	0.10831842	5.67588542	0.10749558	5.63276836	0.11901855	6.23657197
37	38	0.11131269	5.83278498	0.11302853	5.92269498	0.1121706	5.87773932	0.12418396	6.50723963
38	39	0.23316525	12.2178593	0.23676069	12.4062602	0.23496294	12.3120581	0.26013718	13.631188
38	45	0.05067527	2.65538426	0.0514565	2.69632034	0.05106588	2.67585198	0.05653563	2.96246713
39	40	0.03110375	1.62983638	0.03158327	1.65496351	0.03134351	1.64239974	0.03470093	1.81832894
18	42	0.16677967	8.73925488	0.16935204	8.87404705	0.16806583	8.80664967	0.18607729	9.75045001
42	43	0.09121896	4.77987349	0.0926252	4.85356071	0.09192207	4.81671653	0.10176793	5.33263943
43	44	0.03040758	1.59335738	0.03087637	1.61792184	0.03064197	1.60563942	0.03392422	1.77762889
45	46	0.2483317	13.0125811	0.25216054	13.2132125	0.25024609	13.1128952	0.27705424	14.517642
46	48	0.15180192	7.95442063	0.15413852	8.07685858	0.15297022	8.01563937	0.16932731	8.8727513
48	49	0.07590345	3.97734087	0.07707183	4.03856389	0.07648764	4.00795225	0.08466676	4.436538
49	50	0.01518096	0.79548205	0.01541464	0.80772709	0.0152978	0.80160454	0.01693368	0.88732488
48	47	0.06072104	3.18178253	0.06165569	3.23075814	0.06118836	3.20627024	0.06773126	3.54911816
42	19	0.29294224	15.3501733	0.29745936	15.5868706	0.29520076	15.4685199	0.32682834	17.1258049
Maximum Current		**0.65123946**	**34.1249475**	**0.66127415**	**34.6507653**	**0.65625674**	**34.3878533**	**0.72651122**	**38.0691882**

From Bus	To Bus	Hr-17: 001110		Hr-18: 111000		Hr-19: 111000		Hr-20: 111000	
		I (p.u.)	I (Amp)	I (p.u.)	I (Amp)	I (p.u.)	I (Amp)	I (p.u.)	I (Amp)
0	3	0.03666155	1.92106525	0.04344397	2.27646419	0.05559931	2.91340404	0.05092368	2.6684007
1	2	0.7867479	41.2255901	1.39614279	73.1578822	1.78893289	93.7400835	1.63773019	85.8170619
2	3	0.10998289	5.76310344	0.13032945	6.82926292	0.16679389	8.73999972	0.15276763	8.00502394
2	4	0.65844284	34.5024046	1.24409368	65.1905088	1.59434311	83.5435789	1.45950388	76.4780035
4	5	0.60342373	31.6194036	1.17885485	61.7719942	1.51082452	79.1672048	1.3830181	72.4701487
5	6	0.49334771	25.8514202	1.0482832	54.9300398	1.34363309	70.4063737	1.22991725	64.447664
6	7	0.41995004	22.0053821	0.961193	50.3665132	1.23210243	64.5621671	1.12779161	59.0962802
7	8	0.30982651	16.2349093	0.83045905	43.5160541	1.06464432	55.7873623	0.97446732	51.0620875
8	9	0.23637557	12.3860799	0.74314885	38.9409997	0.95275189	49.9241989	0.87203866	45.6948256
9	10	0.12623975	6.61496291	0.61209673	32.0738687	0.78477035	41.1219664	0.71827602	37.6376635
10	11	0.09190506	4.81582492	0.10928615	5.72659444	0.1401098	7.34175362	0.12824035	6.71979412
10	12	0.18715193	9.80676132	0.19621981	10.2819179	0.25138178	13.172405	0.23014972	12.0598454
12	13	0.35244687	18.468216	1.843E-08	9.6573E-07	1.841E-08	9.647E-07	1.8418E-08	9.651E-07
13	14	0.53598434	28.0855792	0.28338386	14.8493143	0.3630335	19.0229554	0.33237689	17.4165491
13	15	0.11013968	5.7713194	0.41403422	21.6953932	0.53035386	27.7905421	0.4855859	25.4447009
10	16	0.20287237	10.6305122	0.48096194	25.2024057	0.61665267	32.3126001	0.56439941	29.5745293
16	17	0.07294211	3.82216638	0.15304908	8.0197719	0.19623359	10.2826404	0.17960333	9.41121458
17	18	0.18315493	9.59731813	0.02186491	1.1457213	0.02803461	1.46901371	0.02565866	1.34451374
18	24	0.75749286	39.692626	0.16001888	8.38498924	0.20532204	10.7588747	0.18786779	9.84427238
19	20	0.13390222	7.0164761	0.16001889	8.38498978	0.20532205	10.7588753	0.1878678	9.84427292
20	21	0.11557297	6.05602352	0.13811797	7.23738139	0.17722787	9.28674064	0.16215937	8.49715084
21	22	0.0788954	4.13411888	0.09428865	4.94072534	0.12099421	6.34009641	0.11070458	5.80092008
22	23	0.00551282	0.28887183	0.00657943	0.34476203	0.00844339	0.44243362	0.00772518	0.40479951
24	25	0.0422644	2.21465435	0.05044145	2.64313217	0.06473126	3.39191825	0.05922524	3.10340232
25	26	0.09738066	5.10274656	0.11621856	6.08985263	0.14913676	7.81476621	0.13645331	7.15015352
26	27	0.11568795	6.06204876	0.11645966	6.10248632	0.1494811	7.83280953	0.13675602	7.1660154
27	28	0.00665886	0.34892428	0.25459676	13.3408705	0.32674134	17.1212461	0.29894221	15.6645719
27	41	0.38194581	20.0139606	1.8902E-08	9.9045E-07	1.8845E-08	9.875E-07	1.8867E-08	9.8864E-07
28	29	0.19292706	10.1093779	0.02871621	1.50472959	0.03687257	1.93212283	0.03372871	1.76738436
28	30	0.15618099	8.18388373	0.01517296	0.79506328	0.01945745	1.01957039	0.01780733	0.9331039
30	31	0.04597407	2.4090413	0.05488145	2.8757878	0.07044895	3.69152505	0.06444956	3.3771568
31	32	0.09186983	4.81397929	0.09199121	4.82033964	0.11806141	6.1864177	0.10801575	5.66002543
31	33	0.00444599	0.23296993	0.20171002	10.5696051	0.25888659	13.5656571	0.23685403	12.4111514
33	34	0.0735432	3.85366367	0.0877795	4.59964578	0.11266737	5.9037702	0.1030767	5.40121929
33	35	0.0371938	1.94895504	0.24558223	12.8685088	0.31519131	16.5160248	0.28836817	15.1104921
34	36	0.05548631	2.90748279	0.26750633	14.0173318	0.34332385	17.99017	0.31410866	16.4592939
36	37	0.12890078	6.75440067	0.35516457	18.6106236	0.45579096	23.8834465	0.41701791	21.8517385
37	38	0.1344851	7.04701903	0.41428739	21.7086592	0.5315224	27.8517737	0.48635727	25.4851211
38	39	0.28172494	14.7623866	0.79130929	41.4646068	1.01533587	53.2035998	0.92902359	48.6808363
38	45	0.0612259	3.20823705	0.32681983	17.1253593	0.41936994	21.9749847	0.38371122	20.1064681
39	40	0.03757992	1.96918801	0.29837043	15.6346107	0.38288337	20.0630884	0.35032028	18.3567829
18	42	0.20152344	10.5598283	0.6918132	36.2510118	0.88735345	46.497321	0.81203326	42.5505428
42	43	0.11021065	5.77503806	0.7790036	40.8197889	0.99904924	52.3501804	0.9142971	47.909168
43	44	0.03673873	1.92510935	0.82252922	43.1005309	1.05478272	55.2706146	0.96533318	50.5834586
45	46	0.30004258	15.7222312	1.63559398	85.7051243	2.09797329	109.933801	1.91986472	100.600911
46	48	0.18334909	9.60749229	0.63157447	33.0945024	0.80887588	42.3850962	0.74064485	38.8097902
48	49	0.09167818	4.80393644	0.10872016	5.69693645	0.13917899	7.29297932	0.12746073	6.67894246
49	50	0.01833602	0.96080755	0.02174458	1.13941584	0.02783669	1.4586427	0.0254929	1.33582776
48	47	0.07334003	3.8430175	0.50111696	26.2585289	0.64187203	33.6340945	0.58770115	30.7955404
42	19	0.35394995	18.5469775	0.64155861	33.6176709	0.82293063	43.1215651	0.75306599	39.4606581
Maximum Current		**0.7867479**	**41.2255901**	**1.63559398**	**85.7051243**	**2.09797329**	**109.933801**	**1.91986472**	**100.600911**

From Bus	To Bus	Hr-21: 111000		Hr-22: 111000		Hr-23: 111000		Hr-24: 111000	
		I (p.u.)	I (Amp)	I (p.u.)	I (Amp)	I (p.u.)	I (Amp)	I (p.u.)	I (Amp)
0	3	0.04367769	2.28871093	0.04367769	2.28871093	0.04180767	2.1907221	0.04227542	2.21523
1	2	1.40368614	73.5531537	1.40368614	73.5531537	1.32217257	69.2818425	1.35843208	71.1818
2	3	0.13103057	6.86600173	0.13103057	6.86600173	0.12542073	6.57204625	0.1268239	6.64557
2	4	1.25081907	65.5429195	1.25081907	65.5429195	1.17585016	61.6145482	1.21047267	63.4288
4	5	1.18522888	62.1059934	1.18522888	62.1059934	1.11307249	58.3249984	1.14699056	60.1023
5	6	1.05395349	55.2271627	1.05395349	55.2271627	0.98743176	51.7414241	1.01993735	53.4447
6	7	0.96639366	50.6390279	0.96639366	50.6390279	0.90363281	47.3503595	0.93519505	49.0042
7	8	0.8349542	43.7516002	0.8349542	43.7516002	0.77784518	40.7590875	0.8079882	42.3386
8	9	0.74717199	39.1518122	0.74717199	39.1518122	0.69384782	36.3576255	0.72303765	37.8872
9	10	0.61541091	32.2475315	0.61541091	32.2475315	0.56777381	29.7513478	0.59552965	31.2058
10	11	0.10987779	5.757596	0.10987779	5.757596	0.10513092	5.50886029	0.10632865	5.57162
10	12	0.19727935	10.3374379	0.19727935	10.3374379	0.18880441	9.89335104	0.19092285	10.0044
12	13	1.843E-08	9.6571E-07	1.843E-08	9.6571E-07	1.8433E-08	9.6587E-07	1.8432E-08	9.7E-07
13	14	0.28491382	14.9294843	0.28491382	14.9294843	0.27267605	14.2882251	0.27573508	14.4485
13	15	0.41626878	21.812484	0.41626878	21.812484	0.39839491	20.8758931	0.40286282	21.11
10	16	0.48356625	25.3388714	0.48356625	25.3388714	0.44162466	23.1411324	0.46794341	24.5202
16	17	0.1538779	8.0632018	0.1538779	8.0632018	0.12618924	6.61231642	0.14890598	7.80267
17	18	0.02198332	1.151926	0.02198332	1.151926	1.192E-08	6.2461E-07	0.021273	1.11471
18	24	0.16088771	8.43051621	0.16088771	8.43051621	0.36545134	19.1496501	0.15567609	8.15743
19	20	0.16088772	8.43051675	0.16088772	8.43051675	0.15431504	8.08610799	0.1556761	8.15743
20	21	0.138868	7.27668294	0.138868	7.27668294	0.13319414	6.97937288	0.13436904	7.04094
21	22	0.09480077	4.96756033	0.09480077	4.96756033	0.09092674	4.76456132	0.09172891	4.80659
22	23	0.00661517	0.34663492	0.00661517	0.34663492	0.00633116	0.33175266	0.00640078	0.3354
24	25	0.05071547	2.6574905	0.05071547	2.6574905	0.04853811	2.54339705	0.04907185	2.57136
25	26	0.11684981	6.12292998	0.11684981	6.12292998	0.11183379	5.86009082	0.11306338	5.92452
26	27	0.11709274	6.13565971	0.11709274	6.13565971	0.11206235	5.87206697	0.1132954	5.93668
27	28	0.25598009	13.4133569	0.25598009	13.4133569	0.24498806	12.8373741	0.2476825	12.9786
27	41	1.8901E-08	9.9039E-07	1.8901E-08	9.9039E-07	1.8904E-08	9.9056E-07	1.8907E-08	9.9E-07
28	29	0.02887253	1.51292039	0.02887253	1.51292039	0.02763055	1.44784087	0.02793496	1.46379
28	30	0.01525518	0.79937138	0.01525518	0.79937138	0.01460181	0.76513476	0.01476199	0.77353
30	31	0.05517988	2.89142558	0.05517988	2.89142558	0.05280861	2.76717094	0.05338984	2.79763
31	32	0.09249108	4.84653273	0.09249108	4.84653273	0.08851911	4.63840112	0.08949274	4.68942
31	33	0.20280627	10.6270486	0.20280627	10.6270486	0.19409549	10.1706037	0.19623071	10.2825
33	34	0.08825665	4.6246485	0.08825665	4.6246485	0.08446524	4.42597877	0.0853946	4.47468
33	35	0.24691686	12.9384436	0.24691686	12.9384436	0.23631187	12.3827419	0.23891141	12.519
34	36	0.26896002	14.0935053	0.26896002	14.0935053	0.25740895	13.4882287	0.2602404	13.6366
36	37	0.35709409	18.7117303	0.35709409	18.7117303	0.34176192	17.9083245	0.34552027	18.1053
37	38	0.41653597	21.826485	0.41653597	21.826485	0.39866772	20.8901883	0.40304794	21.1197
38	39	0.79560572	41.6897398	0.79560572	41.6897398	0.76146486	39.9007589	0.76983401	40.3393
38	45	0.32859468	17.2183611	0.32859468	17.2183611	0.31449131	16.4793448	0.31794851	16.6605
39	40	0.29999107	15.7195319	0.29999107	15.7195319	0.2871132	15.0447315	0.29026996	15.2101
18	42	0.69556466	36.4475882	0.69556466	36.4475882	0.87813685	46.0143711	0.67306114	35.2684
42	43	0.78322578	41.0410309	0.78322578	41.0410309	0.96210048	50.4140651	0.75789827	39.7139
43	44	0.82698599	43.334066	0.82698599	43.334066	1.0039995	52.6095738	0.80025097	41.9332
45	46	1.64446441	86.1699349	1.64446441	86.1699349	1.78640525	93.6076353	1.59125438	83.3817
46	48	0.63498108	33.2730084	0.63498108	33.2730084	0.60773158	31.8451347	0.61454324	32.2021
48	49	0.10930564	5.72761571	0.10930564	5.72761571	0.10462208	5.48219684	0.10579291	5.54355
49	50	0.02186168	1.145552	0.02186168	1.145552	0.02092492	1.0964658	0.0211591	1.10874
48	47	0.50382106	26.4002236	0.50382106	26.4002236	0.48219127	25.2668228	0.48759808	25.5501
42	19	0.64503809	33.7999961	0.64503809	33.7999961	0.82971075	43.4768431	0.6241661	32.7063
Maximum Current		**1.64446441**	**86.1699349**	**1.64446441**	**86.1699349**	**1.78640525**	**93.6076353**	**1.59125438**	**83.3817**

ANNEX G: PYTHON CODE FOR SIMULATION

```
import numpy as np
import pandas as pd
import numpy as np
from pyswarm import pso
from tabulate import tabulate
from scipy.special import expit  # Sigmoid function
import csv  # For saving results to CSV files


# ANSI escape codes for bold and underline
bold = '\033[1m'
underline = '\033[4m'
reset = '\033[0m'  # Reset to default style

#Setting Base Values
I_base = 1
# Read bus data: Load the Excel file
excel_file = 'bus_data_24.xlsx'

#Storing Switch Combinations/VD/Ploss in csv file
min_P_loss = 0.1  # Example value, replace with actual value
Switch_Combination_Final = "Str"  # Example string, replace with actual value
min_VD = 0.1  # Example value, replace with actual value
Switch_Combination_Final_VD = "str"
filename = 'SC_Final.csv'
data = []

# Open the CSV file in append mode to preserve previous values
with open(filename, mode='a', newline='') as file:
    writer = csv.writer(file)
    # Optional: Write header the first time (if the file is empty)
    file.seek(0, 2)  # Move to the end of the file
    if file.tell() == 0:
        writer.writerow(["Iteration", "Variable1", "Variable2", "Variable3", "Variable4"])


#Loop for claculating load flow for different time of days ie 24 hours
for u in range(1, 25):  # 1 to 24
    #Printing Calculation Time of Day
    print(f"\n{bold}{underline}For Hour {u:0d}:{reset}")
    # Convert sheet number to string (since sheet names are string)
    sheet_name = str(u)

    # Read the sheet data into the bus_data variable
    bus_df = pd.read_excel(excel_file, sheet_name=sheet_name)
    bus_data = bus_df.to_numpy()  # Convert to NumPy array
```

```
  # Initialize a large value for min_P_loss (or use np.inf to ensure the first comparison works)
  min_P_loss = float('inf')
  min_VD = float('inf')


  #Loop for calculating load flow for different tie switch combinations
  for n in range(8):
    #Printing switching combinations
    print(f"\n Switch Combination: {n:03b}")

    LD_file_name =  f"{n:03b}.csv"
    line_df = pd.read_csv(LD_file_name)

    # Read line data from CSV
    #line_df = pd.read_csv("line_data.csv")  # Replace with actual file path if needed
    line_data = line_df.to_numpy()  # Convert to NumPy array

    # Extract the number of buses from the bus data
    n_bus = len(bus_data)

    # Identify bus types
    PQ_buses = list(bus_df[bus_df["Type"] == 1].index)
    PV_buses = list(bus_df[bus_df["Type"] == 2].index)
    slack_bus = bus_df[bus_df["Type"] == 3].index[0]  # Assuming one slack bus

    """
    print("Bus Data Loaded Successfully!")
    print("Line Data Loaded Successfully!")
    # Print the loaded data (optional)
    print("\nBus Data:")
    print(bus_df)
    print("\nLine Data:")
    print(line_df)
    """

    # Admittance matrix calculation
    Ybus = np.zeros((n_bus, n_bus), dtype=complex)
    for line in line_data:
      from_bus = int(line[0])
      to_bus = int(line[1])
      R = line[2]
      X = line[3]
      B = line[4]
      Z = R + 1j * X
      Y = 1 / Z
      Ybus[from_bus, to_bus] -= Y
      Ybus[to_bus, from_bus] -= Y
      Ybus[from_bus, from_bus] += Y + 1j * B
```

```
    Ybus[to_bus, to_bus] += Y + 1j * B

# Newton-Raphson method
def newton_raphson_load_flow(bus_data, Ybus, tol=1e-6, max_iter=10):
    n_bus = len(bus_data)
    V = bus_data[:, 2]  # Initial voltage magnitudes
    theta = bus_data[:, 3]  # Initial voltage angles
    P = bus_data[:, 4]  # Active power injections
    Q = bus_data[:, 5]  # Reactive power injections
    Qmin = bus_data[:, 6]  # Minimum reactive power limits
    Qmax = bus_data[:, 7]  # Maximum reactive power limits

    for iter in range(max_iter):
        # Calculate power mismatches
        P_calc = np.zeros(n_bus)
        Q_calc = np.zeros(n_bus)
        for i in range(n_bus):
            for j in range(n_bus):
                P_calc[i] += V[i] * V[j] * (np.real(Ybus[i, j]) * np.cos(theta[i] - theta[j]) +
                                            np.imag(Ybus[i, j]) * np.sin(theta[i] - theta[j]))
                Q_calc[i] += V[i] * V[j] * (np.real(Ybus[i, j]) * np.sin(theta[i] - theta[j]) -
                                            np.imag(Ybus[i, j]) * np.cos(theta[i] - theta[j]))

        # Power mismatches
        dP = P - P_calc
        dQ = Q - Q_calc

        # Check for convergence
        if np.max(np.abs(np.concatenate((dP[PQ_buses], dQ[PQ_buses])))) < tol:
            #print(f"Converged in {iter} iterations.")
            break

        # Jacobian matrix
        J1 = np.zeros((len(PQ_buses), len(PQ_buses)))  # dP/dtheta
        J2 = np.zeros((len(PQ_buses), len(PQ_buses)))  # dP/dV
        J3 = np.zeros((len(PQ_buses), len(PQ_buses)))  # dQ/dtheta
        J4 = np.zeros((len(PQ_buses), len(PQ_buses)))  # dQ/dV

        for i, m in enumerate(PQ_buses):
            for j, n in enumerate(PQ_buses):
                if m == n:
                    J1[i, j] = -Q_calc[m] - (V[m] ** 2) * np.imag(Ybus[m, m])
                    J2[i, j] = P_calc[m] / V[m] + V[m] * np.real(Ybus[m, m])
                    J3[i, j] = P_calc[m] - (V[m] ** 2) * np.real(Ybus[m, m])
                    J4[i, j] = Q_calc[m] / V[m] - V[m] * np.imag(Ybus[m, m])
                else:
                    J1[i, j] = V[m] * V[n] * (np.real(Ybus[m, n]) * np.sin(theta[m] - theta[n]) -
                                              np.imag(Ybus[m, n]) * np.cos(theta[m] - theta[n]))
```

```
                J2[i, j] = V[m] * (np.real(Ybus[m, n]) * np.cos(theta[m] - theta[n]) +
                                   np.imag(Ybus[m, n]) * np.sin(theta[m] - theta[n]))
                J3[i, j] = -V[m] * V[n] * (np.real(Ybus[m, n]) * np.cos(theta[m] - theta[n]) +
                                           np.imag(Ybus[m, n]) * np.sin(theta[m] - theta[n]))
                J4[i, j] = V[m] * (np.real(Ybus[m, n]) * np.sin(theta[m] - theta[n]) -
                                   np.imag(Ybus[m, n]) * np.cos(theta[m] - theta[n]))

        J = np.vstack((np.hstack((J1, J2)), np.hstack((J3, J4))))
        mismatch = np.concatenate((dP[PQ_buses], dQ[PQ_buses]))

        # Update voltage angles and magnitudes
        dX = np.linalg.solve(J, mismatch)
        dtheta = dX[:len(PQ_buses)]
        dV = dX[len(PQ_buses):]

        theta[PQ_buses] += dtheta
         V[PQ_buses] += dV

        # Handle PV bus reactive power limits
        for i in PV_buses:
            Q_calc[i] = np.sum(V[i] * V * (np.real(Ybus[i, :]) * np.sin(theta[i] - theta) -
                                           np.imag(Ybus[i, :]) * np.cos(theta[i] - theta)))
            if Q_calc[i] < Qmin[i]:
                print(f"PV bus {i} violates Qmin limit. Q_calc = {Q_calc[i]:.4f}, Qmin =
{Qmin[i]:.4f}")
                Q_calc[i] = Qmin[i]
                bus_data[i, 2] = Qmin[i] / V[i]  # Adjust voltage magnitude
            elif Q_calc[i] > Qmax[i]:
                 print(f"PV bus {i} violates Qmax limit. Q_calc = {Q_calc[i]:.4f}, Qmax =
{Qmax[i]:.4f}")
                 Q_calc[i] = Qmax[i]
                bus_data[i, 2] = Qmax[i] / V[i]  # Adjust voltage magnitude

    return V, theta, P_calc, Q_calc

# Run load flow
V, theta, P_calc, Q_calc = newton_raphson_load_flow(bus_data, Ybus)

# Compute slack bus power
def compute_slack_bus_power(V, theta, Ybus, slack_bus):
    P_slack = 0
    Q_slack = 0
    for j in range(len(V)):
        P_slack += V[slack_bus] * V[j] * (
            np.real(Ybus[slack_bus, j]) * np.cos(theta[slack_bus] - theta[j]) +
            np.imag(Ybus[slack_bus, j]) * np.sin(theta[slack_bus] - theta[j])
        )
        Q_slack += V[slack_bus] * V[j] * (
            np.real(Ybus[slack_bus, j]) * np.sin(theta[slack_bus] - theta[j]) -
```

```
            np.imag(Ybus[slack_bus, j]) * np.cos(theta[slack_bus] - theta[j])
        )
    return P_slack, Q_slack

# Compute slack bus power
P_slack, Q_slack = compute_slack_bus_power(V, theta, Ybus, slack_bus)

# Prepare results for tabular display
results = []
for i in range(len(V)):
    if i == slack_bus:
        # Use computed slack bus power
        results.append([
            i,  # Bus number
            f"{V[i]:.6f}",  # Voltage magnitude
            f"{np.degrees(theta[i]):.6f}",  # Voltage angle in degrees
            f"{P_slack:.6f}",  # Active power injection (computed)
            f"{Q_slack:.6f}",  # Reactive power injection (computed)
        ])
    else:
        results.append([
            i,  # Bus number
            f"{V[i]:.6f}",  # Voltage magnitude
            f"{np.degrees(theta[i]):.6f}",  # Voltage angle in degrees
            f"{P_calc[i]:.6f}",  # Active power injection
            f"{Q_calc[i]:.6f}",  # Reactive power injection
        ])

# Print bus results in table format
headers = ["Bus", "Voltage (pu)", "Angle (deg)", "P (pu)", "Q (pu)"]
#print("\nBus Results:")
#print(tabulate(results, headers=headers, tablefmt="grid"))

# Compute branch losses
def compute_branch_losses(V, theta, line_data):
    losses = []
    for line in line_data:
        from_bus = int(line[0])
        to_bus = int(line[1])
        R = line[2]
        X = line[3]
        Z = R + 1j * X
        Y = 1 / Z

        # Voltage difference
        V_from = V[from_bus] * np.exp(1j * theta[from_bus])
        V_to = V[to_bus] * np.exp(1j * theta[to_bus])
        dV = V_from - V_to
```

```
            # Current in the branch
            I = dV * Y
            Branch_I = abs(I)*I_base
            print(Branch_I)
             #print(from_bus)
            #print(to_bus)

            # Power loss in the branch
            P_loss = abs(I)*abs(I)*R
            Q_loss = abs(I)*abs(I)*X

            losses.append((from_bus, to_bus, P_loss, Q_loss))
        return losses

    # Calculate and print branch losses
    branch_losses = compute_branch_losses(V, theta, line_data)
    #print("\nBranch Losses:")
    #print("From Bus | To Bus | Active Power Loss (P_loss) | Reactive Power Loss (Q_loss)")
    #for loss in branch_losses:
        #print(f"{loss[0]:^8} | {loss[1]:^6} | {loss[2]:^24.6f} | {loss[3]:^24.6f}")

     # Verify power balance
    total_P_gen = P_slack + np.sum(P_calc[PV_buses])  # Total active power generated
    total_Q_gen = Q_slack + np.sum(Q_calc[PV_buses])  # Total reactive power generated
    total_P_load = -np.sum(P_calc[PQ_buses])  # Total active power load
    total_Q_load = -np.sum(Q_calc[PQ_buses])  # Total reactive power load
    total_P_loss = np.sum([loss[2] for loss in branch_losses])  # Total active power loss
    total_Q_loss = np.sum([loss[3] for loss in branch_losses])  # Total reactive power loss

    #Calculation of Minimal Total Power Loss and Combination of Tie Switches for Minimal Power Loss
    if total_P_loss < min_P_loss:
         min_P_loss = total_P_loss
        Switch_Combination = f"{n:03b}"
        # Invert the binary string: Replace '1' with '0' and '0' with '1'
         opposite_logic = ''.join('0' if bit == '1' else '1' for bit in Switch_Combination)

        # Concatenate the original and inverted strings
         Switch_Combination_Final = Switch_Combination + opposite_logic

    min_VD_value = float(min(row[1] for row in results)) #Convert str to float for data in list named "results"
     if min_VD_value < min_VD:
        min_VD = min_VD_value
        Switch_Combination_VD = f"{n:03b}"
        # Invert the binary string: Replace '1' with '0' and '0' with '1'
        opposite_logic_VD = ''.join('0' if bit == '1' else '1' for bit in Switch_Combination_VD)
```

```
            # Concatenate the original and inverted strings
            Switch_Combination_Final_VD = Switch_Combination_VD + opposite_logic_VD

        """
        print(f"\nPower Balance Verification for Switch Combination of:{n:03b}")
        print(f"Total P Generated: {total_P_gen:.6f}")
        print(f"Total P Load: {total_P_load:.6f}")
        print(f"Total P Loss: {total_P_loss:.6f}")
        print(f"Total P Generated = Total P Load + Total P Loss: {np.isclose(total_P_gen, total_P_load + total_P_loss, atol=1e-6)}")

        print(f"\nTotal Q Generated: {total_Q_gen:.6f}")
        print(f"Total Q Load: {total_Q_load:.6f}")
        print(f"Total Q Loss: {total_Q_loss:.6f}")
        print(f"Total Q Generated = Total Q Load + Total Q Loss: {np.isclose(total_Q_gen, total_Q_load + total_Q_loss, atol=1e-6)}")
        """
        #Saving in CSV File

         # Save bus results to a CSV file
        bus_results_file = f"Hour_{u:0d}_Bus_Result_for_SC_{n:03b}.csv"
        with open(bus_results_file, mode="w", newline="") as file:
            writer = csv.writer(file)
            writer.writerow(headers)  # Write headers
            writer.writerows(results)  # Write data rows
        #print(f"\nBus results saved to {bus_results_file}.")

        # Save branch losses to a CSV file
        branch_losses_file = f"Hour_{u:0d}_Branch_Result_for_SC_{n:03b}.csv"
        with open(branch_losses_file, mode="w", newline="") as file:
            writer = csv.writer(file)
            writer.writerow(["From Bus", "To Bus", "Active Power Loss (P_loss)", "Reactive Power Loss (Q_loss)"])
            writer.writerows(branch_losses)
        #print(f"Branch losses saved to {branch_losses_file}.")

    print(f"\n{bold}{underline}For Hour {u:0d}:{reset}")
    print(f"\n Minimal Loss: {min_P_loss}")
    print(f"\n Switch Combination for Power Loss: {Switch_Combination_Final}")

    print(f"\n Minimal VD: {min_VD}")
    print(f"\n Switch Combination for VD: {Switch_Combination_Final_VD}")

    variable1 = np.float64(min_P_loss)  # Example update
    variable2 = str(Switch_Combination_Final)  # Example update, variable2 is a string
    variable3 = np.float64(min_VD)  # Example update
    variable4 = str(Switch_Combination_Final_VD)  # Example update, variable4 is a string

    data.append([u, str(variable1), str(variable2), str(variable3), str(variable4)])
```

```
# Open the CSV file in write mode (overwriting previous content, or creating a new file if it doesn't exist)
with open(filename, mode='w', newline='') as file:
    writer = csv.writer(file)

    # Write the header
    writer.writerow(["Time of Day", "Minimal System Loss", "SC for Minimal Ploss", "Minimum Bus Voltage", "SC for Mininal VD"])
    for row in data:
        # Ensure that the binary-like variables are treated as strings (adding quotes around them)
        row = [f"'{item}'" if isinstance(item, str) and (item.startswith("0") or len(item) > 3) else item for item in row]
        writer.writerow(row)
    # Write all the collected data
    #writer.writerows(data)
#print(data) import numpy as np
import pandas as pd
import numpy as np
from pyswarm import pso
from tabulate import tabulate
from scipy.special import expit  # Sigmoid function
import csv  # For saving results to CSV files


# ANSI escape codes for bold and underline
bold = '\033[1m'
underline = '\033[4m'
reset = '\033[0m'  # Reset to default style

#Setting Base Values
I_base = 1
# Read bus data: Load the Excel file
excel_file = 'bus_data_24.xlsx'

#Storing Switch Combinations/VD/Ploss in csv file
min_P_loss = 0.1  # Example value, replace with actual value
Switch_Combination_Final = "Str"  # Example string, replace with actual value
min_VD = 0.1  # Example value, replace with actual value
Switch_Combination_Final_VD = "str"
filename = 'SC_Final.csv'
data = []

# Open the CSV file in append mode to preserve previous values
with open(filename, mode='a', newline='') as file:
    writer = csv.writer(file)
    # Optional: Write header the first time (if the file is empty)
    file.seek(0, 2)  # Move to the end of the file
    if file.tell() == 0:
```

```
        writer.writerow(["Iteration", "Variable1", "Variable2", "Variable3", "Variable4"])


#Loop for claculating load flow for different time of days ie 24 hours
for u in range(1, 25):  # 1 to 24
    #Printing Calculation Time of Day
    print(f"\n{bold}{underline}For Hour {u:0d}:{reset}")
    # Convert sheet number to string (since sheet names are string)
    sheet_name = str(u)

    # Read the sheet data into the bus_data variable
    bus_df = pd.read_excel(excel_file, sheet_name=sheet_name)
    bus_data = bus_df.to_numpy()  # Convert to NumPy array


    # Initialize a large value for min_P_loss (or use np.inf to ensure the first comparison
works)
    min_P_loss = float('inf')
    min_VD = float('inf')


    #Loop for calculating load flow for different tie switch combinations
    for n in range(8):
        #Printing switching combinations
        print(f"\n Switch Combination: {n:03b}")

        LD_file_name =  f"{n:03b}.csv"
        line_df = pd.read_csv(LD_file_name)

        # Read line data from CSV
        #line_df = pd.read_csv("line_data.csv")  # Replace with actual file path if needed
        line_data = line_df.to_numpy()  # Convert to NumPy array

        # Extract the number of buses from the bus data
        n_bus = len(bus_data)

        # Identify bus types
        PQ_buses = list(bus_df[bus_df["Type"] == 1].index)
        PV_buses = list(bus_df[bus_df["Type"] == 2].index)
        slack_bus = bus_df[bus_df["Type"] == 3].index[0]  # Assuming one slack bus

        """
        print("Bus Data Loaded Successfully!")
        print("Line Data Loaded Successfully!")
        # Print the loaded data (optional)
        print("\nBus Data:")
        print(bus_df)
        print("\nLine Data:")
        print(line_df)
        """
```

```
# Admittance matrix calculation
Ybus = np.zeros((n_bus, n_bus), dtype=complex)
for line in line_data:
    from_bus = int(line[0])
    to_bus = int(line[1])
    R = line[2]
    X = line[3]
    B = line[4]
    Z = R + 1j * X
    Y = 1 / Z
    Ybus[from_bus, to_bus] -= Y
    Ybus[to_bus, from_bus] -= Y
    Ybus[from_bus, from_bus] += Y + 1j * B
    Ybus[to_bus, to_bus] += Y + 1j * B

# Newton-Raphson method
def newton_raphson_load_flow(bus_data, Ybus, tol=1e-6, max_iter=10):
    n_bus = len(bus_data)
    V = bus_data[:, 2]  # Initial voltage magnitudes
    theta = bus_data[:, 3]  # Initial voltage angles
    P = bus_data[:, 4]  # Active power injections
    Q = bus_data[:, 5]  # Reactive power injections
    Qmin = bus_data[:, 6]  # Minimum reactive power limits
    Qmax = bus_data[:, 7]  # Maximum reactive power limits

    for iter in range(max_iter):
        # Calculate power mismatches
        P_calc = np.zeros(n_bus)
        Q_calc = np.zeros(n_bus)
        for i in range(n_bus):
            for j in range(n_bus):
                P_calc[i] += V[i] * V[j] * (np.real(Ybus[i, j]) * np.cos(theta[i] - theta[j]) +
                                            np.imag(Ybus[i, j]) * np.sin(theta[i] - theta[j]))
                Q_calc[i] += V[i] * V[j] * (np.real(Ybus[i, j]) * np.sin(theta[i] - theta[j]) -
                                            np.imag(Ybus[i, j]) * np.cos(theta[i] - theta[j]))

        # Power mismatches
        dP = P - P_calc
        dQ = Q - Q_calc

        # Check for convergence
        if np.max(np.abs(np.concatenate((dP[PQ_buses], dQ[PQ_buses])))) < tol:
            #print(f"Converged in {iter} iterations.")
            break

        # Jacobian matrix
        J1 = np.zeros((len(PQ_buses), len(PQ_buses)))  # dP/dtheta
        J2 = np.zeros((len(PQ_buses), len(PQ_buses)))  # dP/dV
```

```
        J3 = np.zeros((len(PQ_buses), len(PQ_buses)))  # dQ/dtheta
        J4 = np.zeros((len(PQ_buses), len(PQ_buses)))  # dQ/dV

        for i, m in enumerate(PQ_buses):
            for j, n in enumerate(PQ_buses):
                if m == n:
                    J1[i, j] = -Q_calc[m] - (V[m] ** 2) * np.imag(Ybus[m, m])
                    J2[i, j] = P_calc[m] / V[m] + V[m] * np.real(Ybus[m, m])
                    J3[i, j] = P_calc[m] - (V[m] ** 2) * np.real(Ybus[m, m])
                    J4[i, j] = Q_calc[m] / V[m] - V[m] * np.imag(Ybus[m, m])
                else:
                    J1[i, j] = V[m] * V[n] * (np.real(Ybus[m, n]) * np.sin(theta[m] - theta[n]) -
                                              np.imag(Ybus[m, n]) * np.cos(theta[m] - theta[n]))
                    J2[i, j] = V[m] * (np.real(Ybus[m, n]) * np.cos(theta[m] - theta[n]) +
                                       np.imag(Ybus[m, n]) * np.sin(theta[m] - theta[n]))
                    J3[i, j] = -V[m] * V[n] * (np.real(Ybus[m, n]) * np.cos(theta[m] - theta[n]) +
                                               np.imag(Ybus[m, n]) * np.sin(theta[m] - theta[n]))
                    J4[i, j] = V[m] * (np.real(Ybus[m, n]) * np.sin(theta[m] - theta[n]) -
                                       np.imag(Ybus[m, n]) * np.cos(theta[m] - theta[n]))

        J = np.vstack((np.hstack((J1, J2)), np.hstack((J3, J4))))
        mismatch = np.concatenate((dP[PQ_buses], dQ[PQ_buses]))

        # Update voltage angles and magnitudes
        dX = np.linalg.solve(J, mismatch)
        dtheta = dX[:len(PQ_buses)]
        dV = dX[len(PQ_buses):]

        theta[PQ_buses] += dtheta
        V[PQ_buses] += dV

        # Handle PV bus reactive power limits
        for i in PV_buses:
            Q_calc[i] = np.sum(V[i] * V * (np.real(Ybus[i, :]) * np.sin(theta[i] - theta) -
                                           np.imag(Ybus[i, :]) * np.cos(theta[i] - theta)))
            if Q_calc[i] < Qmin[i]:
                print(f"PV bus {i} violates Qmin limit. Q_calc = {Q_calc[i]:.4f}, Qmin =
{Qmin[i]:.4f}")
                Q_calc[i] = Qmin[i]
                bus_data[i, 2] = Qmin[i] / V[i]  # Adjust voltage magnitude
            elif Q_calc[i] > Qmax[i]:
                print(f"PV bus {i} violates Qmax limit. Q_calc = {Q_calc[i]:.4f}, Qmax =
{Qmax[i]:.4f}")
                Q_calc[i] = Qmax[i]
                bus_data[i, 2] = Qmax[i] / V[i]  # Adjust voltage magnitude

    return V, theta, P_calc, Q_calc
```

```
# Run load flow
V, theta, P_calc, Q_calc = newton_raphson_load_flow(bus_data, Ybus)

# Compute slack bus power
def compute_slack_bus_power(V, theta, Ybus, slack_bus):
    P_slack = 0
    Q_slack = 0
    for j in range(len(V)):
        P_slack += V[slack_bus] * V[j] * (
            np.real(Ybus[slack_bus, j]) * np.cos(theta[slack_bus] - theta[j]) +
             np.imag(Ybus[slack_bus, j]) * np.sin(theta[slack_bus] - theta[j])
         )
        Q_slack += V[slack_bus] * V[j] * (
             np.real(Ybus[slack_bus, j]) * np.sin(theta[slack_bus] - theta[j]) -
            np.imag(Ybus[slack_bus, j]) * np.cos(theta[slack_bus] - theta[j])
         )
    return P_slack, Q_slack

# Compute slack bus power
P_slack, Q_slack = compute_slack_bus_power(V, theta, Ybus, slack_bus)

# Prepare results for tabular display
results = []
for i in range(len(V)):
    if i == slack_bus:
        # Use computed slack bus power
        results.append([
            i,  # Bus number
             f"{V[i]:.6f}",  # Voltage magnitude
              f"{np.degrees(theta[i]):.6f}",  # Voltage angle in degrees
             f"{P_slack:.6f}",  # Active power injection (computed)
             f"{Q_slack:.6f}",  # Reactive power injection (computed)
         ])
    else:
         results.append([
             i,  # Bus number
             f"{V[i]:.6f}",  # Voltage magnitude
             f"{np.degrees(theta[i]):.6f}",  # Voltage angle in degrees
             f"{P_calc[i]:.6f}",  # Active power injection
             f"{Q_calc[i]:.6f}",  # Reactive power injection
         ])

# Print bus results in table format
headers = ["Bus", "Voltage (pu)", "Angle (deg)", "P (pu)", "Q (pu)"]
#print("\nBus Results:")
 #print(tabulate(results, headers=headers, tablefmt="grid"))

# Compute branch losses
def compute_branch_losses(V, theta, line_data):
```

```
        losses = []
        for line in line_data:
            from_bus = int(line[0])
            to_bus = int(line[1])
            R = line[2]
            X = line[3]
            Z = R + 1j * X
            Y = 1 / Z

            # Voltage difference
            V_from = V[from_bus] * np.exp(1j * theta[from_bus])
            V_to = V[to_bus] * np.exp(1j * theta[to_bus])
            dV = V_from - V_to

            # Current in the branch
             I = dV * Y
            Branch_I = abs(I)*I_base
            print(Branch_I)
            #print(from_bus)
            #print(to_bus)

             # Power loss in the branch
            P_loss = abs(I)*abs(I)*R
            Q_loss = abs(I)*abs(I)*X

            losses.append((from_bus, to_bus, P_loss, Q_loss))
        return losses

    # Calculate and print branch losses
    branch_losses = compute_branch_losses(V, theta, line_data)
    #print("\nBranch Losses:")
    #print("From Bus | To Bus | Active Power Loss (P_loss) | Reactive Power Loss (Q_loss)")
    #for loss in branch_losses:
        #print(f"{loss[0]:^8} | {loss[1]:^6} | {loss[2]:^24.6f} | {loss[3]:^24.6f}")

    # Verify power balance
    total_P_gen = P_slack + np.sum(P_calc[PV_buses])  # Total active power generated
    total_Q_gen = Q_slack + np.sum(Q_calc[PV_buses])  # Total reactive power generated
    total_P_load = -np.sum(P_calc[PQ_buses])  # Total active power load
    total_Q_load = -np.sum(Q_calc[PQ_buses])  # Total reactive power load
    total_P_loss = np.sum([loss[2] for loss in branch_losses])  # Total active power loss
    total_Q_loss = np.sum([loss[3] for loss in branch_losses])  # Total reactive power loss

    #Calculation of Minimal Total Power Loss and Combination of Tie Switches for Minimal Power Loss
    if total_P_loss < min_P_loss:
        min_P_loss = total_P_loss
        Switch_Combination = f"{n:03b}"
```

```
            # Invert the binary string: Replace '1' with '0' and '0' with '1'
             opposite_logic = ''.join('0' if bit == '1' else '1' for bit in Switch_Combination)

            # Concatenate the original and inverted strings
             Switch_Combination_Final = Switch_Combination + opposite_logic

        min_VD_value = float(min(row[1] for row in results)) #Convert str to float for data in list named "results"
        if min_VD_value < min_VD:
            min_VD = min_VD_value
            Switch_Combination_VD = f"{n:03b}"
            # Invert the binary string: Replace '1' with '0' and '0' with '1'
            opposite_logic_VD = ''.join('0' if bit == '1' else '1' for bit in Switch_Combination_VD)

            # Concatenate the original and inverted strings
            Switch_Combination_Final_VD = Switch_Combination_VD + opposite_logic_VD

        """
        print(f"\nPower Balance Verification for Switch Combination of:{n:03b}")
        print(f"Total P Generated: {total_P_gen:.6f}")
        print(f"Total P Load: {total_P_load:.6f}")
        print(f"Total P Loss: {total_P_loss:.6f}")
        print(f"Total P Generated = Total P Load + Total P Loss: {np.isclose(total_P_gen, total_P_load + total_P_loss, atol=1e-6)}")

        print(f"\nTotal Q Generated: {total_Q_gen:.6f}")
        print(f"Total Q Load: {total_Q_load:.6f}")
        print(f"Total Q Loss: {total_Q_loss:.6f}")
        print(f"Total Q Generated = Total Q Load + Total Q Loss: {np.isclose(total_Q_gen, total_Q_load + total_Q_loss, atol=1e-6)}")
        """
        #Saving in CSV File

         # Save bus results to a CSV file
        bus_results_file = f"Hour_{u:0d}_Bus_Result_for_SC_{n:03b}.csv"
        with open(bus_results_file, mode="w", newline="") as file:
            writer = csv.writer(file)
             writer.writerow(headers)  # Write headers
            writer.writerows(results)  # Write data rows
        #print(f"\nBus results saved to {bus_results_file}.")

        # Save branch losses to a CSV file
        branch_losses_file = f"Hour_{u:0d}_Branch_Result_for_SC_{n:03b}.csv"
        with open(branch_losses_file, mode="w", newline="") as file:
            writer = csv.writer(file)
            writer.writerow(["From Bus", "To Bus", "Active Power Loss (P_loss)", "Reactive Power Loss (Q_loss)"])
            writer.writerows(branch_losses)
        #print(f"Branch losses saved to {branch_losses_file}.")
```

```
    print(f"\n{bold}{underline}For Hour {u:0d}:{reset}")
    print(f"\n Minimal Loss: {min_P_loss}")
    print(f"\n Switch Combination for Power Loss: {Switch_Combination_Final}")

    print(f"\n Minimal VD: {min_VD}")
    print(f"\n Switch Combination for VD: {Switch_Combination_Final_VD}")

    variable1 = np.float64(min_P_loss)  # Example update
    variable2 = str(Switch_Combination_Final)  # Example update, variable2 is a string
    variable3 = np.float64(min_VD)  # Example update
    variable4 = str(Switch_Combination_Final_VD)  # Example update, variable4 is a string

    data.append([u, str(variable1), str(variable2), str(variable3), str(variable4)])

# Open the CSV file in write mode (overwriting previous content, or creating a new file if it doesn't exist)
with open(filename, mode='w', newline='') as file:
    writer = csv.writer(file)

    # Write the header
    writer.writerow(["Time of Day", "Minimal System Loss", "SC for Minimal Ploss", "Minimum Bus Voltage", "SC for Mininal VD"])
    for row in data:
        # Ensure that the binary-like variables are treated as strings (adding quotes around them)
        row = [f"'{item}'" if isinstance(item, str) and (item.startswith("0") or len(item) > 3) else item for item in row]
        writer.writerow(row)
    # Write all the collected data
    #writer.writerows(data)
#print(data)
```

ANNEX H: PUBLICATION PAPER

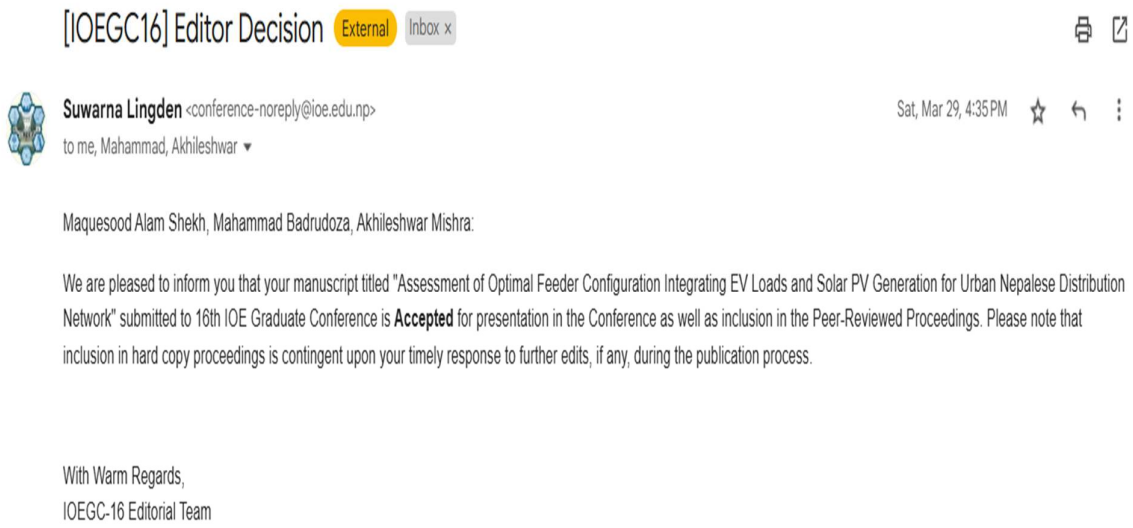

[IOEGC16] Editor Decision External Inbox x

Suwarna Lingden <conference-noreply@ioe.edu.np> Sat, Mar 29, 4:35 PM

to me, Mahammad, Akhileshwar

Maquesood Alam Shekh, Mahammad Badrudoza, Akhileshwar Mishra:

We are pleased to inform you that your manuscript titled "Assessment of Optimal Feeder Configuration Integrating EV Loads and Solar PV Generation for Urban Nepalese Distribution Network" submitted to 16th IOE Graduate Conference is **Accepted** for presentation in the Conference as well as inclusion in the Peer-Reviewed Proceedings. Please note that inclusion in hard copy proceedings is contingent upon your timely response to further edits, if any, during the publication process.

With Warm Regards,
IOEGC-16 Editorial Team

Assessment of Optimal Feeder Configuration Integrating EV Loads and Solar PV Generation for Urban Nepalese Distribution Network

Shekh Maquesood Alam [a], Mahammad Badrudoza [b], Akhileshwar Mishra [c]

[a,b,c] *Department of Electrical Engineering, Institute of Engineering, Pulchowk Campus*

[a] 079mspse021.shekh@pcampus.edu.np [b] mbadrudoza@ioe.edu.np [c] akhileshwar@ioe.edu.np

Abstract

With Nepal's ongoing transition to renewable energy sources and the increasing adoption of electric vehicles, the existing distribution networks are encountering critical challenges, including power losses, voltage instability, and inefficiencies in energy usage. This work investigates the optimization of radial-loop configurations for urban distribution networks in Nepal, focusing on the integration of Electric Vehicle (EV) charging loads and solar Photovoltaic (PV) systems. The most efficient radial-loop configurations that minimize line losses, reduce voltage fluctuations, and improve overall system performance is proposed and tested for an urban distribution network at Nepal Electricity Authority (NEA), Nuwakot Distribution Center (NDC). Through advanced simulation and modeling techniques, this study evaluates the impact of various configurations on the power flow, line losses, and voltage profile of the distribution system. Additionally, it explores the potential benefits of incorporating solar PV systems and EV charging infrastructure, aiming to optimize power distribution while enhancing reliability and minimizing operational costs. The results of the study present an effective control strategy for radial and loop distribution feeders by utilizing optimal tie switch operations for utility operators. Also, the findings of this research will provide valuable insights and practical recommendations for policymakers, utility operators, and engineers, supporting the design of more sustainable, resilient, and efficient urban power distribution networks in Nepal.

Keywords

Radial-Loop Configuration, Electric Vehicle (EV), Solar Photovoltaic (PV), Urban Distribution, Power Losses, Voltage Stability

1. Introduction

1.1 Background

The integration of renewable energy sources such as solar photovoltaic (PV) systems and the increasing penetration of electric vehicles (EVs) present significant opportunities and challenges for modern electrical distribution networks. As the transition to clean energy accelerates, optimizing the design and operation of distribution systems has become essential to ensure reliability, efficiency, and sustainability. Among various network configurations, radial-loop systems offer a promising solution by balancing the trade-off between installation cost, system reliability, and operational efficiency [1]. In particular, the addition of EVs and solar PV systems into the grid poses unique challenges, primarily concerning the management of increased energy demand and intermittent renewable generation. EVs, with their growing adoption, represent a substantial load on distribution networks, potentially exacerbating issues like voltage fluctuation and line loss [2]. Meanwhile, solar PV systems, though beneficial for reducing the carbon footprint, contribute to voltage fluctuations due to their variable generation patterns [3]. Thus, it is critical to assess and optimize the radial-loop configuration of distribution networks, considering these new loads and generation sources, to minimize line losses and maintain voltage stability.

The rapid growth of renewable energy technologies and electric mobility presents both significant opportunities and challenges for power distribution networks worldwide. In Nepal, the increasing integration of solar Photovoltaic (PV) systems and the growing adoption of Electric Vehicles (EVs) are transforming the energy landscape, especially in urban areas. Nepal's energy sector, historically reliant on hydropower, is undergoing a shift towards decentralized renewable energy sources such as solar PV, which contributes to reducing dependency on conventional grid power [4]. However, the integration of these technologies into the existing distribution networks, particularly in urban areas, poses several challenges, including voltage instability and higher line losses, due to the unpredictable nature of renewable generation and the fluctuating demand from EV charging stations [5]. Conventional radial distribution systems, which are commonly used in Nepalese cities, have limitations in handling bidirectional power flow and distributed energy resources. These systems often face issues such as line losses, voltage drops, and low system reliability when new loads like EVs and renewable generation sources like solar PV are integrated [6]. As such, there is a pressing need to optimize the configuration of these networks to ensure better integration of distributed energy, mitigate losses, and enhance voltage stability.

This research aims to assess the optimal radial-loop configuration for urban Nepalese distribution networks, focusing on the integration of EV loads and solar PV systems. By evaluating different radial-loop configurations, the study will explore strategies to minimize line losses and reduce voltage fluctuations, thus enhancing the efficiency and reliability of the network. The results of this work are expected to provide valuable insights for policymakers, utility companies, and engineers in Nepal, helping to design more robust and efficient distribution systems that can better accommodate the increasing demand for renewable energy

and electric vehicles in urban areas. This research will contribute to the growing body of knowledge on optimizing power distribution networks in developing countries, with a specific focus on Nepal's unique energy challenges.

1.2 Problem Statement

The integration of renewable energy sources, particularly solar Photovoltaic (PV) systems, and the increasing adoption of Electric Vehicles (EVs) in urban areas present significant challenges for power distribution networks. In Nepal, the transition towards decentralized energy generation and electric mobility is accelerating, but the existing distribution infrastructure, especially in urban centers, is not adequately equipped to handle the complexities introduced by these technologies. As a result, issues such as increased line losses, voltage fluctuations, and grid instability have become prominent, jeopardizing the reliability and efficiency of power supply in urban Nepalese distribution networks.

Traditional radial distribution networks, which are commonly employed in Nepal, are inherently limited in their ability to manage bidirectional power flow, a characteristic feature of distributed generation systems such as solar PV. Additionally, the unpredictable charging demands of EVs, particularly during peak hours, exacerbate these challenges, leading to inefficiencies in power distribution. Current feeder configurations, which primarily focus on conventional loads and infrastructure, fail to optimize for the dual integration of renewable energy and EVs, leaving the distribution system vulnerable to inefficiencies and performance degradation.

This research seeks to address these issues by exploring the optimal radial-loop configuration for urban Nepalese distribution networks, specifically incorporating the integration of EV loads and solar PV systems. The primary objective is to identify a configuration that minimizes line losses, reduces voltage fluctuations, and enhances overall system stability and reliability in the face of increasing demand and renewable energy generation. The study will develop models and optimization techniques tailored to the specific needs of Nepalese distribution systems, focusing on their unique operational challenges, such as high line losses, voltage instability, and the lack of advanced grid management infrastructure.

The problem is multifaceted, as it involves:

- The need for an optimized configuration that accounts for both solar PV generation and EV load demands, which vary throughout the day.
- The requirement for advanced optimization algorithms that can address these challenges in a computationally efficient manner, suitable for real-time application in a developing country context.
- The necessity of proposing a configuration that not only minimizes technical losses but also ensures voltage stability, thereby improving the quality and reliability of electricity supply in urban areas.

Addressing this problem will contribute to the development of more sustainable, resilient, and efficient power distribution networks in Nepal, enabling the successful integration of renewable energy sources and electric mobility into the national grid. The results of this study have the potential to inform energy policy and utility strategies, ultimately helping to enhance the performance and stability of Nepal's urban power distribution systems.

1.3 Research Objective

The main objective of this research is to assess and identify the optimal radial-loop configuration for the urban distribution network at NEA, Nuwakot Distribution Center that integrates Electric Vehicle (EV) loads and solar Photovoltaic (PV) systems, intending to minimize line losses, reducing voltage fluctuations, and improving overall system stability and reliability. This optimization will enhance the efficiency of the distribution network while accommodating the growing adoption of renewable energy and electric vehicles in Nuwakot, Nepal. While the specific objectives are:

- To assess how the inclusion of both EV charging stations and solar PV generation affects the performance of distribution networks at the urban area of Nuwakot Distribution Center, particularly in terms of power losses, voltage stability, and load demand fluctuations.
- To develop models of various radial-loop configurations for distribution systems at Nuwakot DC that incorporate EV loads and solar PV systems. Simulate these models to analyze their performance under different operational conditions.
- To optimize the feeder configuration to determine the most efficient feeder configuration that minimizes line losses in the distribution network.
- To improve voltage stability and minimize voltage fluctuations caused by the integration of distributed generation and fluctuating EV charging demand.

1.4 Research Scopes and Limitations

Scope of the study: This research will focus on the assessment of optimal radial-loop configurations for urban Nepalese distribution networks, incorporating Electric Vehicle (EV) loads and solar Photovoltaic (PV) systems. While the findings may have broader applications, the primary context is based on the challenges and characteristics of Nepalese cities, where the integration of renewable energy and EVs is rapidly increasing. This research will consider the integration of solar PV systems and EV charging infrastructure into the existing power distribution network. The study will not cover other forms of renewable energy (such as wind or biomass) or advanced technologies like energy storage systems, which are outside the scope.

The optimization will address issues such as minimizing line losses, improving voltage stability, and enhancing system reliability while integrating the dynamic loads from EVs and the intermittent nature of solar energy. The study will consider different timeframes for the simulation of EV charging demand and solar generation, focusing on daily and seasonal variations. However, it will not delve into long-term grid expansion planning or explore multi-year dynamics. The research will use computer simulations to model various

feeder configurations and evaluate their performance under different operating conditions, considering factors such as load variation, solar generation, and EV demand.

Limitations of Study: Despite the comprehensive approach, several limitations exist in this study:

- The study's findings may be limited by the availability and accuracy of data on the actual distribution network infrastructure, solar PV generation, and EV load profiles in urban Nepalese settings.
- During optimization process, certain assumptions will need to be made, such as uniform load distribution, standard operating conditions, and average solar generation profiles. These assumptions may not fully reflect the complexity of real-world conditions.
- The study will focus on radial-loop feeder configurations, which may not address all potential network optimization scenarios.
- The study will assume representative load profiles, but these assumptions may not fully capture the actual variability in EV charging demand, especially during peak times or in the event of unexpected EV adoption surges.
- The focus of the research will be primarily on solar PV and EVs, without considering other distributed energy resources like wind or energy storage systems.

2. Literature Review

Different studies have been carried out to provide optimal radial and loop feeder configuration in a distribution network reducing the line loss and voltage drop. Following subsections provide review of the different studies carried on distribution system feeder optimization till now and the research gap between past studies and considerations of this research to address such research gap.

2.1 Previous Studies

Over the years, numerous studies have been conducted on the optimization of distribution system feeders, focusing on improving the efficiency and reliability of electrical power distribution networks. These studies have primarily concentrated on minimizing power losses, enhancing voltage stability, and ensuring the effective integration of distributed energy resources (DERs) such as solar PV systems and electric vehicles (EVs). Radial distribution networks are typically the default configuration in many power systems due to their simplicity and low installation costs. However, they are often less reliable, as any fault or failure at a single point can cause a large portion of the network to go offline [7]. In contrast, looped networks, which connect various points in a closed-loop configuration, can provide higher reliability and flexibility by offering alternative paths for electricity flow during faults or disturbances. While looped systems have higher installation costs and are more complex to operate, they can reduce system losses and improve voltage regulation [8].

The literature highlights that the optimal configuration between radial and looped systems often depends on various factors, including cost, reliability, load patterns, and integration of renewable energy sources. A hybrid approach, involving both radial and looped topologies, has been proposed as a solution to combine the cost-efficiency of radial networks with the reliability benefits of looped systems. Studies by [9] suggest that such hybrid configurations could help optimize the trade-off between system losses and reliability, especially when coupled with distributed energy resources like solar PVs and EV charging stations. The incorporation of solar PV systems into distribution networks has been widely recognized for its potential to reduce dependency on fossil-fuel-based generation and decrease greenhouse gas emissions [10]. However, solar PVs also introduce challenges, primarily due to their intermittent and variable nature. As PV output fluctuates with weather conditions, it can lead to voltage instability and significant power quality issues such as voltage fluctuations and over-voltages during periods of high solar generation [3].

Early research in distribution system optimization focused on minimizing power losses through techniques such as load flow analysis, optimal placement of transformers, and feeder reconfiguration. For example, studies by [11] emphasized the importance of reconfiguring feeders in radial distribution networks to reduce losses and enhance voltage profiles. Various optimization algorithms, such as genetic algorithms (GA), particle swarm optimization (PSO), and simulated annealing (SA), were applied to solve these problems, yielding improved efficiency and lower operational costs in the distribution system. Recent advancements in optimization techniques have shown that Particle Swarm Optimization (PSO) is a powerful and efficient method for solving various problems related to optimal feeder configuration. In particular, the integration of Electric Vehicle (EV) charging loads and solar Photovoltaic (PV) generation into the optimization models has presented new challenges and opportunities for improving the efficiency and reliability of distribution systems.

A study on [12] used PSO for optimal feeder reconfiguration to minimize power loss in radial distribution systems. The authors demonstrated that PSO could efficiently optimize feeder switches, resulting in reduced losses and improved voltage stability. Similarly, [13] used PSO to find the optimal placement of distributed generation (DG) units in distribution systems, taking into account both active and reactive power flow, and minimizing feeder losses. This method showed significant improvements in system efficiency and reduced operational costs. Study in [14] proposed a PSO-based method for optimal feeder reconfiguration that integrates the impact of EV charging loads. The study demonstrated that PSO could adapt to fluctuating EV demands, allowing for optimal feeder reconfiguration and load balancing in real-time. The authors highlighted the advantage of PSO in handling the uncertainty and variability of EV charging patterns, which can be highly dynamic, by adjusting the configuration to optimize power distribution.

Another study by [15] focused on the combined optimization of EV charging stations and distribution network configuration. They used PSO to determine the optimal location and size of EV charging stations while minimizing power loss and ensuring voltage stability under varying EV

charging loads. Study by [16] proposed a PSO-based approach for optimal feeder configuration that incorporated both EV charging and solar PV generation. The study focused on reducing power losses and improving the voltage profile while accounting for the variability of both EV and PV. The authors demonstrated that PSO, through its ability to explore a large solution space, was able to find optimal feeder configurations that minimized losses while maintaining voltage stability in the presence of uncertain load and generation patterns. They also highlighted the advantage of PSO in handling the stochastic nature of renewable energy generation and EV charging loads. In [17] extended this work by integrating battery storage systems into the optimization model. The authors used PSO to determine the optimal configuration of feeders, placement of solar PV systems, EV charging stations, and energy storage units. The study aimed to reduce the impact of EV charging on the feeder network and to enhance the reliability of the system under varying renewable energy generation. The results showed that PSO effectively managed the dynamic fluctuations in both solar power generation and EV load while ensuring that voltage profiles were maintained and system losses minimized.

Recent studies have shifted towards integrating renewable energy sources and EVs into distribution systems. For instance, [18] presented a feeder optimization approach for systems incorporating both solar PV and EV loads, aiming to mitigate issues like voltage fluctuations and unbalanced loads. The study highlighted the challenges of bidirectional power flow and the need for dynamic adjustments to the feeder configuration to accommodate the intermittent nature of solar energy and the variable demand from EV charging stations. Similarly, [19] explored the optimal configuration of distribution feeders in the presence of EVs and distributed energy sources, proposing a hybrid optimization technique that considers both operational constraints and economic factors.

In the context of Nepal, which is experiencing an increasing adoption of solar PV and EVs, several studies have been carried out to assess the integration of these technologies into the country's distribution networks. For example, [20] examined the impact of solar PV integration on the existing radial distribution systems in urban Nepal, identifying issues related to voltage instability and high line losses. They proposed the use of advanced optimization techniques to enhance the distribution network's performance, including feeder reconfiguration and voltage regulation. Overall, the body of literature demonstrates the growing importance of optimizing distribution system feeders in the face of new challenges posed by renewable energy integration and electric mobility. Many studies suggest that an optimal radial-loop configuration, particularly in urban areas, can significantly improve system performance by minimizing line losses and voltage deviations. However, research on optimizing feeders for Nepal's specific distribution systems, considering both EV loads and solar PV systems, remains limited and warrants further investigation.

2.2 Research Gap

While significant progress has been made in the optimization of distribution system feeders, particularly with the integration of renewable energy sources (such as solar PV) and Electric Vehicle (EV) loads, several gaps remain in the existing literature. These gaps highlight areas where further research is required to improve the performance and efficiency of distribution networks, especially in the context of urban areas in developing countries like Nepal. This subsection discusses the research gaps identified from past studies and outlines the considerations of this research to address these gaps.

One of the primary gaps in past studies is the limited focus on the integration of both solar PV systems and EV loads simultaneously in the optimization of distribution system feeders. While many studies have addressed feeder optimization with either solar energy or EV loads in isolation, there is a lack of research that simultaneously considers the interaction between these two emerging technologies. The combined impact of variable solar generation and fluctuating EV charging demands on the distribution network has not been fully explored, especially in the context of urban Nepalese networks, where the adoption of both technologies is growing rapidly. Most studies [18], [19] have concentrated on optimizing distribution feeders for either renewable energy or EVs, but not both in an integrated manner, leading to a limited understanding of how these factors interact within a single network.

Another significant gap is the application of optimization techniques to Nepal's specific distribution system configurations. Much of the existing research, such as that by [11] and [20], has primarily focused on developed countries with advanced infrastructure or on generalized models of distribution networks. These studies do not adequately address the unique characteristics of Nepal's distribution systems, which are often more decentralized, face high levels of power loss, and experience voltage instability due to the lack of robust grid infrastructure. The optimal radial-loop configuration for such networks has not been thoroughly studied in Nepal, and the integration of EVs and solar PV systems has not been specifically optimized for Nepalese urban environments. Additionally, while optimization algorithms such as genetic algorithms (GA), particle swarm optimization (PSO), and simulated annealing (SA) have been widely used to solve distribution network optimization problems [11], [18] there is a need for more context-specific and computationally efficient methods, particularly when considering the unique operational challenges in Nepalese networks. Many of the existing optimization models are computationally expensive and may not be well-suited for real-time implementation in developing countries where computational resources and access to large-scale simulation platforms are often limited. There is, therefore, a need for more accessible, low-complexity optimization approaches that can be effectively implemented in these settings.

This research aims to fill these gaps by exploring the optimal radial-loop configuration for urban Nepalese distribution networks with the integration of both EV loads and solar PV systems. Specifically, this study will simultaneously consider solar PV and EV loads. This research will assess the combined

impact of both technologies on power loss, voltage deviations, and system stability, addressing the gap in understanding their interactions in urban distribution networks. It will develop a specific optimization techniques to the unique features of Nepalese distribution networks, considering local conditions such as grid infrastructure, power loss, and voltage fluctuations, which have been inadequately addressed in prior studies. The research will adopt or develop low-complexity optimization algorithms to ensure that the solutions are practical for real-world implementation in Nepal, where computational resources may be limited. By addressing these gaps, this research will contribute to the development of more efficient, reliable, and sustainable distribution networks in urban Nepal, offering valuable insights that can be applied to similar contexts in other developing countries facing similar challenges with renewable energy integration and electric mobility.

3. Methodology

3.1 Review of Past Studies

The first step of this study is to discuss research carried out related to distribution system optimization with the integration of EV loads and Solar PV generators. As discussed in literature review, there are various research carried out mainly focused on optimization of radial distribution feeders with reduced uncertainties and least computational costs. Even though number of studies have been carried out, research on optimizing feeders for Nepal's specific distribution systems, considering both EV loads and solar PV systems, remains limited and requires further investigation. With reference from different literatures, Particle Swarm Optimization (PSO) will be used for the proposed optimization. Particle Swarm Optimization (PSO) is a heuristic optimization technique inspired by the social behavior of birds flocking or fish schooling. It is widely used for solving complex optimization problems because of its simplicity and ability to find near-optimal solutions in a reasonable amount of time. In the context of distribution feeder optimization, PSO has been applied to various problems related to the efficient design and operation of electrical distribution systems. When applied to distribution feeder optimization, which involves tasks like minimizing power losses, enhancing voltage profiles, optimal placement of EVs and Distributed generations, capacitor placement, and reconfiguration, PSO has several distinct advantages over other optimization techniques. These benefits arise from PSO's inherent characteristics, making it particularly well-suited for the complex and dynamic nature of electrical distribution systems.

3.2 Generalized Flow of Algorithm

3.2.1 System Modeling

The first step involves development of a comprehensive model of the urban distribution network taking system data from NEA, Nuwakot Distribution Center, including both conventional and distributed energy resources such as solar PV and EV charging stations. The distribution network is modeled using standard electrical network elements (such as feeders, transformers, and buses) in MATLAB Simulink. The power flow equations are derived and used for simulations to assess network performance under different configurations.

3.2.2 Load Profile and Solar Generation Modeling

The next step involves modeling the load profiles, specifically focusing on the variability of EV loads and the intermittency of solar generation. EV load profiles is based on representative charging patterns, including both residential and public EV charging demand. A hypothetical solar PV generation is modeled as a function of time of day, season, and geographical location, using typical meteorological data for urban Nepalese environments near Bidur Municipality of Nuwakot District to evaluate the model performance in the presence of solar PV generators.

3.2.3 Feeder Reconfiguration

The various radial-loop configurations are evaluated with the help of optimization of different tie switch combinations. Radial-loop configurations are chosen for their practicality in urban distribution systems, where looped configurations allow for flexibility in power distribution and improved reliability compared to purely radial networks. The optimization will focus on determining which configurations minimize line losses and enhance voltage stability.

3.2.4 Optimization Algorithm

Particle Swarm Optimization (PSO) technique is employed to determine the optimal radial-loop configuration. Given the complexity of the problem, metaheuristic algorithms, PSO algorithm is well-suited for solving nonlinear, non-convex optimization problems that arise in network configuration and operation.

3.2.5 Performance Analysis and Validation

Various simulation scenarios have been executed to evaluate the performance of different feeder configurations with different tie switch combinations. The key performance indicators (KPIs), including line losses, voltage profiles, conductor ampacity, and power flow stability under varying solar generation and EV charging demand is assessed. The results are compared for each configuration to determine the optimal configuration for the urban distribution network at NEA, NDC.

3.3 Mathematical Formulation

In reference to the study carried out in [21], the mathematical formulation of the research objective and constraints are discussed in the following subsections.

3.3.1 Objective Function

The objective is to minimize the total line losses and voltage deviations across the distribution network. The objective function can be expressed as:

$$MinJ = \sum_{i=1}^{n} P_{loss}(i) + \lambda * \sum_{j=1}^{m} \Delta(j) \quad (1)$$

Where, Ploss(i): is the power loss in feeder segment i.

Δ (j): is the voltage deviation at bus j

n: is the number of feeder segments.

m: is the number of buses (nodes) in the network

λ: is the weighting factor to balance the importance of line losses and voltage deviations in the objective function.

3.3.2 Power Flow Equations

The network's power flow is governed by equations derived from Kirchhoff's laws, which include both active and reactive power. The distribution network consists of a set of nodes (buses) connected by lines (or branches) that are either in a radial or loop configuration. Each line has a resistance R and reactance X and each bus i has a voltage Vi, load Pi, and reactive power Qi. The power flow equations for the network are given by:

$$P_i = V_i * \sum_{k=1}^{n} V_k[G_{ik} * cos(\theta_i - \theta_k) + B_{ik} * sin(\theta_i - \theta_k)] \quad (2)$$

$$Q_i = V_i * \sum_{k=1}^{n} V_k[G_{ik} * sin(\theta_i - \theta_k) - B_{ik} * cos(\theta_i - \theta_k)] \quad (3)$$

Here, P_i and Q_i are the active and reactive power at the bus i. V_i and θ_i are the voltage magnitude and phase angle at bus i. G_{ik} and B_{ik} are the real and imaginary part of the bus-to-bus admittance matrix.

3.3.3 Line Loss Computation

The power losses in each feeder are calculated based on the difference between the power supplied and the power consumed:

$$P_{Loss}(i) = \sum_{j=1}^{n} [(V_i - V_j) * G_{ij}] \quad (4)$$

Where, G_{ij} is the conductance of the feeder between buses i and j.

3.3.4 Optimization Constraints

Voltage Constraints: Voltage constraints are enforced to maintain voltage within a permissible range at each bus:

$V_{min} \leq V_i \leq V_{max}$ for all i

Where, V_{min} and V_{max} are the minimum and maximum allowable voltages for each bus, ensuring voltage stability. **Power Balance Constraints:** EV charging demand and solar generation are variable and are modeled as time-varying load profiles. These profiles must be incorporated into the power flow equations as dynamic loads. The load at each bus, particularly for EVs, will be constrained by the maximum charging capacity and the solar power generation will be bounded by the available irradiance at each time step. The total power generated (including from solar PV systems) and the total load (including EVs) must balance:

$$P_{Grid}(i) + P_{PV}(i) = P_{Load}(i) + P_{EV}(i) \quad (5)$$

Line Flow Limits: The power flowing through each line must not exceed its thermal limit:

$P_{Line}(i) \leq P_{Thermal}$ for all branches i

By solving the above optimization problem bu using different tie switch combinations, the optimal radial-loop configuration is determined which minimizes line losses, reduces voltage fluctuations, and enhances overall system reliability and efficiency.

4. Numerical Testing of Proposed Methodology

4.1 System Under Consideration

The system considered for this research will focus on the typical urban distribution network in Nepal, integrating Electric Vehicle (EV) loads and solar Photovoltaic (PV) systems into the existing power grid. The test system for the proposed methodology will be based on the radial-loop configuration of the Nuwakot Distribution Center, operated by the Nepal Electricity Authority, located in Nuwakot, Nepal. Nuwakot, situated in the Bagmati Province and to the immediate north of Kathmandu, the capital city of Nepal, is known for its diverse cultural landscape and rapidly growing economy. The demand for agricultural, industrial, and commercial electricity is increasing significantly, driven in part by its strategic location along a major highway connecting Nepal's capital with China. The Nuwakot Distribution Center includes six 33/11 kV sub-stations and 19 radial 11 kV distribution feeders. Additionally, there are approximately 742 11/0.4 kV distribution transformers installed across the district, served by a total of 613 kilometers of radial 11 kV feeders. The district's various consumer categories are supplied through 400/230 V low-tension distribution lines, consuming approximately 40 million units of electrical energy annually.

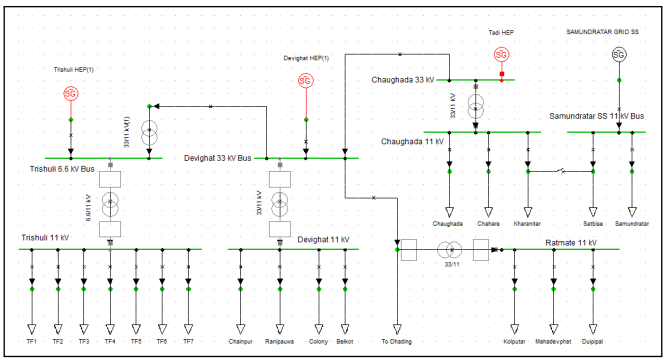

Figure 1: Typical Layout of Feeder and Substation Arrangements at Nuwakot DC

The Figure 1 illustrates the typical distribution layout of the NEA, Nuwakot Distribution Center. The feeder under consideration is the radially configured Battar Feeder (TF4), which originates from the Trishuli Hydropower Station substation, along with Feeders No. 5 and 3 from the Devighat Hydropower Station. These feeders collectively supply the major load centers in Bidur Municipality, Nuwakot District. The proposed methodology will be used to determine the optimal radial and loop configuration, as well as the best

locations for Electric Vehicle (EV) charging stations and Solar Photovoltaic (PV) generation within these areas.

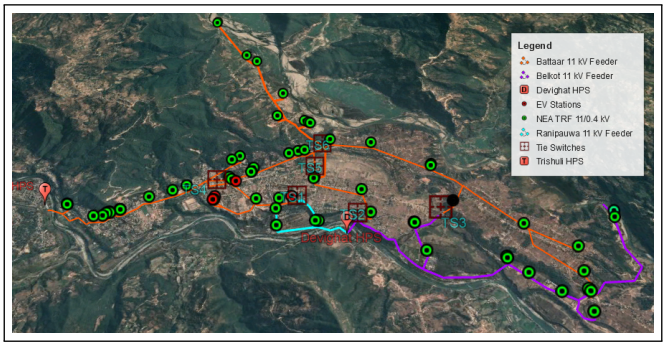

Figure 2: Layout of Existing Distribution System for the Study

The main urban area of Nuwakot District is located within Bidur Municipality, which accounts for approximately one-fourth of the total energy consumption in the district. There are currently six operational EV charging stations in this area, with an additional 20 stations under installation. Bidur Municipality also has high solar generation potential, as it falls within a region with strong solar radiation. Notably, the largest solar project in Nepal, a 25 MW peak capacity plant, is located within Bidur Municipality. This makes the area highly suitable for connecting rooftop PV installations and small solar PV farms to the low-voltage distribution system. The Nepal Electricity Authority (NEA) is in the process of developing policies for the implementation of net metering systems, which further enhances the feasibility of integrating solar generation. The key characteristics of the system to be considered are as follows:

Urban Distribution Network: The study modeled a radial-loop configuration of distribution network, under urban area of Nuwakot Distribution Center, Nuwakot District, Nepal. The network consists of the typical distribution components such as buses, feeders, transformers, EV charging station, Solar PV generators and substations. Various network topologies is simulated, and the effects of different radial-loop configurations along with effect of EV loads and solar generators on line losses, voltage stability, and overall system performance will be assessed.

Electric Vehicle (EV) Loads: EV charging stations is incorporated into the network as time-varying loads. The load profiles of different EV charging stations are collected from the data provided by Advance Metering Infrastructure installed at NEA and a load profile is analyzed accordingly. The EV charging load profiles is modeled based on typical urban driving and charging behaviors. This includes both residential EVs (charging at home) and public EV charging stations (e.g., fast-charging stations located in key urban areas). The variability in charging demand based on factors such as time of day, seasonality, and location is considered.

Solar Photovoltaic (PV) Systems: Solar PV systems is included as distributed generation sources within the distribution network. These systems is modeled at various locations within the urban network, considering factors like geographical position, installation capacity, and local solar radiation. The intermittent nature of solar power generation is taken into account, and its impact on the power flow and voltage stability is analyzed.

Power Flow Analysis: Power flow is analyzed using both active and reactive power equations. The interaction between EV charging, solar generation, and conventional loads is simulated to assess the performance of the network under varying conditions. Line losses, voltage profiles, and load balancing is key indicators to optimize the system's efficiency.

Optimization Techniques: Particle Swarm Optimization (PSO) algorithm is applied to determine the most efficient radial-loop configuration that minimizes line losses and voltage deviations while maintaining the stability and reliability of the network. The optimization considers the dynamic integration of EV loads and solar PV generation.

Network Constraints: Constraints such as voltage limits, capacity limits of feeders, and power supply limitations are incorporated into the model. The proposed system is operated within these constraints while achieving the optimal configuration for minimizing losses and improving voltage stability.

4.2 Simulation Results

For the urban radial distribution system, as represented in Figure 2, the system line data and bus data have been gathered. Since this distribution network consists of various conductor types, such as ACSR Weasel, ACSR Rabbit, and 100 and 50 Sq. mm XLPE Conductors, the distribution line parameters—specifically resistance, reactance, and charging susceptance—vary accordingly. The specific conductor type used in each branch of the distribution network has been obtained from the records of the NEA Nuwakot Distribution Center. The standard per-unit values for these conductor parameters have been sourced from various standards and are then multiplied by the length of each branch to determine the actual line parameters for each specific branch of the distribution network.

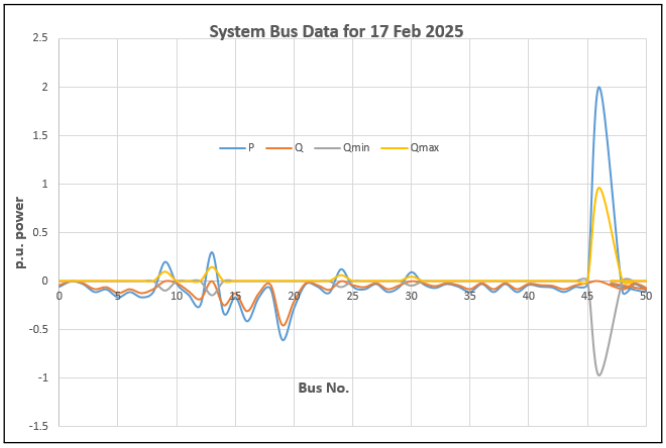

Figure 3: System Bus Data for Testing System on 17th Feb 2025, 12:00 PM

Similarly, the bus data has been collected from the database of the NEA Nuwakot Distribution Center. The bus data primarily consists of three types of buses. One of these is the generator bus, which represents the power generation sources in the

system. Two hydropower stations, the Trishuli Hydropower Station and the Devighat Hydropower Station, are available at the NEA NDC and are included as generator buses in the system. For the purpose of this study, a bus located near a region with the potential for solar PV generation installation is also considered as a generation bus. The solar PV generation is included hypothetically to study its behavior within the proposed methodology. Since solar PV generation is variable, the generation bus data is also subject to changes over a 24-hour period, as shown in Figure 3.

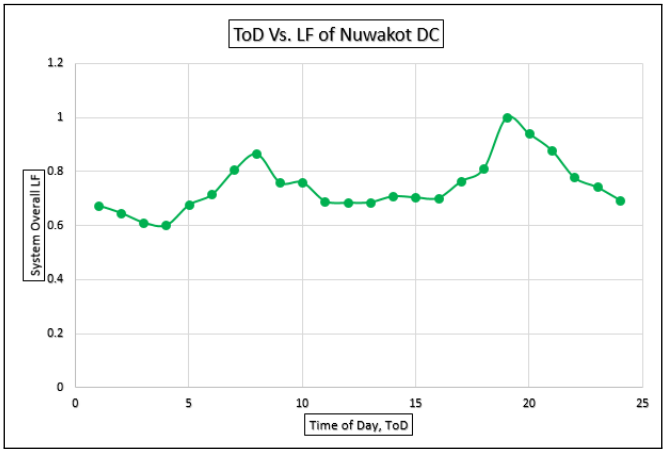

Figure 4: Overall System Load Factor behaviour for Different Time of Day at NEA, NDC

Additionally, the remaining buses are considered load buses. The load consumed by existing consumers of NEA, NDC from various categories is treated as the system load. Around sixty-five 11/0.4 kV distribution transformers are used to supply different consumer classes of NEA, NDC. The behavior of the system load is analyzed using the overall system load curve of NEA, NDC, as shown in Figure 4.

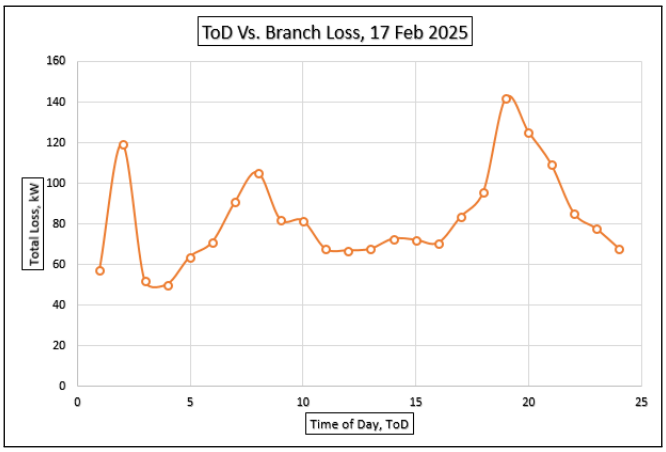

Figure 5: TOD Vs Total Branch Loss Plot for NEA NDC on 17th Feb 2025

The hourly demand at each individual system load bus is evaluated to replicate the system load curve, using measured data from different sub-stations of NEA, NDC. Another type of load bus is connected to EV charging stations, which exhibit variable loads since the charging demand changes throughout the day. Figure 3 illustrates the total system bus data for the proposed test system on the 17th of February, 2025, at 12:00 PM. Different bus data sets are generated for various times of day, as solar PV generation, system loads, and EV charging loads fluctuate with time.

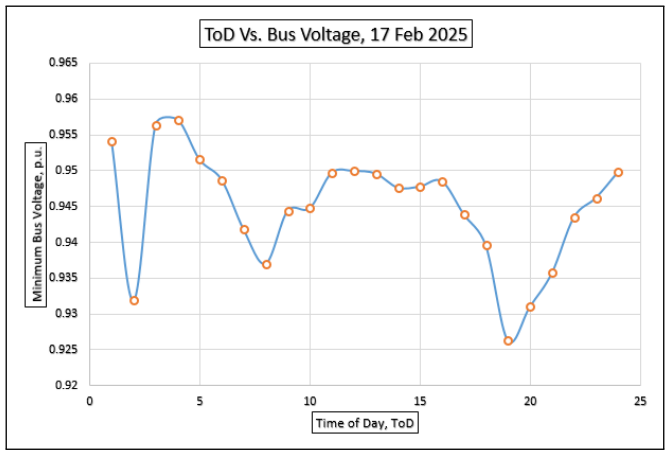

Figure 6: TOD Vs Minimum Bus Voltage Plot for NEA NDC on 17th Feb 2025

Table 1: Total Active Power Loss and Minimum Bus Voltage Magnitude for Different Switch Combination

SN	Total Loss (kW)	Min. Voltage (p.u.)
000111	137.2665338	0.955057
001110	128.9592695	0.954188
010101	73.96483496	0.9785
011100	69.19762876	0.980229
100011	109.9574929	0.959381
101010	101.3288711	0.95949
110001	59.07886672	0.980706
111000	57.08989461	0.980229
	Total	299

Using this bus and line data, load flow analysis is conducted, incorporating different combinations of tie switches, as shown in Figure 2. These tie switch combinations are controlled to avoid islanding operations of load buses. For each combination of tie switches, hourly load flow analysis is performed to minimize the total branch losses and bus voltage deviations. For illustration, Table 1 shows the total branch loss data and minimal bus voltage data for various tie switch combinations in the test system. In these switch combinations, logic "0" represents the off/open condition of a tie switch, while logic "1" represents the on/closed condition. The first digit in the logic represents tie switch TS1, and it continues up to the 6th digit for tie switch TS6. In one case, a minimal branch loss of 57.089 kW is observed when the tie switch combination is 111000 (i.e., TS1, TS2, and TS3 are closed, while TS4, TS5, and TS6 are open). Similarly, a minimal bus voltage of 0.954188 p.u. is observed when the tie switch combination is 001110 (i.e., TS1, TS2, and TS6 are open, while TS3, TS4, and TS5 are closed).

The minimal total branch losses for different time of day on the date of 17th February 2025, is represented in the Figure 5. Similarly, minimal bus voltage measured among of all 47 buses for different time of day is represented in the Figure 6. Here for

each hour of time of day, branch loss and minimal bus voltage for eight tie switch combination is evaluated. Some of this combinations are removed as it results the islanded operation of few load buses.

5. Conslusions

In conclusion, the study investigates the performance and behavior of an urban radial distribution system using detailed line and bus data. The system incorporates different conductor types, generation sources including hydropower and a hypothetical solar PV installation, and varying loads from both existing consumers and electric vehicle (EV) charging stations. Load flow analysis is conducted at various times of the day, considering different tie switch combinations to minimize branch losses and bus voltage deviations. The findings highlight the impact of these combinations on system efficiency, with some configurations offering minimal losses and voltage deviations, while others may result in islanding operations of load buses. This dynamic approach ensures optimal system performance and can be adapted to real-time changes in generation and consumption patterns.

Acknowledgments

This work has been supported by the Department of Electrical Engineering, Pulchowk Campus, Institute of Engineering, Tribhuvan University, Nepal.

References

[1] S. Chakraborty and S. Sen. Optimal configuration of radial and looped distribution networks considering power quality indices. *Journal of Electrical Engineering Technology*, 15:1078–1086, 2020.

[2] X. Zhang X. Huang and Y. Wu. Electric vehicle charging optimization in smart grids: A review of methodologies and applications. *IEEE Transactions on Smart Grid*, 10:3470–3481, 2019.

[3] Z. Li B. Zhao and X. Zhang. Voltage fluctuation and line loss reduction in distribution systems with renewable energy integration. *Renewable and Sustainable Energy Reviews*, 121, 2020.

[4] B. Koirala S. Shrestha and T. Sharma. Solar energy potential and its integration into nepal's energy grid. *Energy Policy Journal*, pages 89–102, 2020.

[5] S. Shrestha S. Karki and B. Upreti. Challenges and opportunities in integrating solar energy and electric vehicles into nepal's power grid. *Nepal Journal of Science and Technology*, pages 25–38, 2021.

[6] K. Bhattarai A. Sapkota and R. Sharma. Optimization of distribution network configuration for sustainable energy integration: A case study of nepal. *Renewable Energy Review*, pages 112–125, 2022.

[7] M. F. Hossain R. Akbar and S. Chowdhury. Analysis of radial and looped distribution network configurations for optimal energy delivery. *IEEE Transactions on Power Systems*, 33:394–403, 2018.

[8] S. Kumar and R. Saini. A review of the optimal configuration of distribution systems: Radial and looped networks. *International Journal of Electrical Power Energy Systems*, 106:435–442, 2019.

[9] S. R. Pandit A. Gupta and A. Patel. Optimization of hybrid radial-loop distribution network in the presence of renewable energy resources. *Energy Reports*, 6:681–690, 2020.

[10] L. Wang M. Hossain and S. Khan. Solar power integration in distribution networks: Challenges and opportunities. *International Journal of Electrical Power Energy Systems*, 119, 2020.

[11] J. Martinez R. Romero and S. Gracia. Feeder reconfiguration techniques in radial distribution networks to reduce line losses. *Electric Power Systems Research*, pages 246–253, 2017.

[12] A. Singh. Optimal feeder reconfiguration using particle swarm optimization. *International Journal of Electrical Power Energy Systems*, 57:213–221, 2014.

[13] S. Ghosh. Optimal placement of distributed generation in a distribution system using particle swarm optimization. *International Journal of Electrical Power Energy Systems*, 65:338–348, 2015.

[14] H. Khatib. Pso-based optimal feeder reconfiguration considering ev charging load. *Energy Conversion and Management*, 204, 2020.

[15] M. Rohit. Fuzzy dynamic thermal rating of transmission linesoptimization of ev charging stations in distribution networks using pso. *International Journal of Electrical Power Energy Systems*, 124, 2021.

[16] W. Zhao. Optimal feeder reconfiguration in distribution systems with ev load and solar pv using pso. *Renewable and Sustainable Energy Reviews*, 129, 2020.

[17] Z. Li. Optimal feeder configuration with ev load and solar pv generation using particle swarm optimization. *Renewable Energy*, 165:749–758, 2021.

[18] Z. Liu W. Zhang and L. Li. Optimization of distribution feeders with solar and ev load integration. *Renewable Energy*, pages 925–935, 2019.

[19] P. Sharma A. Gupta and A. Singh. Hybrid optimization techniques for distribution system feeders with electric vehicles and distributed energy resources. *Journal of Electrical Engineering and Technology*, 2021.

[20] S. Shrestha B. Koirala and R. Sharma. Impact of solar pv integration on nepal's urban distribution networks. *International Journal of Electrical Power Energy Systems*, 2020.

[21] T. Anegawa H. Hokazono A. Kaneko, Y. Hayashi and Y. Kuwashita. Evaluation of an optimal radial-loop configuration for a distribution network with pv systems to minimize power loss. *IEEE Access*, 8:220408–220421, 2020.

ANNEX I: PLAGIARISM REPORT

Shekh Maquesood Alam

final report for plag.pdf

Tribhuvan University

Document Details

Submission ID
trn:oid:::3117:450695141

Submission Date
Apr 20, 2025, 3:22 PM GMT+5:45

Download Date
Apr 20, 2025, 3:23 PM GMT+5:45

File Name
final report for plag.pdf

File Size
1.7 MB

52 Pages

14,163 Words

79,028 Characters

11% Overall Similarity

The combined total of all matches, including overlapping sources, for each database.

Match Groups

134 Not Cited or Quoted 9%
Matches with neither in-text citation nor quotation marks

14 Missing Quotations 1%
Matches that are still very similar to source material

11 Missing Citation 1%
Matches that have quotation marks, but no in-text citation

0 Cited and Quoted 0%
Matches with in-text citation present, but no quotation marks

Top Sources

7% Internet sources

9% Publications

0% Submitted works (Student Papers)

Integrity Flags

0 Integrity Flags for Review

No suspicious text manipulations found.

Our system's algorithms look deeply at a document for any inconsistencies that would set it apart from a normal submission. If we notice something strange, we flag it for you to review.

A Flag is not necessarily an indicator of a problem. However, we'd recommend you focus your attention there for further review.

Match Groups

- **134** Not Cited or Quoted 9%
  Matches with neither in-text citation nor quotation marks
- **14** Missing Quotations 1%
  Matches that are still very similar to source material
- **11** Missing Citation 1%
  Matches that have quotation marks, but no in-text citation
- **0** Cited and Quoted 0%
  Matches with in-text citation present, but no quotation marks

Top Sources

- 7% Internet sources
- 9% Publications
- 0% Submitted works (Student Papers)

Top Sources

The sources with the highest number of matches within the submission. Overlapping sources will not be displayed.

1	Internet	
www.mdpi.com		<1%
2	Publication	
Doğan Çelik, Muhammad Adnan Khan, Nima Khosravi, Muhammad Waseem, Hafi...		<1%
3	Publication	
Yue Wu, Weiguo Qiao, Yanzhi Li, Yabing Jiao, Shuai Zhang, Zonghao Zhang, Huini ...		<1%
4	Publication	
"International Conference on Signal, Machines, Automation, and Algorithm", Spri...		<1%
5	Publication	
Safia Babikir Bashir, Ali A. Adam, A. Elnady, Mena Maurice Farag, Abdul-Kadir Ha...		<1%
6	Internet	
ris.utwente.nl		<1%
7	Internet	
coek.info		<1%
8	Internet	
elibrary.tucl.edu.np		<1%
9	Publication	
Joel H. Van Sickel, Kwang Y. Lee, Jin S. Heo. "Differential Evolution and its Applicat...		<1%
10	Internet	
avesis.yildiz.edu.tr		<1%

11 Internet
www.ijeat.org <1%

12 Internet
www.ijrer.com <1%

13 Publication
Islam, Md Rabiul. "Managing Unbalanced Distribution Grid with Distributed Rene... <1%

14 Internet
ijece.iaescore.com <1%

15 Publication
Sajjan Kumar, Kamal Krishna Mandal, Niladri Chakraborty. "Optimal placement o... <1%

16 Internet
scopedatabase.com <1%

17 Internet
www.researchgate.net <1%

18 Internet
ej-eng.org <1%

19 Internet
gmsarnjournal.com <1%

20 Internet
19january2017snapshot.epa.gov <1%

21 Internet
back.skoltech.ru <1%

22 Publication
Amit Kumar Tyagi, Shrikant Tiwari. "AI and Blockchain in Smart Grids - Fundamen... <1%

23 Internet
core.ac.uk <1%

24 Publication
Ahmed. T. Hachemi, Fares Sadaoui, Abdelhakim Saim, Mohamed Ebeed, Salem Ari... <1%

25 Internet
dergipark.org.tr <1%

26 Internet
www.spellchecker.net <1%

27 Internet
www.jetir.org <1%

28 Internet
www.ncbi.nlm.nih.gov <1%

29 Internet
besaust.com.au <1%

30 Internet
eprints.usm.my <1%

31 Publication
Xie, Wanni. "A Dynamic Knowledge Graph Approach for Studying the Decarbonisa... <1%

32 Publication
Damanjeet Kaur, Jaydev Sharma. "Optimal conductor sizing in radial distribution ... <1%

33 Publication
Gulshan Sharma, Pitshou N. Bokoro, Sudeep Tanwar. "Energy 4.0 - Trends, Challe... <1%

34 Publication
Azizivahed, Ali. "Energy Management in Reconfigurable Distribution Network Inc... <1%

35 Publication
Liu, Haifeng, Licheng Jin, David Le, and A. A. Chowdhury. "Impact of high penetra... <1%

36 Publication
Ahmad Tavakoli, Sajeeb Saha, Mohammad Taufiqul Arif, Md Enamul Haque, Nisha... <1%

37 Publication
Sivaraman Palanisamy, Sharmeela Chenniappan, Sanjeevikumar Padmanaban. "F... <1%

38 Publication
Arvind R. Singh, Pradeep Vishnuram, Sureshkumar Alagarsamy, Mohit Bajaj et al. ... <1%

39 Publication

Iacopo Carnacina, Mawada Abdellatif, Manolia Andredaki, James Cooper, Darren ... <1%

40 Internet

d197for5662m48.cloudfront.net <1%

41 Internet

discovery.researcher.life <1%

42 Internet

it.ajou.ac.kr <1%

43 Publication

Janak, Urmisha Reddy. "Detection of Cyber Attacks on Power Distribution System ... <1%

44 Publication

Meijuan Zhang, Qingyou Yan, Yajuan Guan, Ni Da, Gibran David Agundis Tinajero.... <1%

45 Internet

lutpub.lut.fi <1%

46 Internet

pastel.archives-ouvertes.fr <1%

47 Publication

Young-Jae Jeon, Jae-Chul Kim, Jin-O Kim, Joong-Rin Shin, K.Y. Lee. "An efficient si... <1%

48 Internet

digital-library.theiet.org <1%

49 Internet

dokumen.pub <1%

50 Internet

drpress.org <1%

51 Internet

iris.polito.it <1%

52 Internet

knr.uns.ac.rs <1%

53 Internet
rangoli.rect.ernet.in <1%

54 Internet
worldwidescience.org <1%

55 Internet
www.coursehero.com <1%

56 Publication
Yordan Garbatov, C. Guedes Soares. "Innovation in the Analysis and Design of Ma... <1%

57 Internet
pmc.ncbi.nlm.nih.gov <1%

58 Internet
pure.tue.nl <1%

59 Internet
www-emerald-com-443.webvpn.sxu.edu.cn <1%

60 Internet
www.ijeert.org <1%

61 Internet
www.nginfra.nl <1%

62 Publication
"Decarbonisation of Transport Through Electrification and Synthetic Fuels", Riga ... <1%

63 Publication
"Smart Energy and Advancement in Power Technologies", Springer Science and B... <1%

64 Publication
Barazesh, Mohammadreza, Javad Saebi, and D. B. M. Hossein Javidi. "Optimal dist... <1%

65 Publication
Bindeshwar Singh, Charitra Pal, V. Mukherjee, Prabhakar Tiwari, Manish Kumar Y... <1%

66 Publication
G. Gurumoorthi, S. Senthilkumar, G. Karthikeyan, Faisal Alsaif. "A hybrid deep lea... <1%

67 Publication

Jung-Beom Lee. "Review on Environmentally-Friendly Vehicle Charging Station Lo... <1%

68 Publication

Junhui Li, Tong Zhao, Dapeng Sun, Jie Ma, Haozheng Yu, Gangui Yan, Xingxu Zhu, ... <1%

69 Publication

Jyotsna Singh, Rajive Tiwari. "Reconfiguration and Coordination of V2G EVs in Dist... <1%

70 Publication

Madhab Chandra Mandal, Nripen Mondal, Amitava Ray. "An expert system based ... <1%

71 Publication

Montoya, F.G.. "Minimization of voltage deviation and power losses in power net... <1%

72 Publication

Omid Ziaee, Omid Alizadeh-Mousavi, F. Fred Choobineh. "Co-Optimization of Tran... <1%

73 Publication

Rao, PVV Rama, and S Sivanaga Raju. "Voltage regulator placement in radial distri... <1%

74 Publication

Seyed Amir Hosseini, Behrooz Taheri, Seyed Hossein Hesamedin Sadeghi, Adel Na... <1%

75 Publication

Vaccaro, Alfredo, and Ahmed F. Zobaa. "Voltage regulation in active networks by ... <1%

76 Internet

acikerisim.atlas.edu.tr <1%

77 Internet

ajeee.co.in <1%

78 Internet

dream-go.ipp.pt <1%

79 Internet

flex.flinders.edu.au <1%

80 Internet

library.unisel.edu.my <1%

81 Internet
orbi.uliege.be <1%

82 Internet
ouci.dntb.gov.ua <1%

83 Internet
publications.polymtl.ca <1%

84 Internet
researchspace.ukzn.ac.za <1%

85 Internet
s3-ap-southeast-1.amazonaws.com <1%

86 Internet
waseda.repo.nii.ac.jp <1%

87 Internet
www.appropedia.org <1%

88 Internet
www.hindawi.com <1%

89 Internet
www.ijera.com <1%

90 Publication
Radian Belu. "Building Electrical Systems and Distribution Networks - An Introduc... <1%

91 Publication
Sirote Khunkitti, Natsawat Pompern, Suttichai Premrudeepreechacharn, Apirat Si... <1%

92 Publication
Zhilin Lyu, Xingyu Ni, Xiaoqing Bai, Chongyang Wang, Bin Liu. "CNN data-driven a... <1%

93 Publication
Akihisa Kaneko, Yasuhiro Hayashi, Takaya Anegawa, Hideyasu Hokazono, Yukiyas... <1%

94 Publication
Hossein Kiani, Behrooz Vahidi, Seyed Hossein Hosseinian, George Cristian Lazaroi... <1%

95 Publication

Jingshi Cui, Yi Cao, Bo Wang, Jiaman Wu. "Multi-stage adaptive expansion of EV ch... <1%

96 Publication

Milad Rahimipour Behbahani, Alireza Jalilian, Alireza Bahmanyar, Damien Ernst. "... <1%

97 Publication

Oscar Danilo Montoya, Walter Gil-González, Luis Fernando Grisales-Noreña. "Opti... <1%

98 Publication

Pitchai Pandiyan, Subramanian Saravanan, Kothandaraman Usha, Raju Kannadas... <1%